# Biogenesis Dynamics and Functions of Cargo vesicles in early secretory pathway and in extracellular milieu

**By**

**Sudeshna Roy Chowdhury**

**(LIFE09201504010)**

**Tata Memorial Centre, Mumbai**

A thesis submitted to the

Board of Studies in Life Sciences

In partial fulfilment of requirements

For the Degree of

**DOCTOR OF PHILOSOPHY**

**OF**

**HOMI BHABHA NATIONAL INSTITUTE**

**July, 2021**

# Homi Bhabha National Institute

## Recommendations of the Viva Voce Committee

As members of the Viva Voce Committee, we certify that we have read the dissertation prepared by Ms. Sudeshna Roy Chowdhury entitled "Biogenesis, Dynamics and Functions of Cargo vesicles in early secretory pathway and in extracellular milieu" and recommend that it may be accepted as fulfilling the thesis requirement for the award of Degree of Doctor of Philosophy.

S.N. Dalal 11/08/2021

Chairperson – Dr. Sorab N. Dalal Date:

Dibyendu Bhattacharyya

Guide/Convener – Dr. Dibyendu Bhattacharyya Date: 23 July 2021

Roop Mallik

External Examiner – Dr. Roop Mallik Date: 23 July 2021

Prasanna

11/08/2021

Member – Dr. Prasanna Venkatraman Date:

Abhijit De 11/08/2021

Member – Dr. Abhijit De Date:

---

Final approval and acceptance of this thesis is contingent upon the candidate's submission of the final copies of the thesis to HBNI.
I hereby certify that I have read this thesis prepared under my direction and recommend that it may be accepted as fulfilling the thesis requirement.

Date: 23.07.21
Place: Navi Mumbai

Dibyendu Bhattacharyya
Dr. Dibyendu Bhattacharyya
Guide

## 1.1 Background of the Thesis

A cell is compartmentalized into different organelles, each of which utilizes a specific set of proteins to carry out unique functions. This enrichment of proteins is carried out by vesicles that originate from the endomembrane system and function in intracellular communication in the form of membrane trafficking. Vesicular trafficking extends to intercellular communication and communication between the cell and its surroundings in exchanging information in the form of nutrients or signalling. This system is tightly regulated by various effector biomolecules, failure of which might affect cellular homeostasis and lead to a diseased condition (Yarwood *et al.*, 2020). An efficient system requires proper organization. There are three primary stages of vesicle transport; vesicle formation or budding from the donor membrane, release and directed transfer to its destination and, vesicle recognition and fusion or uptake at the acceptor membrane (Bonifacino and Glick, 2004). It is proposed that vesicle formation and tethering must occur at particular sites on the membrane (Spang, 2009). Furthermore, the respective constituent protein machinery's self-organization can create micro-domains on the donor and acceptor membrane (Glick, 2014).

## 1.2 Hypothesis

In the early secretory pathway, cargo proteins are transported to Golgi in COPII vesicles that originate from the Endoplasmic Reticulum (ER) at specialized sub-domains called ER Exit Sites (ERES). However, the site of the arrival of retrograde COPI vesicles at the ER membrane is poorly understood. We utilized the budding yeast, *P. pastoris,* that provides a simple system consisting of 4-5 stacked Golgi units positioned next to ERES. Dsl1 complex acts as the tether that links the COPI vesicles to the ER membrane before fusion and might act as the potential candidate for organizing the ER Arrival Sites (ERAS). We aimed to test this in our thesis. Also,

we tried to understand ERAS's spatial and functional relationship with ERES based on earlier reports on the proximity between COPI and COPII vesicles (Fig 1.1A).

A B

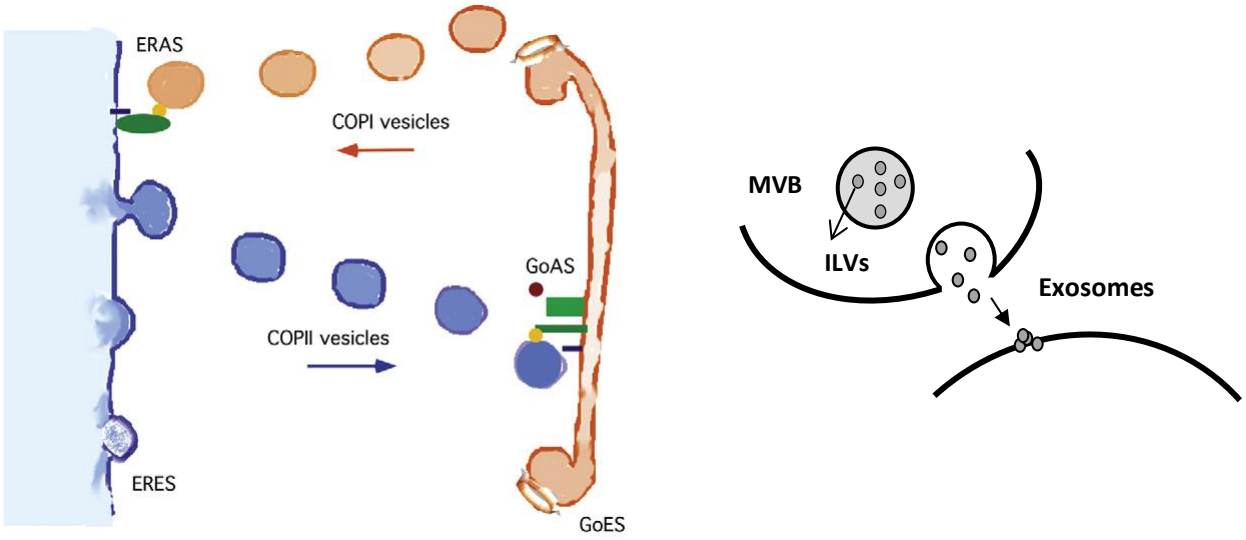


**Figure** Error! No text of specified style in document**..1: The proposal of ERAS and EES.** (Adapted from Spang, 2009)

We also hypothesize that, extracellular vesicles such as exosomes follow the same concept of entering through designated sites in the recipient cells. We tested this in the mammalian system (Fig1.1B).

## 1.1 Objectives

**I. To study the biogenesis, dynamics and functions of cargo vesicles in the early secretory pathway.**

A. To characterize ER Arrival Sites in budding yeast, *Pichia pastoris*.

B. To study the correlation between ER Arrival Sites and ER Exit Sites.

**II. To study the biogenesis, dynamics and functions of cargo vesicles in the extracellular milieu.**

A. To investigate the existence of Exosome Entry Site (EES)

B. To understand the mechanism of exosome entry

## 1.2 Work done

The results and discussion of the work carried out under the objectives mentioned above are presented as two chapters with the following headings:

**Chapter 4.1** – ER Arrival sites in the budding yeast *P. pastoris*, together with ER exit sites, form a bidirectional transport portal.

**Chapter 4.2 –** Exosome Entry Sites in mammalian cells.

**Thesis Abstract**

**Name:** Sudeshna Roy Chowdhury

**Enrollment Number:** LIFE09201504010

**Thesis Title:** Biogenesis Dynamics and Functions of Cargo vesicles in early secretory pathway and extracellular milieu

Many distinct vesicles operate an efficient cargo trafficking system to execute intracellular and extracellular communications in a tightly regulated manner. In the early secretory pathway, cargo proteins are transported to Golgi via anterograde COPII vesicles originating from specialized sub-domains at the Endoplasmic Reticulum called ER Exit Sites (ERES). However, the site of the arrival of Golgi-derived retrograde COPI vesicles at the ER membrane is poorly understood. We utilized the budding yeast, *P. pastoris*, a simple system consisting of 4-5 stacked Golgi units positioned next to ERES. Dsl1 complex acts as the tether that links the COPI vesicles to the ER-localized SNAREs for fusion and might act as the potential candidate for organizing the ER Arrival Sites (ERAS).

We tested this by fluorescently labeling the Dsl1 complex components which formed distinct punctate domains that more or less entirely colocalized with COPI vesicles (marked by the coat protein, Sec26). These ER Arrival sites (ERAS) always localize around the ERES, such that together they behave as a bipartite ultrastructure that form *de novo*, grow in size and undergo fusion. To investigate the functional connection between the ERES and ERAS, we employed two different techniques (anchor away and auxin induced degradation) to deplete one of the sites and examine its effect on the other. We found that loss of ERES lead to dispersal of the ERAS, however, the viva versa was not true. Interestingly, loss of COPI vesicles also disrupted the ERAS. We further showed depletion of ERES lead to the loss of typical tightly stacked Golgi that failed to produce COPI vesicles. On the other hand, perturbation of ERAS lead to accumulation of COPI vesicles and a vesiculated and enlarged Golgi. All these results suggested that the biogenesis of ERAS depends on the function of ERES.

We also observed that extracellular vesicles, such as exosomes follow the same concept of entering through designated sites in the recipient cells.

.....

Signature: .....
Student: Sudeshna Roy Chowdhury

Signature: .....
Guide: Dr. Dibyendu Bhattacharyya

Forwarded through:

Dr. Sorab N. Dalal, 11/08/2024
Chairperson, Academic &
Training Programme, ACTREC

**(Dr. Sorab N. Dalal)**
Chairperson, Academic & Training Programme
Tata Memorial Center, ACTREC,
Kharghar, Navi Mumbai - 410210

14/8/24
Dr. S. D. Banavali,
Dean (Academics)
T.M.C.

PROF. S. D. BANAVALI, MD
DEAN (ACADEMICS)
TATA MEMORIAL CENTRE
MUMBAI - 400 012.

# 1. Introduction

## 1.1 Background of the Thesis

A cell is compartmentalized into different organelles, each of which utilizes a specific set of proteins to carry out unique functions. This enrichment of proteins is carried out by vesicles that originate from the endomembrane system and function in intracellular communication in the form of membrane trafficking. Vesicular trafficking extends to intercellular communication and communication between the cell and its surroundings in exchanging information in the form of nutrients or signalling. This system is tightly regulated by various effector biomolecules, failure of which might affect cellular homeostasis and lead to a diseased condition (Yarwood *et al.*, 2020). An efficient system requires proper organization. There are three primary stages of vesicle transport; vesicle formation or budding from the donor membrane, release and directed transfer to its destination and, vesicle recognition and fusion or uptake at the acceptor membrane (Bonifacino and Glick, 2004). It is proposed that vesicle formation and tethering must occur at particular sites on the membrane (Spang, 2009). Furthermore, the respective constituent protein machinery's self-organization can create micro-domains on the donor and acceptor membrane (Glick, 2014).

## 1.2 Hypothesis

In the early secretory pathway, cargo proteins are transported to Golgi in COPII vesicles that originate from the Endoplasmic Reticulum (ER) at specialized sub-domains called ER Exit Sites (ERES). However, the site of the arrival of retrograde COPI vesicles at the ER membrane is poorly understood. We utilized the budding yeast, *P. pastoris,* that provides a simple system consisting of 4-5 stacked Golgi units positioned next to ERES. Dsl1 complex acts as the tether that links the COPI vesicles to the ER membrane before fusion and might act as the potential candidate for organizing the ER Arrival Sites (ERAS). We aimed to test this in our thesis. Also,

we tried to understand ERAS's spatial and functional relationship with ERES based on earlier reports on the proximity between COPI and COPII vesicles (Fig 1.1A).

A B

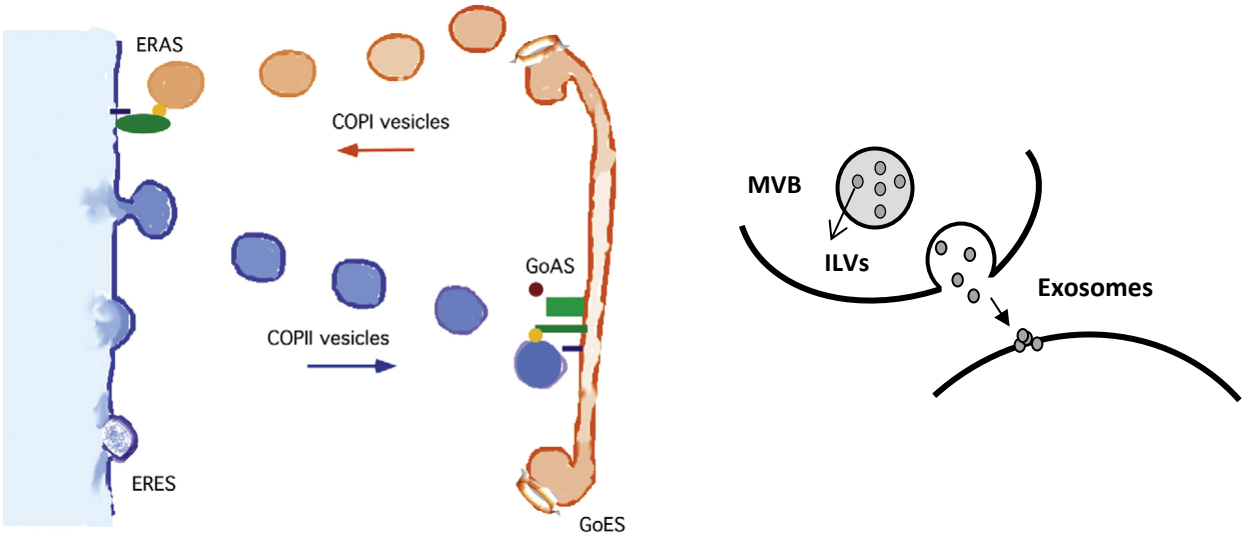


**Figure 1.1: The proposal of ERAS and EES.**

(Adapted from Spang, 2009)

We also hypothesize that, extracellular vesicles such as exosomes follow the same concept of entering through designated sites in the recipient cells. We tested this in the mammalian system (Fig1.1B).

## 1.1 Objectives

**I. To study the biogenesis, dynamics and functions of cargo vesicles in the early secretory pathway.**

A. To characterize ER Arrival Sites in budding yeast, *Pichia pastoris*.

B. To study the correlation between ER Arrival Sites and ER Exit Sites.

**II. To study the biogenesis, dynamics and functions of cargo vesicles in the extracellular milieu.**

A. To investigate the existence of Exosome Entry Site (EES)

B. To understand the mechanism of exosome entry

## 1.2 Work done

The results and discussion of the work carried out under the objectives mentioned above are presented as two chapters with the following headings:

**Chapter 4.1** – ER Arrival sites in the budding yeast *P. pastoris*, together with ER exit sites, form a bidirectional transport portal.

**Chapter 4.2 –** Exosome Entry Sites in mammalian cells.

# 2. Review of Literature

## 2.1 Vesicular trafficking:

A eukaryotic cell is compartmentalized into different membrane-bound organelles, most of which form part of the complex endomembrane system; the endoplasmic reticulum (ER), the Golgi apparatus, endosomes, lysosomes and plasma membrane. These compartments are defined by enriching a unique set of proteins and lipids (organelle markers) to execute organelle-specific functions to maintain cellular homeostasis. Coordinated and regulated communication is required among these compartments in orchestrating cellular functions. Small membranous vesicles carry out most intracellular and extracellular transport of biologically active biomolecules (Palade, 1975) (Fig 2.1). They originate from a donor compartment and fuse with the acceptor compartment releasing the cargo molecules. A plethora of distinct vesicles operates in this endomembrane trafficking. Other organelles like mitochondria, chloroplasts and peroxisomes that do not form part of the endomembrane system

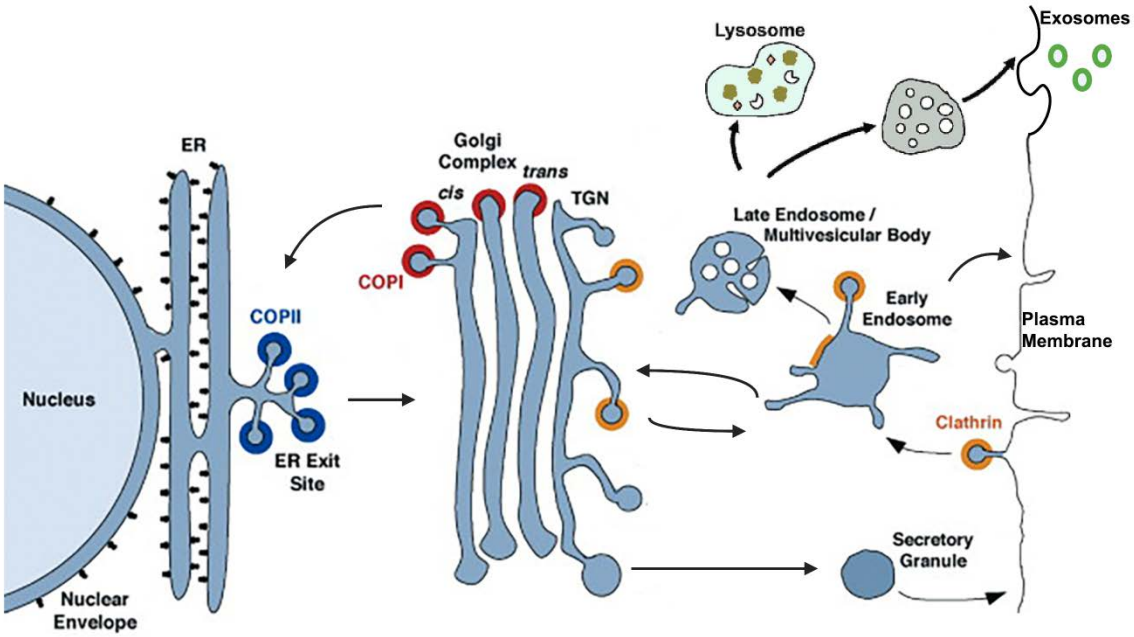


**Figure 2.1: Vesicular trafficking.**
(Created by biorender.com; adapted from Bonifacino and Glick, 2004; Hasegawa *et al.*, 2017)
The schematic shows the plethora of distinct vesicles that operate in the intracellular and extracellular trafficking of cargo biomolecules.

utilize different communication platforms. Mitochondria are often observed to physically contact the ER membrane at sites formed by protein complexes known as ERMES

(endoplasmic reticulum (ER)-mitochondria encounter structure) (Kornmann and Walter, 2010). The vesicular transport is broadly divided into the endocytic pathway; that sort and internalize extracellular contents such as nutrients or toxins and recycle cell membrane contents and the secretory pathway; that transport material at ER-Golgi interface, from Golgi to endosomes and secretory vesicles to the plasma membrane or cell exterior, endosomes to Golgi, and endosomes to lysosomes. In an alternative pathway, the early endosomes that mature into multivesicular bodies fuse to the plasma membrane and release exosomes in the extracellular milieu.

The fidelity of vesicle trafficking depends on the interplay of multiple proteins that functions at various stages to ensure specificity and directionality of the cargo vesicles from their originating compartment to their target compartment (Cai, Reinisch and Ferro-Novick, 2007)

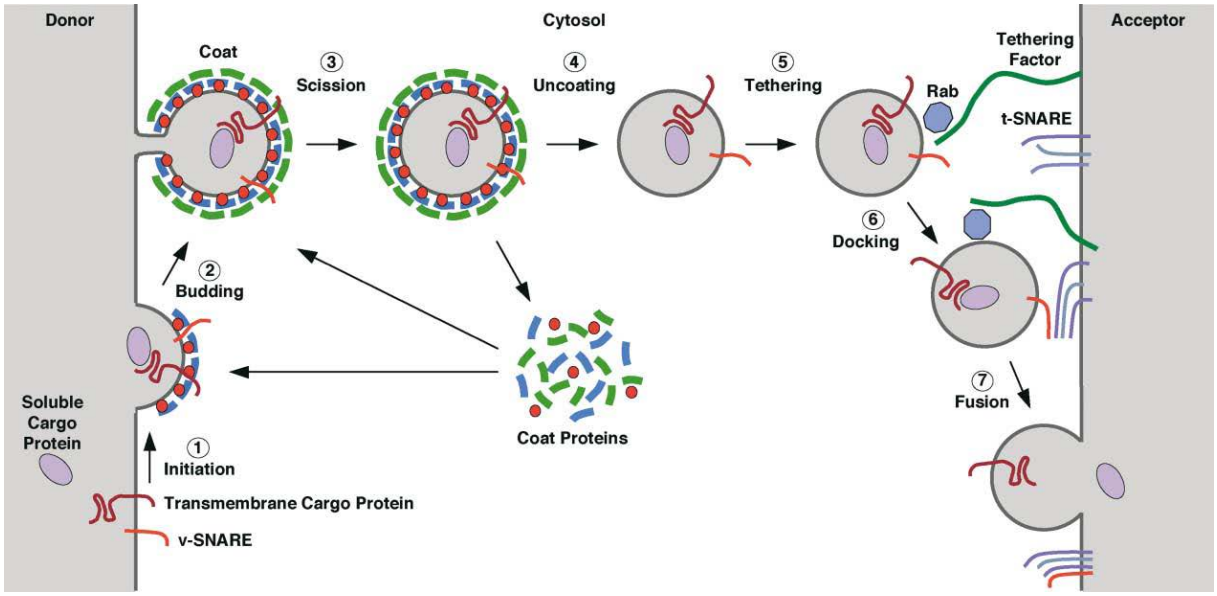


**Figure 2.2: Mechanism of vesicle transport.**
(Adapted from Bonifacino and Glick, 2004)
Rabs, tethers, coats and SNAREs work together to maintain the fidelity of vesicular trafficking.

(Fig 2.2). Rabs impart GTP/GDP regulation in recruiting various effector proteins in the trafficking cascade, coats induce membrane deformation at the donor membrane and assists cargo selection for the formation of the nascent vesicle, tethers capture the vesicle and dock

them to the acceptor membrane and finally, SNAREs execute fusion between the vesicle and target membrane. Alterations in any of the proteins or insufficiency in the transport can impair the cell function and lead to a diseased condition (Howell *et al.*, 2006).

## 2.2 Endocytic Pathway:

The internalization of exterior components and recycling of plasma membrane contents can occur in one of the following ways (Fig 2.3):

### 2.2.1 Clathrin-Coated Vesicle / receptor-mediated endocytosis

Clathrin-coated vesicles (Kaksonen and Roux, 2018) are formed at the cytoplasmic side of TGN (trans Golgi network), endosomes and plasma membrane. The 600kDa clathrin complex forms a triskelion (three-legged) that polymerizes in a cage-like lattice that deforms the membrane into a budding vesicle. Clathrin associated Adaptor protein (AP) complexes recognize the cargo proteins' cytoplasmic signal sequences and load them into the vesicles. Different adaptor protein complexes have been identified that function at different locations in vesicle formation, for example, AP1 function in vesicle trafficking between TGN to endosomes or plasma membrane, AP2 is involved in the internalization of cell membrane receptors, and AP3 mediates vesicle transport from early endosome to late endosome or lysosome. The GTPase dynamin brings about clathrin-coated vesicle release from the plasma membrane. The clathrin-coat disassembles before fusion with the endosomes, which further mediate cargo sorting to either fuse to the plasma membrane for recycling, TGN or lysosomes. Lysosomes are organelles that contain degradative enzymes like proteases, lipases and hydrolases and maintain an acidic environment. Endosomes carry material to lysosomes for lysosomal degradation or transport lysosome-resident proteins from TGN. Early endosomes utilize Rab5 GTPase regulated EEA1 tether for contacting the target membrane.

### 2.2.2 Caveolae mediated vesicle transport

Caveolae (Bastiani and Parton, 2010) are found as flask-shaped invaginations in the plasma membrane of specific cell types such as endothelial cells, smooth muscle cells and adipocytes. Caveolae are also detected in TGN to plasma membrane transport. Caveolin proteins (Cav-1, 2 and 3) form the structural unit of the Caveolae. Other than the classical vesicle fission and fusion machinery such as dynamin and SNAREs, caveolae contain a combination of GPI-anchored proteins, transmembrane proteins and cholesterol. Caveolae derived vesicles do not disassemble but retain their protein and lipid components and fuse into an endocytic compartment called caveosome, which further move to the early endosome.

### 2.2.3 Phagocytosis

Large particulate materials are internalized using cell-surface receptors such as Fc receptors that activate tyrosine kinases and Rho GTPases to signal actin cytoskeleton remodelling and

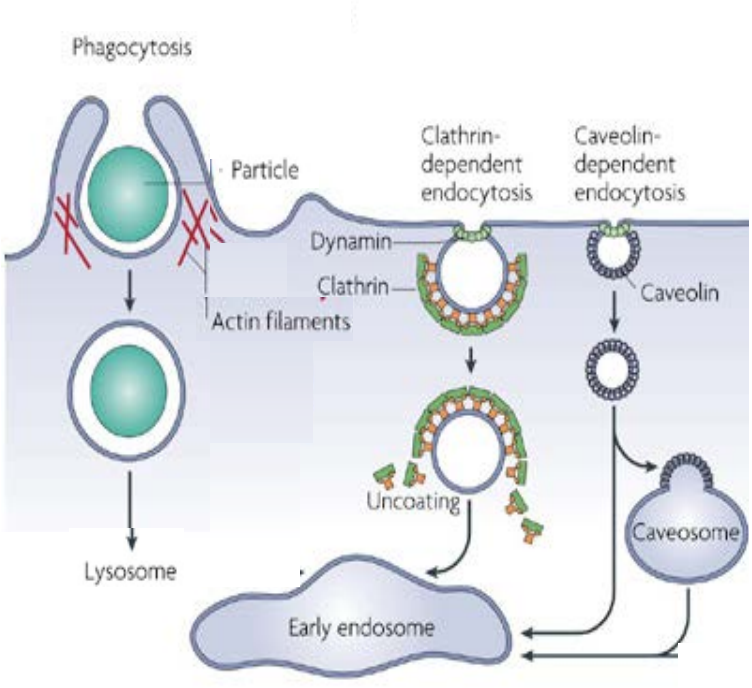


**Figure 2.3: Endocytic pathways.**
(Adapted from Mayor and Pagano, 2007)
The schematic shows internalization of exterior components or recycling of plasma membrane contents via different endocytic pathways.

formation of pseudopodia-like structures that engulfs the outer material. The resultant endocytic compartment called phagosome fuses with a lysosome leading to degradation and digestion of the foreign material (Flannagan, Jaumouillé and Grinstein, 2012).

## 2.3 The Secretory pathway:

Pioneering work in Schekman and Rothman lab led to the beginning of understanding the mechanisms of the vesicular trafficking in the secretory pathway (Malhotra *et al.*, 1989; Kaiser and Schekman, 1990). Secretory proteins or proteins destined for transport to organelles of the endomembrane system or plasma membrane begin their journey in the endoplasmic reticulum (ER). These proteins are translocated co-translationally or post-translation into the ER (Fig 2.4). During translation on the ribosome, the nascent polypeptide chain is recognized by the Signal Recognition Particle (SRP) via its hydrophobic transmembrane signal sequence and recruited to the SRP receptor on the ER membrane (Wild *et al.*, 2004). Translated proteins are

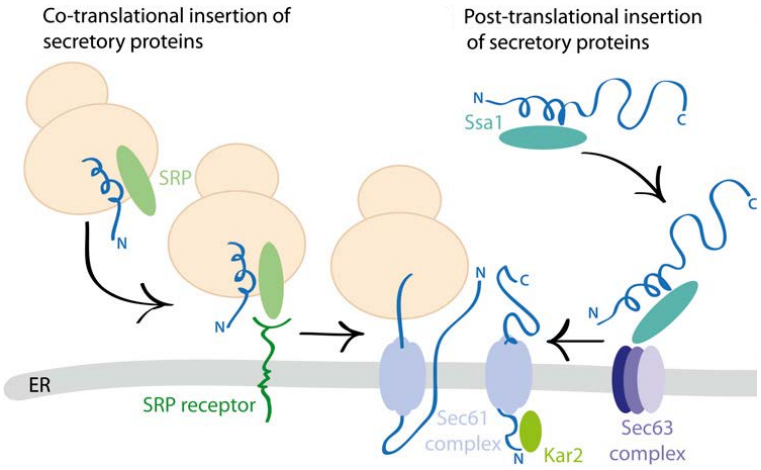


**Figure 2.4: Co-translation and post-translation translocation of proteins.**
(Adapted from Barlowe and Miller, 2013)
The nascent polypeptide chain associated with ribosome during translation can be recognized by the Signal Recognition Particle (SRP) and recruited to the SRP receptor on ER, or a fully translated nascent polypeptide chain associated with chaperons can be recognized by the Sec63 complex on the ER for translocation through the Sec61 pore complex.

maintained by cytosolic chaperons, Hsp70 ATPases like Ssa1 keeping the unfolded nascent proteins in a competent state for translocation. The N-terminal signal sequences in these proteins are recognized by the Sec63 complex comprised of Sec62, Sec63, Sec71 and Sec72 in the ER membrane (Deshaies *et al.*, 1991). Sec61 complex forms a translocation pore that, along with associated luminal protein Kar2, directs the nascent polypeptide chain in the ER membrane or lumen co-translationally or post-translation. The nascent polypeptides undergo several post-translational modifications, mature and are correctly folded in the ER. Initially, during translocation through the Sec61 complex, the N-terminal signal sequence is cleaved by the signal peptidase complex (SPC) comprising Spc1, Spc2, Spc3 and Sec11 (YaDeau, Klein and Blobel, 1991) located close to the translocon exit. A core 14 residue oligosaccharide assembled on dolichol pyrophosphate is added en bloc to N-X-S/T consensus sequence by oligosaccharyltransferase (OST) enzyme. The nascent N-linked glycoproteins render solubility and thermodynamic stability that aid protein folding (Kelleher and Gilmore, 2006). Some proteins undergo O-linked glycosylation at S/T residues by adding mannose residues using dolichol-mannose by protein O-mannosyltransferases (Pmts) (Willer, 2003). Further C-terminal ω residue of some proteins are covalently linked to lipid-anchored glycosylphosphatidylinositol (GPI) moiety by the GPI transmidase complex (Orlean and Menon, 2007). The formation of disulfide bonds that assist protein folding occurs in the ER lumen by disulfide isomerases like Pdi1 that utilizes FAD-linked Ero1 for oxidation (Tu and Weissman, 2002). Finally, the 14 residues $Glc_3Man_9GlcNAc_2$ of N-linked glycan on the proteins are trimmed sequentially to facilitate protein folding and quality control (Helenius and Aebi, 2004). Three terminal Glucose residues are removed by the enzymes, glucosidase I and II. If the nascent protein fails to fold correctly, UDP-glucose glycoprotein glucosyltransferase (UGGT) adds back one Glucose residue, due to which it binds to the chaperone calnexin that retains the unassembled protein in ER. Further, the mannosidase Mns1 removes the terminal

mannosyl residue to yield $Man_8GlcNAc_2$ linked to properly folded protein that exits the ER. However, the incorrectly folded proteins undergo another round of mannosidase trimming by Htm1 to remove another mannosyl residue, the resultant $Man_7GlcNAc_2$ linked protein is recognized by Yos9 that targets it to the transmembrane E3 ubiquitin ligase. These terminally misfolded proteins are ubiquitylated and dislocated to cytosol where they undergo proteosomal degradation (Smith, Ploegh and Weissman, 2011). This is known as ER associated degradation (ERAD) (Fig 2.5). The correctly folded proteins exit the ER in small COPII coated vesicles from the ER exit sites and are delivered to the Golgi apparatus for further processing.

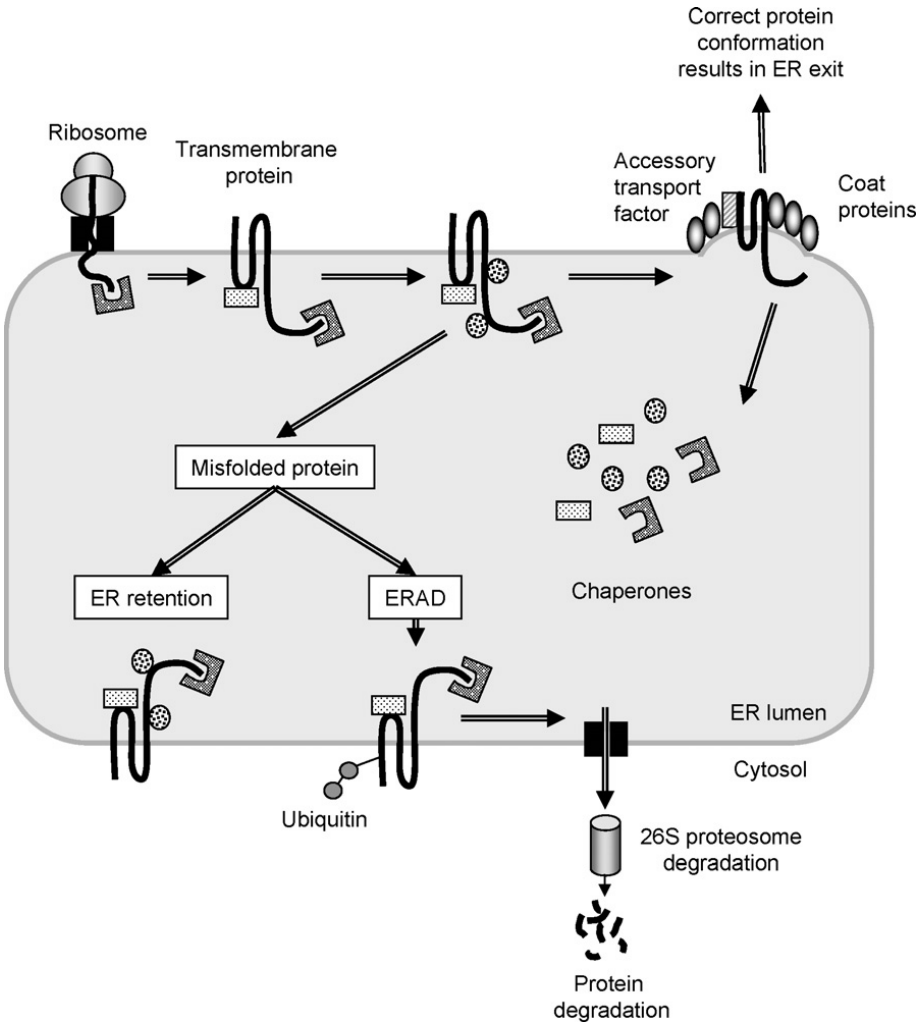


**Figure 2.5: Quality control in the ER for protein exit or degradation.**
(Adapted from Yarwood *et al.*, 2020)
The incorrectly folded proteins undergo ER associated degradation (ERAD) while the correctly folded proteins exit the ER.

There are two prevalent models of protein transport through Golgi (Fig 2.6). The vesicular transport model proposes the Golgi to be stable with distinct compartments / cisternae consisting of a unique set of proteins that facilitate cargo processing (Rothman, 1981). The cargoes exit ER in COPII vesicles that fuse to the cis-Golgi cisternae. Further, the secretory proteins are carried from one compartment to the next in anterograde COPI-coated vesicles distinguishable from retrograde COPI vesicles that recycle ER-resident proteins from Golgi to ER (Orci *et al.*, 1997). In the cisternal maturation model, the cisterna is proposed to be dynamic. Homotypic fusion of COPII vesicles generates cis Golgi cisternae that further progress with the protein cargo and matures into medial then trans by replenishment of cisterna specific Golgi-resident proteins via retrograde COPI vesicles (Glick, Elston and Oster, 1997). Finally, the mature TGN cisternae vesiculate to transport cargo to their final destinations; endosomes, secretory granules or plasma membrane. This model is the most accepted in the early secretory

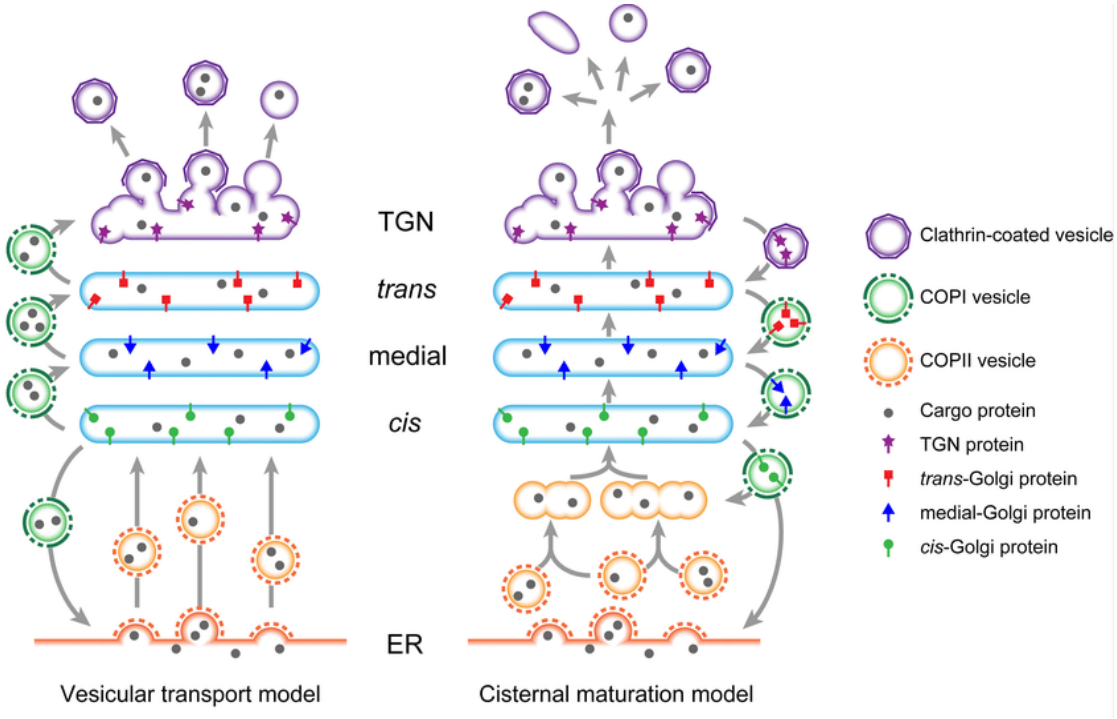


**Figure 2.6: Intra Golgi transport models.**
(Adapted from Ito, Uemura and Nakano, 2014)
The schematic of two prevalent models of protein transport through Golgi; vesicular transport model proposes the Golgi to be stable and the cisternal maturation model, the cisterna is proposed to be dynamic.

pathway. The COG multi-subunit tether complex interacts with γ-subunit of retrograde COPI vesicles and docks them for fusion using the SNAREs; Sed5 (Qa), Gos1 (Qb), Sft1 (Qc) and Ykt6/Sec22 (Shestakova *et al.*, 2007).

α-1,6-mannose is added to the N-linked proteoglycans in the cis-Golgi. Further, α-1,2- and α-1,3 mannose residues are added in the medial-Golgi (Graham and Emr, 1991). Finally, the proteins undergo proteolytic processing in the trans-Golgi by Kex2 endopeptidase.

## 2.4 COPII vesicles:

COPII (Coat protein complex II) vesicles originate from the ER, from where they load membrane or luminal cargo proteins and lipids and transport them to the adjacent organelle of the endomembrane system, Golgi. COPII-coated vesicles' formation requires the coat proteins; Sec23, Sec24, Sec13 and Sec31 and the small GTPase Sar1 (Fig 2.7). These proteins deform the ER membrane into a budded structure and simultaneously select cargo either directly or using cargo adaptors into the nascent vesicle.

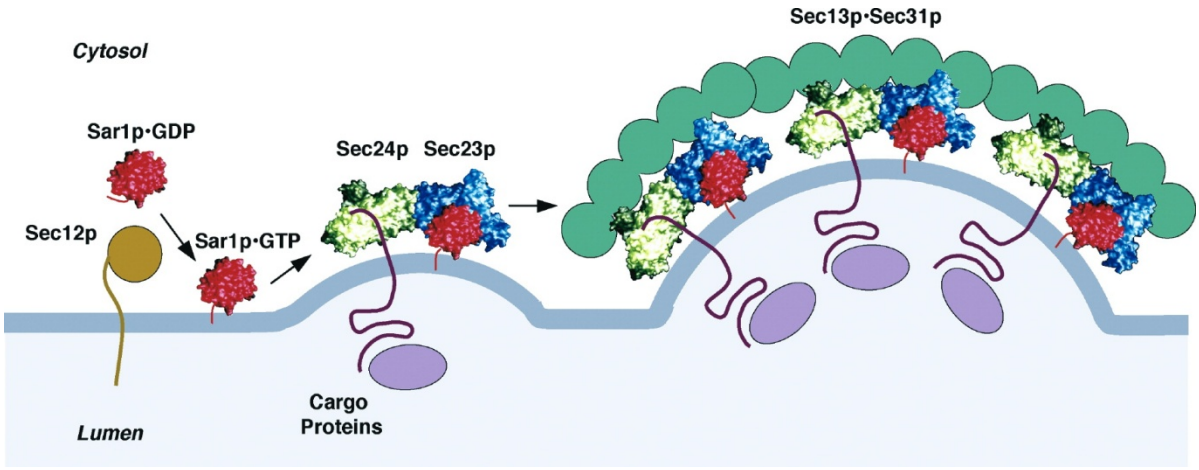


**Figure 2.7: COPII coat assembly.**
(Adapted from Bonifacino and Glick, 2004)
The schematic showing activation of Sar1 followed by recruitment of Sec23-Sec24 heterodimer and Sec13- Sec31 heterotetramer in a sequential manner for COPII assembly.

The COPII assembly is initiated by the small GTPase Sar1 (Secretion-Associated, Ras-related). It is present in the cytoplasm in an inactive GDP-bound state. Sec12 acts as the guanine exchange factor (GEF) to activate Sar1 (Weissman, Plutner and Balch, 2001). Sec12 is an ER-bound transmembrane protein that catalyzes the replacement of GDP with GTP in Sar1. Activated Sar1 undergoes conformational changes that expose its N-terminal amphipathic α-helix with the help of which it embeds itself into the ER membrane and induces membrane curvature (Lee *et al.*, 2005). Sar1 recruits the Sec23-Sec24 heterodimer by direct interaction with Sec23. The Sec23-Sec24 heterodimer forms the cargo-selecting inner layer of the COPII coat. Sar1, together with Sec23/24 heterodimer, is called the pre-budding complex.

Sec24 contains various cargo binding pockets at the proximal membrane surface identified as A-, B- and C-sites, which recognizes export signal sequences on transmembrane cargo proteins' cytoplasmic domains (Miller *et al.*, 2003). A-site binds to YxxNPF motif on the SNARE protein Sed5. The C-site recognizes a domain on the SNARE protein Sec22. The B-site is multivalent that interacts with different sorting signals, such as the acidic motifs on the SNARE protein Bet1. Membrane proteins transported from the ER exhibit di-acidic, di-hydrophobic or aromatic motifs at their C-terminal (Barlowe, 2003). Some proteins bind to integral membrane cargo receptors/ adaptors that simultaneously interact with the COPII coat subunit. Erv29 mediates the loading of soluble luminal secretory proteins such as pro-α factor and carboxypeptidase Y (CPY) (Belden and Barlowe, 2001). The p24 proteins like Emp24 facilitate COPII packaging of GPI-anchored proteins such as Gas1, which do not expose amino acid residues to the cytoplasm (Belden and Barlowe, 1996). Few transmembrane proteins that lack an export signal or require chaperon-like assistance depend on receptor/adaptor proteins like Erv14 and Erv26 for loading into COPII (Powers and Barlowe, 2002; Bue, Bentivoglio and Barlowe, 2006). Further, some proteins enter the COPII vesicles passively in a bulk flow diffusion (Thor *et al.*, 2009).

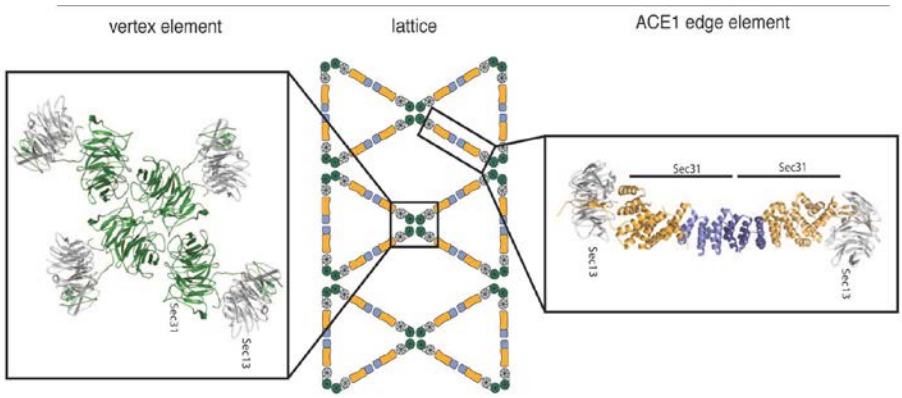


**Figure 2.8: Cage lattice of COPII.**
(Adapted from Leksa and Schwartz, 2010)
The COPII coat forms a flexible cage lattice of cuboctahedron geometry with square and triangular faces that makes vesicles roughly 60-70nm in size.

The pre-budding complex resembles a bow-tie shaped structure with its concave side rich in positively charged amino acids facing the negatively charged phospholipid layer of the ER membrane (Bi, Corpina and Goldberg, 2002). The pre-budding complex recruits the Sec13-Sec31 heterotetramer that forms the membrane distal outer layer of the COPII-coat. Direct interaction is reported between Sec31 and Sec23 (Shaywitz *et al.*, 1997). Sec13/31 complex exerts membrane bending force and provides a structural framework to the COPII vesicle (Fig 2.8). It forms a flexible cage lattice of cuboctahedron geometry with square and triangular faces that makes the COPII vesicles roughly 60-70nm in size (Stagg *et al.*, 2006).

Complete polymerization of the coat proteins facilitates Sar1-GTP hydrolysis followed by COPII uncoating leading to vesicle scission and pinching off from the ER membrane. Sar1, although having an intrinsic GTPase activity, requires a GTPase activating protein (GAP) for GTP hydrolysis and subsequent COPII disassembly. Sec23 acts as the GAP for Sar1 that stimulates its GTPase activity by inserting an arginine side chain into the active site of Sar1 (Yoshihisa, Barlowe and Schekman, 1993; Bi, Corpina and Goldberg, 2002). Sec31 further accelerates the GTP hydrolysis reaction by binding across Sec23/Sar1 complex and embedding amino-acid side chains in the vicinity of the Sar1 active site (Antonny *et al.*, 2001; Bi, Mancias and Goldberg, 2007). The GTP hydrolysis reaction on Sar1 is a paradox that couples COPII

coat's assembly and disassembly (Fig 2.9). The Sar1 is constantly reactivated by membrane-bound Sec12 as the coat complex remain stably associated with the assembled cargo. Once the complete COPII coat is assembled and attains proper enrichment of cargo proteins, the GTPase activity overpowers, leading to the release of Sar1 and subsequent disassembly of COPII coat proteins (Sato and Nakano, 2005).

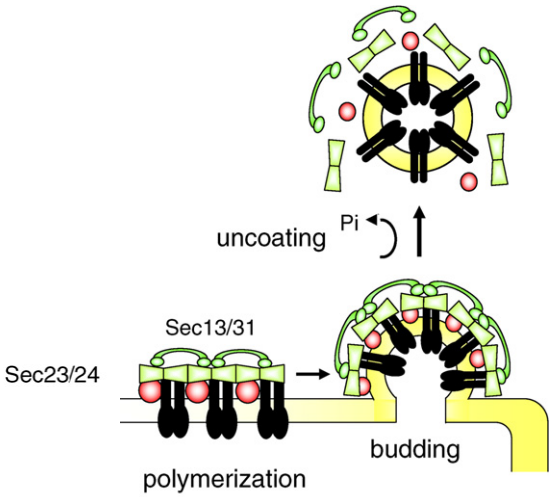


**Figure 2.9: GTP hydrolysis of Sar1 and COPII uncoating.**
(Adapted from Sato and Nakano, 2007)
Complete assembly of a COPII vesicle with sufficiently enriched cargo triggers hydrolysis of Sar1 with subsequent disassembly of coat protein followed by vesicle release.

Vesicle scission releases the nascent COPII vesicles that are tethered to the Golgi membranes. TRAPP I multi-subunit tether complex associates with partially coated COPII vesicles. TRAPPI have six subunits; Bet3, Bet5, Trs20, Trs23, Trs3 and Trs33. Bet3 directly interacts with Sec23. This interaction is regulated by a Golgi associated kinase Hrr25, which phosphorylates Sec23/24 complex. TRAPP I acts as a GEF, and its components, Bet3, Bet5, Trs23 and Trs31, bind and activate Ypt1 GTPase (Wang, Sacher and Ferro-Novick, 2000). The activated form of Ypt1 recruits and coordinate with the coiled-coil tether Uso1 on the Golgi membrane to exert a long-range capture of COPII vesicles to the Golgi membrane (Cao, Ballew and Barlowe, 1998). Once tethered, the formation of the trans SNARE complex renders COPII vesicle fusion with the Golgi membrane (Fig 2.10). Four SNARE proteins contribute to the complex; Qa-Sed5, Qb-Bos1, Qc-Bet1 (providing glutamine residue), and R-Sec22 (providing

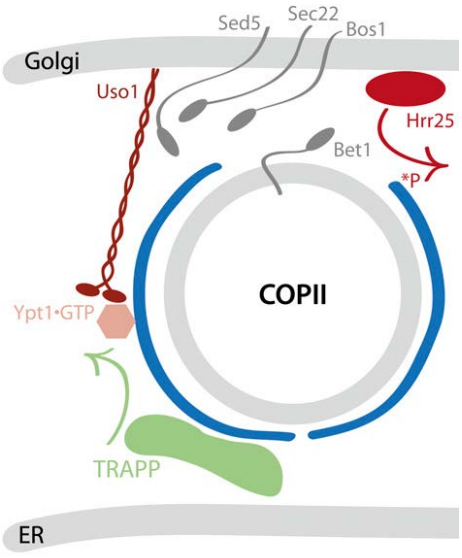


**Figure 2.10: COPII vesicle tethering and fusion machinery.**
(Adapted from Barlowe and Miller, 2013)
TRAPP I (GEF) activates Ypt1(Rab GTPase) that recruits Uso1(coiled-coil tether) at the Golgi membrane to tether COPII vesicles released from ER for fusion with the help of Sed5-Bos1-Bet1-Sec22 SNARE complex.

arginine residue) form a parallel coiled-coil α-helical bundle using their conserved ~70 amino acid heptad repeats motifs that zipper the bilayer lipid of the apposing COPII and Golgi membranes (Newman, Shim and Ferro-Novick, 1990). The Sec1/Munc18-1 (SM) family of

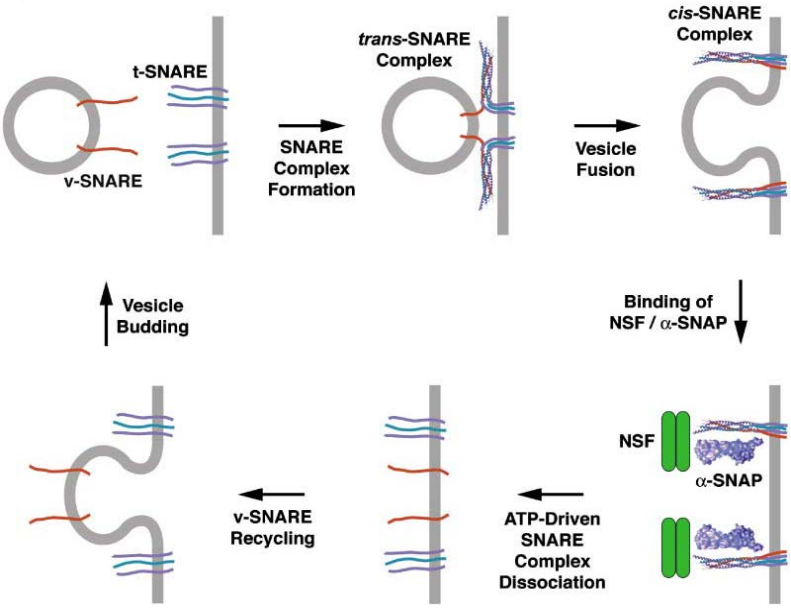


**Figure 2.11: General mechanism of vesicle fusion with the target membrane.**
(Adapted from Bonifacino and Glick, 2004)
The v-SNARE and the t-SNAREs form the trans-SNARE complex leading to vesicle fusion. The resultant cis-SNARE complex on the target membrane disassembled by Sec17(α-SNAP) /Sec18(NSF) that recycles the v-SNARE.

protein, Sly1 binds to Sec5 and acts as a clamp to stabilize the trans SNARE complex formed by Sed5, Bos1, Bet1 and Sec22 (Peng and Gallwitz, 2002). Sec17 (α-SNAP) recruits Sec18 (NSF) ATPase to disassemble the cis SNARE complex on the target Golgi membrane and recycle the SNARE proteins (Fig 2.11)

## 2.5 ER Exit Sites (ERES):

COPII vesicles mediating ER to Golgi cargo transport, bud in specialized microdomains in a ribosome free zone amidst the rough Endoplasmic Reticulum (ER), forming a functionally distinct highly ordered structure (Mogelsvang *et al.*, 2003; Kurokawa and Nakano, 2019). These subdomains of the endoplasmic reticulum are known as ER exit sites (earlier called the transitional ER) and are defined by high COPII producing activity. These regions are enriched in COPII coat proteins, Sec23, Sec24, Sec13 and Sec31, along with the accessory proteins; Sec12 and Sec16 that regulate ERES organization (Budnik and Stephens, 2009) (Fig 2.12). The ERES have a selective preference to reside in a region of high membrane curvature as they co-localize with curvature stabilizing protein, reticulon Rtn1 that concentrates on high-curvature ER membranes (Okamoto *et al.*, 2012). These domains are stable (~0.5µm in diameter), long-

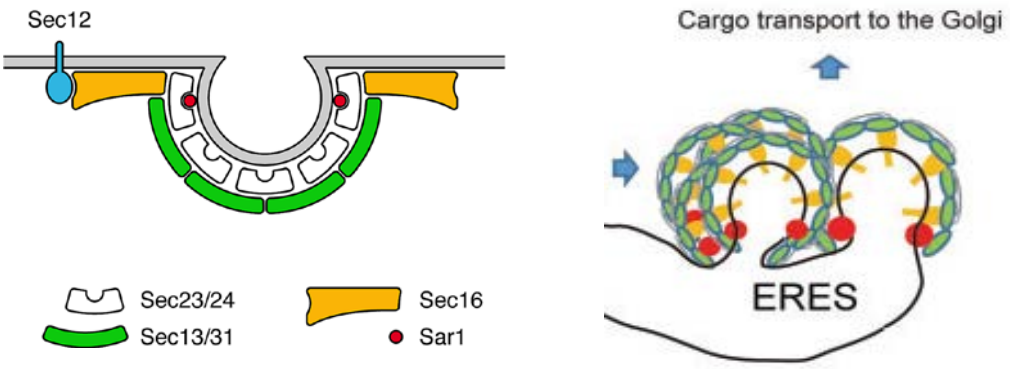


**Figure 2.12: The ERES and its components.**
(Adapted from Bharucha *et al.*, 2013; Kurokawa and Nakano, 2019)
ER exits sites are specific subdomains on the Endoplasmic Reticulum that defined by high COPII producing activity and enriched in COPII coat proteins and associated regulatory proteins and lipids.

lived and dynamic that moves over short distances. ERES has been observed to appear *de novo* as a small spot increasing to the optimum size and persists. They exhibit the ability to fuse among themselves to attain a larger domain and undergo fission or shrinkage to return to its steady-state size (Hammond and Glick, 2000; Bevis *et al.*, 2002; Stephens, 2003).

The number of ERES varies in different organisms. The ERES organization among organisms can be correlated with its association with pre-/early Golgi membranes (Rossanese *et al.*, 1999). In vertebrate cells, the Golgi is organized into a tight, complex stacked ribbon-like structure positioned in the perinuclear region. Numerous ERES are spread over the ER membrane, distant from the Golgi ribbon but in juxtaposition to ERGIC (ER-Golgi intermediate compartment) that receives cargo from ER. In plant cells, many ERES is found in tight association with the stacked Golgi unit's cis-face throughout the cytoplasm. The yeast S. cerevisiae consists of an unstacked Golgi, with individual cisternae floating in the cytoplasm, and numerous ERES are observed on the ER membranes, most of which co-localize with the cis-Golgi cisterna. The budding yeast *Pichia pastoris* has a few discrete and definable ERES (2-6 in number), each of which lies next to a stacked Golgi unit proximal to cis/early Golgi cisterna. This simplicity makes *P. pastoris* an excellent model organism to study the early secretory pathway (Fig 2.13).

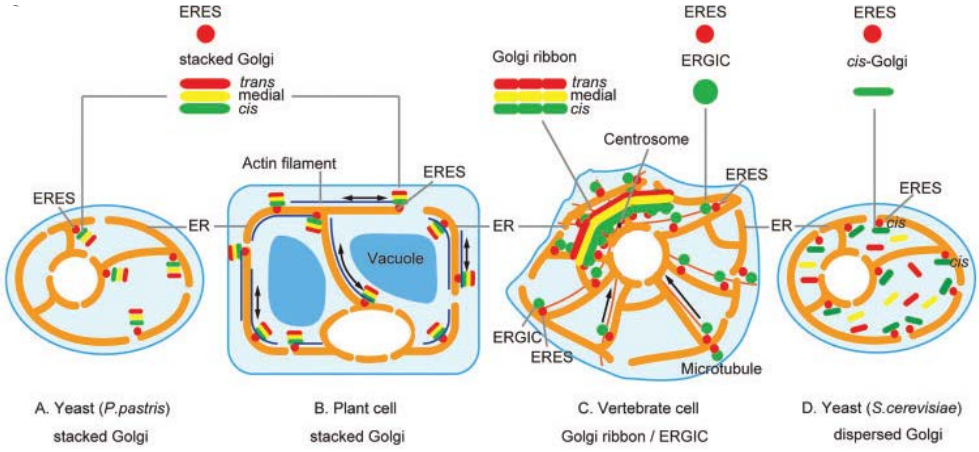


**Figure 2.13: Distribution of ERES in different model organisms.**
(Adapted from Kurokawa and Nakano, 2019)
The distribution of ERES varies in different organisms but their organization can be correlated with their association with pre-/early Golgi membranes together making up the secretory unit.

Many reports from Glick lab have shed insights into the organization of ERES. ERES might follow the concept of self-assembly, which implicate that similar membrane components incorporate themselves into a domain undergoing expansion and shrinkage to attain an optimum size in a dynamic equilibrium (Glick and Edu, 2014). Sec16, a peripheral membrane protein, has been shown to play an essential role in ERES organization (Connerly *et al.*, 2005; Montegna *et al.*, 2012; Bharucha *et al.*, 2013). Sec16 interacts with all the subunits of the COPII complex and the GEF Sec12 as well. Sec16 binds to the cytosolic domain of the transmembrane protein, Sec12, with its C-terminal. This binding is saturable such that abolition of Sec16 C-terminal fragment perturbs its ability to recruit Sec12 into the ERES. This data suggested that Sec16 might act as a scaffold protein for organizing the ERES. It can crosslink COPII complex molecules into an organized ultrastructure. Further studies revealed that the depletion of Sec16 did not wholly abolish ERES structures but increased their formation rate. The ERES became smaller in size, numerous in number and highly dynamic. However, disruption of COPII coat components delocalized Sec16 from ERES, suggesting Sec16 functions downstream of COPII coat formation. Interestingly, the Sar1 GDP locked mutant can reverse the effect of Sec16 loss on ERES. Thus, Sec16 negatively regulates COPII turnover by suppressing Sar1 GTPase activity and stabilize ERES organization.

## 2.6 COPI vesicles:

COPI (coat protein complex I) vesicles function to retrieve lipids and proteins between Golgi cisternae and the ER-Golgi interface. As with other coat protein complexes, the COPI operates in initiating membrane curvature for vesicle formation and cargo loading for sorting to the destined location. COPI vesicles operate in the retrograde transport where they recycle the ER- or Golgi-resident components back to where they belong. The coat protein complex I (COPI) is made up of seven subunits (Fig 2.14). This large heptameric coatomer is formed en bloc in

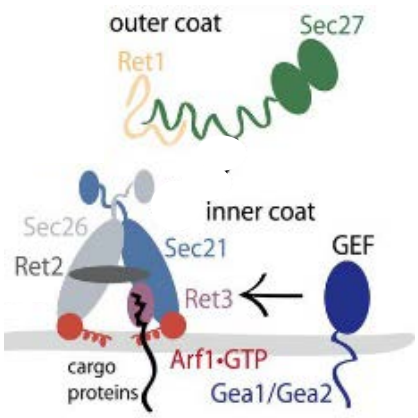


| | |
|---|---|
| Ret1/Cop1 | α-COP |
| Sec27 | β′-COP |
| Sec28 | ε-COP |
| Sec26 | β-COP |
| Ret2 | δ-COP |
| Sec21 | γ1-COP<br>γ2-COP |
| Ret3 | ζ1-COP<br>ζ2-COP |

**Figure 2.14: COPI subunits.**
(Adapted from Barlowe and Miller, 2013; Arakel and Schwappach, 2018)
The coat protein complex I (COPI) is made up of seven subunits, α-, β′-, and ε-COP form the outer putative cage and γ-, ζ-, β- and δ-COP subunits form the inner cargo-binding layer.

the cytoplasm from where it is recruited to the Golgi membrane (Hara-Kuge *et al.*, 1994). Although present in a single complex, the COPI structure resembles a clathrin-adaptor complex that can be dissected into an inner adaptor-like complex that interacts with the cargo and an outer cage-like shell providing mechanical shape to the vesicle (Lowe and Kreis, 1995). The reversible disassembly of the COPI hetero-oligomeric complex revealed the partial complex of α-, β′-, and ε-COP and direct interactions between γ- and ζ-COP as well as β- and δ-COP. α-, β′-, and ε-COP form the outer putative cage and γ-, ζ-, β- and δ-COP subunits form the inner cargo-binding layer.

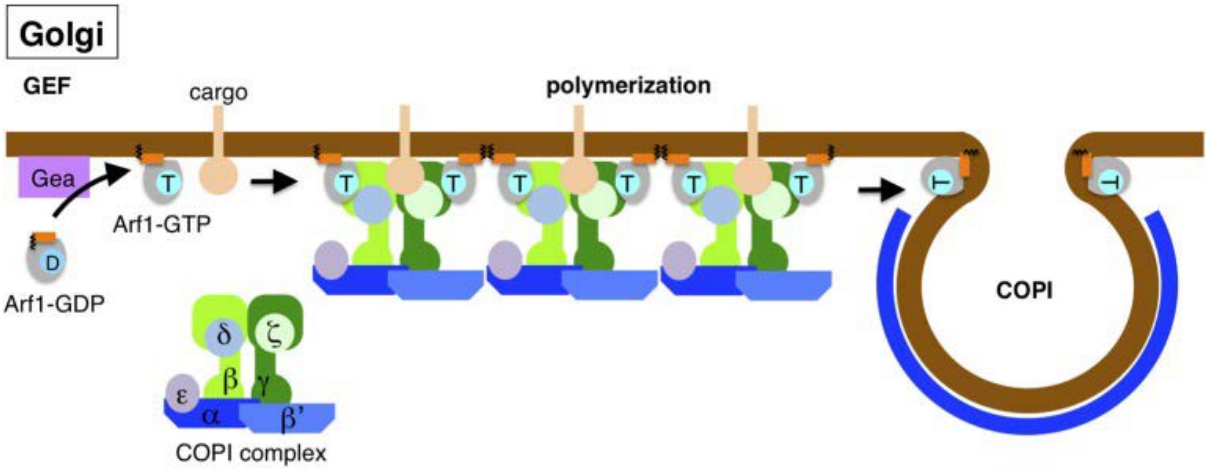


**Figure 2.15: Formation of COPI vesicle.**
(Adapted from Yorimitsu, Sato and Takeuchi, 2014)
Activation of Arf1 leads to recruitment and polymerization of the COPI coat complex with concomitant cargo loading.

The small GTPase Arf1 (ADP ribosylation factor) initiates COPI vesicles' formation on the Golgi membrane. Arf1 is activated by Guanine Exchange Factors (GEFs) that catalyze the exchange of GTP for GDP. Trans-Golgi localized Sec7 and cis-Golgi localized Gea1, which shares the conserved Sec7 domain, act as the GEFs for Arf1 for intra-Golgi and Golgi-ER retrograde transport, respectively recruited by the membrane-associated Arf1-GTP. Two molecules of activated Arf1 mediates bivalent interaction with the βδ/γζ-COP inner layer at the quasi-equivalent sites on the β-COP and γ-COP subunits. Polymerization of the Arf1 and COPI coat causes membrane curvature and vesicle bud formation (Fig 2.15). Studies in Briggs' lab showed three COPI heptamers (COPI triad) form the basic unit of the symmetrically linked flexible polyhedral cage structure (Fig 2.16). In the process of self-assembly, the coatomer binds to the cargo molecules.

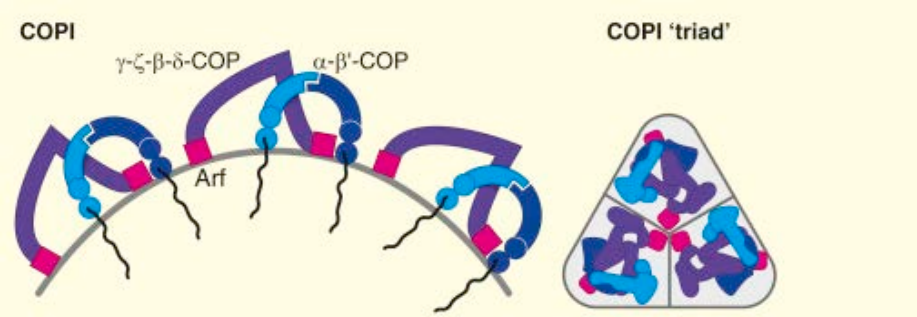


**Figure 2.16 COPI lattice.**
(Adapted from Gomez-Navarro and Miller, 2016)
Three COPI heptamers (COPI triad) form the basic unit of the symmetrically linked flexible polyhedral cage structure.

For transmembrane proteins, di-lysine (K) KKXX and KXKXX motifs on the cytoplasmic domains of the ER-resident proteins are recognized by the α- and β'-COP subunits of the COPI coat (Ma and Goldberg, 2013). COPI also recognize arginine (R) based ER- retrieval signals present on cytoplasmic domains of multimeric receptor or channel-forming proteins which bind at the interface between β- and δ-COP subunits (Zerangue *et al.*, 2001). Protein receptor Erd2 recognize canonical sorting signal K/HDEL present in the soluble luminal ER-destined cargoes and couple them to the COPI coat in a pH-dependent manner (Semenza *et al.*, 1990). The p24 family of proteins found in COPI vesicles recognize diaromatic residues in cargo proteins and

bind the γ-COP subunit of the inner COPI coat (Strating and Martens, 2009). Cargo adaptors such as Rer1, Vps74 and Erv41-46 complex (Shibuya *et al.*, 2015) bind to COPI coat and escaped ER cargo proteins, simultaneously loading them into the retrograde COPI cargo vesicles. The well-characterized multivalent cargo receptor, Rer1, is involved in the ER localization of Sar1 GEF, Sec12 and translocon components, Sec63 and Sec71, by interacting with their transmembrane domains (Sato, Sato and Nakano, 2001). The GOLPH3 (Golgi phosphoprotein 3) family protein Vps74 is involved in intra-Golgi sorting of glycosyltransferases into COPI vesicles (Eckert *et al.*, 2014).

The COPI vesicle formation ends with GTP hydrolysis and dissociation of Arf1 from the Golgi membrane. Arf1 lacks intrinsic GTPase activity; therefore, GTP hydrolysis depends on ArfGAPs (GTPase activating protein). Three mammalian ArfGAPs; ArfGAP1, ArfGAP2 and ArfGAP3 (Weimer *et al.*, 2008) and two yeast ArfGAPs; Gcs1 (ArfGAP1) and Glo3 (ArfGAP2) (Poon *et al.*, 1999) have been identified that catalyze GTP hydrolysis of Arf1. ArfGAP1 binds to the Arf1 bound to β-COP and is dependent on membrane curvature. It processes a lipid-packing sensor motif (Mesmin *et al.*, 2007) that recognizes highly curved membranes at the COPI triad's periphery. ArfGAP2, on the other hand, is COPI coatomer dependent and binds to Arf1 complexed with γ-COP at the centre of the COPI triad. Completion of COPI polymerization leads to vesicle scission (synchronized with GTP hydrolysis) at the site of negative membrane curvature and depends on the ability of Arf1 to dimerize and factors such as BARS (Brefeldin-A ADP-Ribosylated Substrate) (required in bud-neck constriction) and phosphatidic acid (required in bud-neck scission) (Beck *et al.*, 2011; Yang *et al.*, 2005, 2008).

Various Golgi-localized tethers tether the COPI-coated vesicles; Uso1, TRAPP II (trafficking protein particle II) complex and COG (conserved oligomeric Golgi) complex for intra-Golgi

COPI traffic, and ER-localized tether, the Dsl1 complex for Golgi to ER COPI trafficking (Guo *et al.*, 2008; Yamasaki *et al.*, 2009; Miller and Ungar, 2012).

## 2.7 Dsl1 Complex:

A vesicle originating from one compartment in order to fuse with the membrane of the target compartment requires a tethering complex (Chia and Gleeson, 2014) that associates with SNARE (soluble N-ethylmaleimide sensitive factor [NSF] attachment protein receptor) proteins localized on the recipient membrane and recognizes and captures the incoming vesicles. The tethers have binding sites on the vesicle-coat proteins and thus dock the vesicles bringing it closer to the membrane such that the v-SNARE on the vesicle membrane can interact with the t-SNAREs associated with the tethers on the target membrane to bring about fusion of the two lipid bilayers (Fig 2.17).

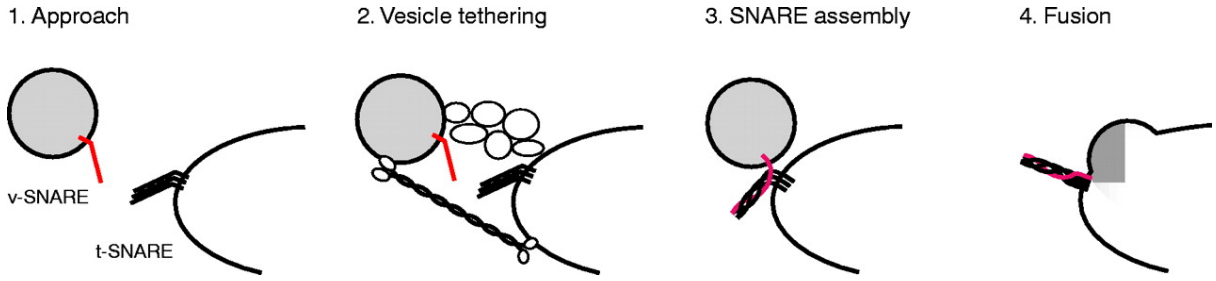


**Figure 2.17: Vesicle tethering.**
(Adapted from Whyte and Munro, 2002).
The schematic of vesicle tethering by coiled-coil tethers or multi-subunit complexes and subsequent fusion with the cognate target membrane.

Tethers are peripheral membrane proteins that are recruited to rapidly establish subdomains on the membranes. Tethers fall under one of the two categories: long coiled-coil proteins or multi-subunit tethering complexes (MTCs) (Gillingham and Munro, 2003; Bröcker, Engelbrecht-Vandré and Ungermann, 2010). Coiled-coil tethers are large rod-like structures comprising of two globular head domains and a long coiled-coil domain. They are hydrophilic and homo-dimeric that can capture vesicles over long distances of ~200nm. They are primarily present

on Golgi apparatus and are called Golgins; they involve capturing vesicles, homotypic membrane tethering of the Golgi cisterna, matrix formation or scaffold formation for the assembly of other tethering factors. Some coiled-coil tethers like EEA1 are also found on endosomes. On the other hand, MTCs form a complex of 3-10 protein subunits, forming a bulky tether of ~250-800 kDa that capture vesicles over a shorter range of apposing compartments. MTCs functioning in the secretory pathway are collectively termed as complexes associated with tethering containing helical rods (CATCHR) and comprises of the Dsl1 complex, COG (conserved oligomeric Golgi) complex, GARP (Golgi-associated retrograde protein) complex and the exocyst. Another class of MTCs function in the endo-lysosomal pathway and comprises class C vacuolar protein sorting (Vps) complexes, HOPS (homotypic fusion and vacuole protein sorting) complex and CORVET (class C core vacuole/endosome tethering) complex. The TRAPP complex is also a multi-subunit complex that functions in the anterograde ER-Golgi, intra-Golgi and retrograde endosome-TGN (trans Golgi network) trafficking.

Dsl1 complex is the simplest known CATCHR (Spang, 2012), comprising three subunits, namely Dsl1, Dsl3 and Tip20. It is known to function in the ER-Golgi interface and tether retrograde COPI vesicles. Tip20 (SEC twenty interacting protein) was the first to be discovered as an 80 kDa cytosolic factor that physically interacted with the 50 kDa integral membrane glycoprotein, Sec20 (Sweet and Pelham, 1993). Tip20 showed similar functions as the ER-localized, Sec20 (Sweet and Pelham, 1992) in the early secretory pathway. Further, both the proteins were shown to be involved in retrieving proteins with a di-lysine signal sequence from Golgi to ER (Cosson *et al.*, 1997). Dsl1 (Dependence on SLy1-20) was later identified by different studies to play an essential role in assisting retrograde Golgi to ER transport (VanRheenen *et al.*, 2001; Reilly *et al.*, 2001; Andag, Neumann and Schmitt, 2001). The 88 kDa essential protein, Dsl1, was first isolated in a screen where its mutation was suppressed by

the SLY1-20 mutant form of Sly1 (t-SNARE-interacting proteins involved in ER to Golgi traffic). Dsl1 mutations caused defects in retrieving ER-resident SNARE proteins, di-lysine motif bearing integral membrane proteins and soluble proteins such as BiP/Kar2p bearing the ER signal sequence, HDEL. Dsl1 co-immunoprecipitated with Tip20/Sec20 complex that further bind to ER t-SNARE Ufe1. Dsl1 was shown to interact with the δ-subunit of the COPI coat, Ret2p and Dsl1 mutation was strongly suppressed by dominant overexpression of the γ-subunit of the COPI coat, Sec21. These findings indicated that the Dsl1, Tip20, Sec20 and Ufe1 function in the retrograde Golgi to ER transport. The third member of the Dsl1 multi-subunit tether complex, Dsl3/Sec39, was first picked up in a genome-wide screen for essential genes required in the ER-Golgi trafficking (Mnaimneh *et al.*, 2004) and later found to interact with Dsl1 in a two-hybrid assay (Kraynack *et al.*, 2005). Further, Dsl3 was shown to bind the ER-localized SNARE protein Use1, forming part of the Dsl1 complex (Fig 2.18).

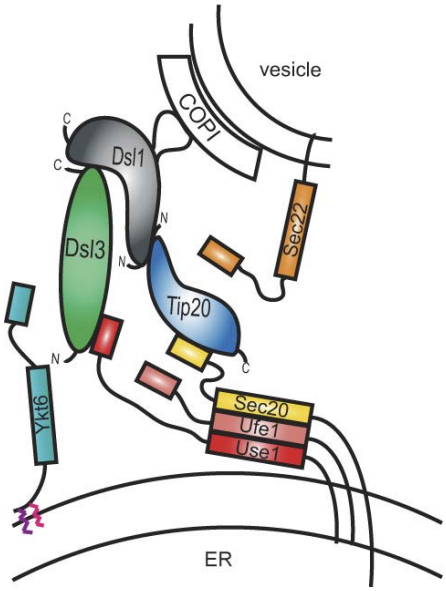


**Figure 2.18: Dsl1 multi-subunit tethering complex.**
(Adapted from Meiringer *et al.*, 2011)
Schematic representation of the Dsl1 complex forming a bridge between the ER-localized SNAREs and COPI vesicle.

N-terminal domains of ER-localized SNAREs, Use1 and Sec20, are associated with N-terminus of Dsl3 and C-terminus of Tip20. Ufe1 does not bind to any member of the Dsl1

complex directly. The two R-SNAREs, Ykt6 and Sec22, also associates with the Dsl1 complex; the non-essential Sec22 acts as the v-SNARE present on COPI while Ykt6 association occurs prior and implicated to have a regulatory role. Studies from Hughson lab have expounded the structure of the Dsl3-Dsl1-Tip20 ternary complex (Tripathi *et al.*, 2009). Tip20 and Dsl3 do not exhibit a direct interacting site but are linked by Dsl1. The Dsl1-N binds to the N-terminus of the Tip20, and Dsl1-C binds to the two C-terminal helices of Sec39/Dsl3. The middle section of the Dsl1p contains a disordered region that forms a flexible lasso loop-like structure reported to harbour interaction sites that bind to α- and δ- COPI coat subunits mediating vesicle recognition and tethering. The binding sites are, however, too close for binding both the subunits at the same time. Possibly, Dsl1 initially interacts with α-COPI that forms part of the outer shell of the coatomer. Moreover, experiments in Schmitt lab showed the interaction site on α-COPI is shared by Dsl1 and other subunits of the COPI coatomer, like ε-COPI (Eugster *et al.*, 2000). Therefore, the binding of Dsl1 impedes the integrity of the COPI coat. Accumulation of coated vesicles is seen in Dsl1 mutants that are unable to bind α-COPI. Dsl1 later interacts with δ-COP that forms part of the coatomer's inner shell and is involved in cargo loading (Michelsen *et al.*, 2007). This binding leads to destabilization and disassociation of the cargo proteins and coat proteins. Uncoating expose the embedded v-SNARE on the vesicle that pair to its cognate t-SNAREs leading to vesicle fusion to the target membrane (Fig 2.19).

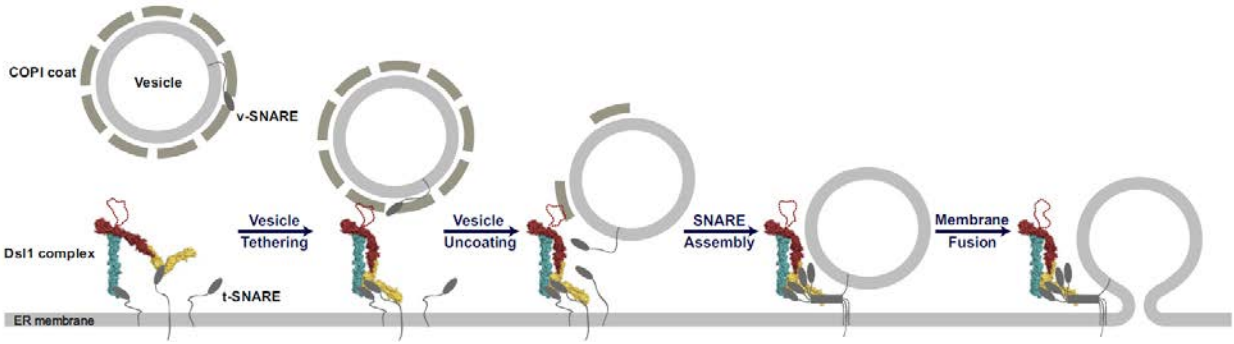


**Figure 2.19: The Dsl1 complex function.**
(Adapted from Ren *et al.*, 2009; Zink *et al.*, 2009)
The Dsl1 complex functions in orchestrating COPI vesicle tethering, disassembly of the COPI coat and its fusion with the ER membrane.

The Dsl1 complex forms a tower-structure with Dsl1 at its apex and Tip20 and Dsl3 forming the two pillars connecting with Sec20 (Qb SNARE) and Use1 (Qc SNARE) anchored at its base. Due to the flexible hinge region in the Dsl1, the legs formed by Dsl3 and Tip20 can attain different conformations simultaneously assisting vesicle capture and positioning the SNAREs into close assembly (Schmitt and Jahn, 2009; Diefenbacher, Thorsteinsdottir and Spang, 2011). The Dsl1 complex recruits the ER-localized SNAREs and accelerates their assembly kinetics. A SNARE protein consists of three domains; the variable N-terminal domain, the central SNARE domain and the C-terminal transmembrane domain (Rothman, 1994). Most v-SNAREs residing on the vesicle membrane contain an arginine residue in their SNARE domain, whereas t-SNAREs on the target organelle contain glutamine or aspartate residue. Hence, they are classified as R-SNAREs and Q-SNAREs, respectively (Fasshauer *et al.*, 1998). The Q-SNAREs are further classified into Qa, Qb and Qc. The Dsl1 complex associates with Qb-Sec20 and Qc-Use1. The SM (Sec1/Munc18) protein Sly1 collaborates with the Qa SNARE Ufe1 (Rizo and Südhof, 2012). As the R-SNARE Sec22 from the COPI vesicle approach, it initially binds to the Sly1-bound Qa-SNARE Ufe1. The Dsl1 complex attains a closed parallel position bringing the Qb-Sec20 and Qc-Use1 close to Qa-Ufe1 and R-SNARE

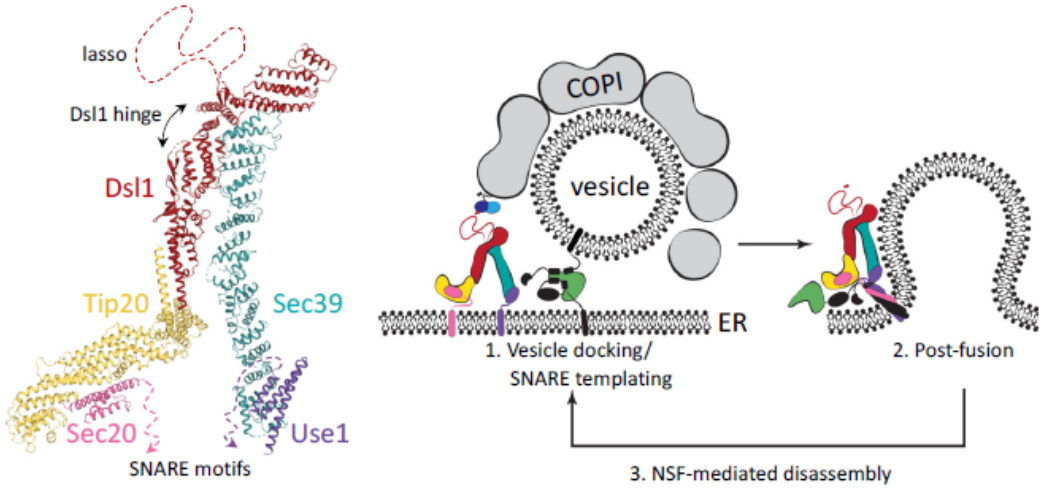


**Figure 2.20: Dsl1 complex association with ER-localized SNAREs.**
(Adapted from Travis *et al.*, 2020)
The Dsl1 complex forms a tower-structure with Dsl1 at its apex linking Tip20 and Dsl3 that form the two pillars connecting with Qb-Sec20 and Qc -Use1 at its base, respectively, positioning the SNAREs into close assembly.

Sec22 such that all the four components engage in a tight trans- SNARE complex with their SNARE domains and form a coiled-coil helix (Ungermann and Langosch, 2005) called a SNAREpin that zipper up the two opposing membranes (Fig 2.20). The binding enthalpy released due to SNARE complex formation is enough to overcome the energy barrier required to create membrane instability and fusion. Initially, a hemifusion intermediate is formed, followed by the complete merging of the bilayer lipid. The resultant single membrane contains the cis-SNARE complex that is disassembled by AAA type ATPase Sec18 (NSF) and its cofactor Sec17 (α -SNAP), freeing the SNAREs for further cycles of membrane fusion (Mayer, Wickner and Haas, 1996).

The mammalian counterpart of the Dsl1 complex is called the NRZ complex; NAG (Sec39/Dsl3), RINT1 (Tip20) and ZW10 (Dsl1), although the amino acid sequence homology among the proteins is low. ZW10 and RINT1 were first identified along with Syntaxin18 (Ufe1), the ER-associated SNARE in an immunoaffinity pool. The NRZ complex is also similarly associated with ER-localized SNAREs, Syntaxin18 (Ufe1), BNIP1 (Sec20), p31 (Use1/Slt1), and Sec22b (Sec22). Interesting, the mammalian Dsl1 complex participates in membrane trafficking and have actively associated roles in different cellular processes such as cell cycle and autophagy (Tagaya *et al.*, 2014) (Fig 2.21).

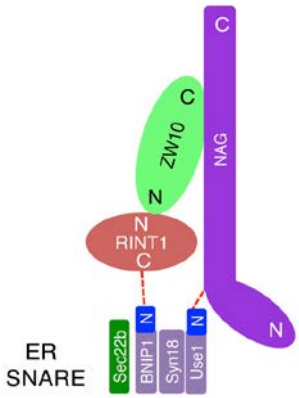


**Figure 2.21: The NRZ complex.**
(Adapted from Tagaya *et al.*, 2014)
The mammalian counterpart of the Dsl1 complex; NAG (Sec39/Dsl3), RINT1 (Tip20) and ZW10 (Dsl1) associated with SNAREs, Syntaxin18 (Ufe1), BNIP1 (Sec20), p31 (Use1/Slt1), and Sec22b (Sec22).

## 2.8 Exosomes

Two groups discovered exosomes in 1983 (Harding, Heuser and Stahl, 1983; Pan and Johnstone, 1983). They showed that transferrin receptors were externalized in small ~50-70 nm vesicles in maturing red blood cells or reticulocytes. The name of these extracellular vesicles was coined exosomes by Rose Johnstone. These vesicles are mediators of extracellular communication through the exchange of proteins, lipids and nucleic acids. Exosomes confer a wide array of functions in immune response, neural signalling, pathogen transmission and cancer. Exosomes have also recently been utilized as drug delivery agents.

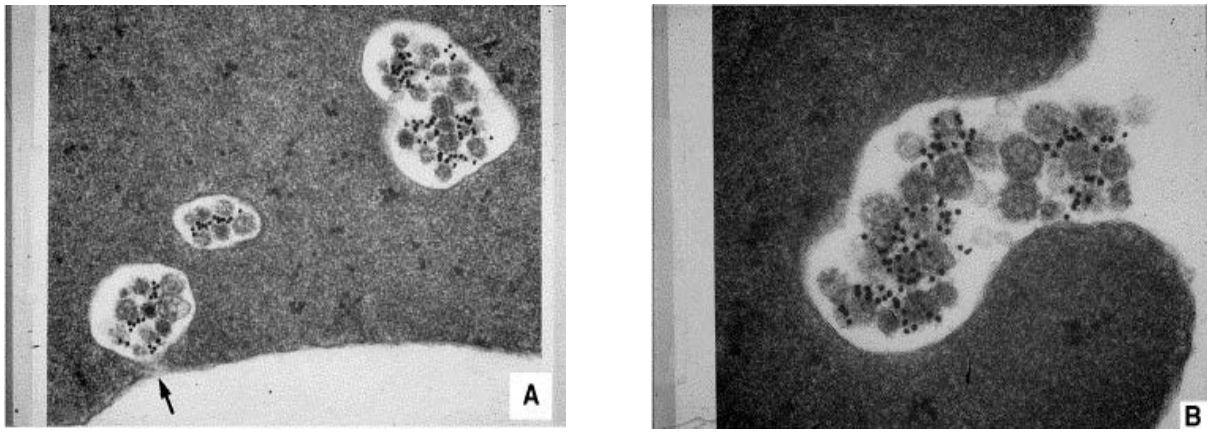


**Figure 2.20: Electron micrograph of exosomes.**
(Data from Johnstone, 2005)
Exosomes are extracellular vesicles ranging from 30-100nm in size formed inside a multivesicular body (MVB) as intraluminal vesicles (ILVs) (A) and are released into the extracellular milieu upon fusion of the MVBs with the plasma membrane (B). They are taken up by other cells where they release their biologically active molecules (such as nucleic acids, proteins or lipids) and bring about phenotypic changes.

### 2.8.1 Exosome biogenesis:

The biogenesis of exosomes begins along the endosomal sorting pathway. Early endosomes sort and sequester membrane proteins, lipids and cytosol (containing mRNA and soluble proteins) in vesicles formed by inward budding of the endosomal membrane. These vesicles are known as intraluminal vesicles (ILVs) that accumulate in the endosomal lumen as it matures into a multivesicular body (MVB). The MVBs either fuse to lysosomes to degrade

their contents or fuse with the plasma membrane to release exosomes (Klumperman and Raposo, 2014). Multiple ways of formation of MVBs have been described in the literature. Depletion of ESCRT (Endosomal sorting Complex Required for Transport) machinery components HRS, STAM1 and TSG101 affected exosome secretion (Tamai *et al.*, 2010; Colombo *et al.*, 2013). The ESCRT component, ALIX, assists intraluminal budding in endosomes by interacting with the syndecan heparan sulphate proteoglycan adaptor, syntenin (Baietti *et al.*, 2012). Moreover, TSG101 and ALIX are also present in exosomes (Théry *et al.*, 2001). The ESCRT machinery comprises four complexes (Schmidt and Teis, 2012); ESCRT-0 assembles on the endosomal membrane, sorts ubiquitinated proteins and recruits ESCRT-1, which in turn recruits ESCRT-II; both of which sorts cargo and is responsible for membrane deformation into bud formation. ESCRT-III transiently assembles and brings about vesicle scission. Later the AAA-ATPase, Vps4, is recruited to catalyze disassembly of ESCRT machinery. MVB biogenesis could progress in the absence of crucial subunits of each ESCRT complex (Stuffers *et al.*, 2009). Ceramide is formed by hydrolysis of sphingomyelin by neutral sphingomyelinase (nSMase), and inhibition of nSMase leads to a decrease in exosome release. Further ceramide enrichment in exosomes implicated its role in exosomes' biogenesis (Trajkovic *et al.*, 2008). Similarly, ARF6 and its effector phospholipase D2 (PLD2) hydrolyses phosphatidylcholine to phosphatidic acid that induces the formation of ILVs (Ghossoub *et al.*, 2014). Moreover, tetraspanins that are selectively enriched in exosomes, such as CD63, are shown to function in cargo sorting in ILVs for secretion in exosomes independent of ESCRT machinery, mainly sorting cargo for lysosomal degradation (van Niel *et al.*, 2011) (Fig 2.23).

### 2.8.2 Exosome Secretion:

Various Rab GTPases are involved in the trafficking of MVBs. Rab11, along with Calcium, mediates docking and homotypic fusion of MVBs (Savina *et al.*, 2005). Inhibition of Rab35 causes accumulation of endosomal vesicles and inhibited exosome secretion, implicating the

role of Rab35 in tethering of MVB (Hsu *et al.*, 2010). Both Rab11 and Rab35 were involved in the transport of early endosomes or MVBs. Rab27a/b isoforms function in MVB transport to the plasma membrane. The RNAi screen identified the proteins and showed silencing of Rab27a and Rab27b caused MVB enlargement and localization to the perinuclear region. Also,

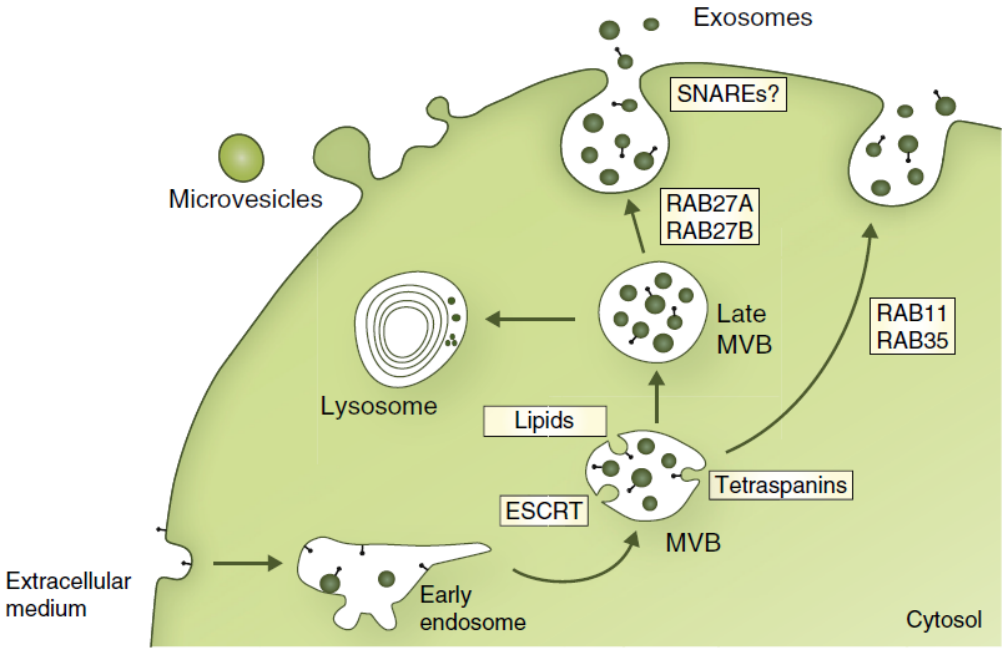


depletion of Rab27 effectors impaired exosome secretion (Ostrowski *et al.*, 2010) (Fig 2.8.2).

**Figure 2.21: Exosome biogenesis and secretion.**
(Adapted from Kowal, Tkach and Théry, 2014)
The ESCRT machinery, lipids and the tetraspanins are involved in the biogenesis of ILVs while Rab GTPases direct MVBs to the plasma membrane.

### 2.8.3 Exosome Uptake:

Methods of exosome internalization are highly debated. Sometimes internalization is not required when exosomes contain surface proteins that induce signal transduction in the target cells. Exosomal proteins interact with cell membrane receptors for signalling as well as allowing internalization. 'Tetraspanins' such as Tspan8 complexed with integrin α4 on exosome binds to CD54 ligand on the cell surface for uptake (Rana *et al.*, 2012). Blocking 'integrins' like αv and β3 on dendritic cells decrease exosome uptake (Morelli *et al.*, 2004). Exosomes co-localized with cell surface heparin sulphate 'Proteoglycans' (HSPG), and its depletion reduced

exosome uptake (Christianson *et al.*, 2013). Inhibition of Dynamin GTPase or administering Chlorpromazine impairs the formation of clathrin-coated vesicles inhibiting the exosome uptake implicating the role of clathrin-mediated endocytosis of exosomes (Tian *et al.*, 2014). One group has shown an association of exosome with lipid rafts where its uptake is negatively regulated by CAV1 (Svensson *et al.*, 2013). Another study showed knockout of CAV-1 suppressed exosome internalization (Nanbo *et al.*, 2013), contradicting the role of caveolin mediated endocytosis in exosome uptake. One report suggested that exosomes were more readily uptaken by phagocytes via phagocytosis and not by caveolae, clathrin or micropinocytosis, and the process was dependent upon actin and phosphatidylinositol 3-kinase (Feng *et al.*, 2010). The exosomes were sorted into phagolysosomes shown by co-localization with phagocytosed latex beads. This internalization method was mostly speculated for clearance of exosomes rather than utilizing its contents (McKelvey *et al.*, 2015). Exosomes could fuse with the target cell in a pH-dependent manner observed via the fluorescent lipid dequenching method (Parolini *et al.*, 2009).

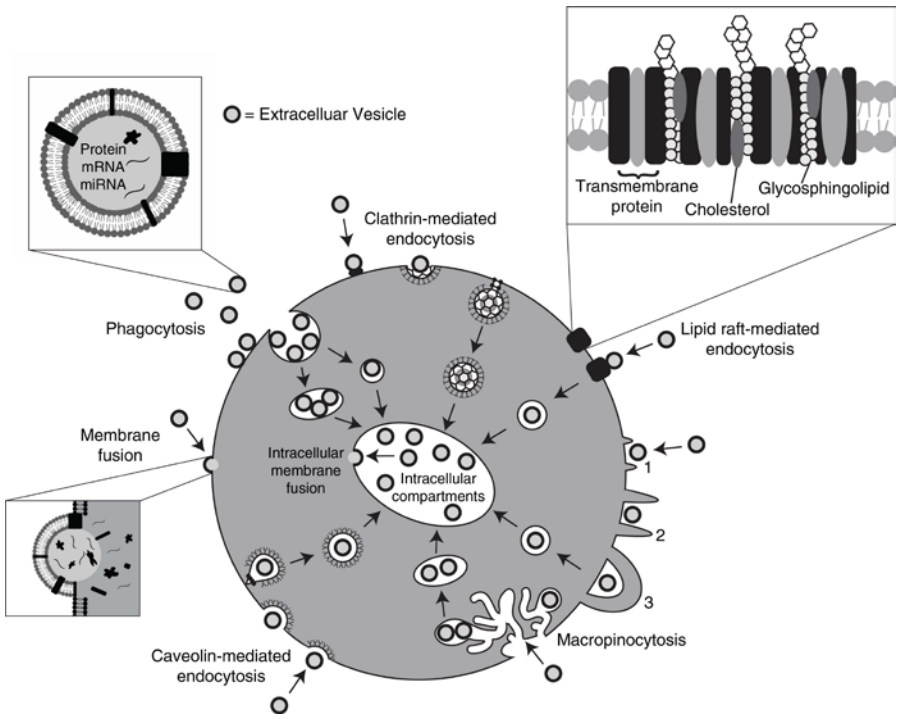


**Figure 2.22: Exosome uptake mechanisms.**
(Adapted from Mulcahy, Pink and Carter, 2014)
Schematic of the different endocytic pathways proposed to function in the exosome uptake.

# 3. Materials and Methods

## 3.1 Molecular Biology Methods

**Host:** *Escherichia coli*

**Strain:** DH5α

**Luria Bertani (LB) broth**: 20g LB powder (HI Media) is dissolved in Milli-Q with the final volume adjusted to 1 litre and autoclaved. For making LB-agar plates, 20g bacteriological grade agar powder (HI Media) is added. The mixture is autoclaved, cooled to 55-60$^{o}$ C (for the addition of antibiotics), poured in 90 mm sterile petri-plates and stored at 4$^{o}$C after solidification.

**Antibiotic Selection:** Final concentrations of 50µg/ml Ampicillin (HI Media) and 30µg/ml Kanamycin (HI Media) are used in LB media.

### 3.1.1 Preparation of ultra-competent E. coli:

DH5α was made ultra-competent for the transformation of recombinant and routine plasmid vectors for high cloning efficiency.

**Super-Optimal Broth (SOB)**: 2% Peptone (Bacteriological) (HI Media), 0.5% yeast extract (HI Media), 10mM NaCl (Fisher Scientific), 2.5mM KCl (SDFCL), 10mM MgCl2 (Merck), 10mM MgSO4 (Merck) is dissolved in Mill-Q and autoclaved.

**Super-Optimal Catabolite (SOC) Media**: To 98ml of sterile SOB, add sterilized 2M glucose (HI Media) and 2M MgCl2.

**Transformation Buffer (TB):** 10mM PIPES (Sigma), 15mM $CaCl_2$ (SDFCL) and 250mM KCl (SDFCL) is dissolved in Milli-Q and adjusted to pH 6.7 with 5N KOH (SDFCL). 55mM MnCl2 was added and sterilized by passing it through 0.2µm membrane filter.

**Protocol:** E. coli DH5α cells from frozen glycerol stock are streaked on an LB agar plate and incubated overnight at 37$^{o}$C (~16 hrs). A single colony is inoculated in 250ml SOB media and incubated in a refrigerated shaker incubator with 200 RPM at 18$^{o}$C until $OD_{600}$ reaches 0.4-0.5.

The culture is incubated on ice for 10 minutes and spun at 2500 x g (3500 RPM) for 10 minutes at 4$^{o}$C. The pellet is resuspended very gently in 80ml of ice-cold transformation buffer and again kept on ice for another 10 minutes. The mixture is spun at 2500 x g (3500 RPM) for 10 minutes at 4$^{o}$C. The pellet is resuspended gently in 20 ml of ice-cold transformation buffer and incubated on ice for 10 minutes. Dimethyl sulfoxide (DMSO) (Sigma) is added to a final concentration of 7% (1.4 ml) to the cell suspension in transformation buffer and mixed gently and thoroughly. 100µl aliquot of cells is prepared in vials that are snap-frozen using liquid nitrogen and stored at -80$^{o}$C.

### 3.1.2 Bacterial Transformation (Inoue, Nojima and Okayama, 1990)

Ultra-competent DH5α cells (100µL aliquot) stored in -80˚C were taken and kept for thawing on ice. 10µl (50-100 ng) of DNA sample is added to the cells. Cells are incubated on ice for 10 minutes. The cells were subjected to heat shock at 42$^{o}$C for 45 seconds and placed on ice immediately for 5 minutes. 200µl of ice-cold SOC medium is added to the cells aseptically. The cells are incubated at 37$^{o}$C with shaking at 200 RPM for 30 minutes. The cells are plated on an LB agar plate with required antibiotic selection and incubated at 37$^{o}$C for 16 hours for colonies to appear.

### 3.1.3 Plasmid DNA isolation

Different methods are used to isolate plasmid DNA.

#### 3.1.3.1: Plasmid Miniprep kit

**Reagent**: Thermo scientific GeneJET Plasmid Miniprep Kit; as per the manufacturer's protocol The kit utilizes a silica-based membrane on a convenient spin column that binds up to 20µg of high copy plasmid DNA molecules at a high salt concentration and allows the adsorbed DNA to be eluted in a small volume of low-salt buffer. The pure plasmid is used for downstream

molecular biology techniques such as PCR, digestion using restriction enzymes, cloning, and sequencing.

**Protocol**: A single bacterial colony is inoculated in 10ml of LB selection (with required antibiotic) media and incubated at 37$^{o}$C for 16 hours at 180 RPM shaker incubator. The bacterial culture is harvested at room temperature for 10 minutes at 5000 RPM. The pellet is vortexed briefly, resuspended in 250µl of Resuspension Buffer (with added RNase A) and transferred to a microcentrifuge tube. 250µl of Lysis Solution is added, and the tube is slowly inverted a few times until the mixture becomes slimy. 350µl of Neutralization Solution is added immediately, and the tube is again inverted few times until the mixture turns white. The lysate is spun at 13,000 RPM for 10 minutes. The clear supernatant is added to the spin column and spun for 1 minute at 13,000 RPM. The flow-through is discarded from the collection tube, and 500µl of Wash Solution (with added Ethanol) is added and spun for 1 minute to remove contaminants. The collection tube is replaced with a new dry one and spun at 13000 RPM for 1 minute to remove any residual alcohol. The column is placed on a clean microcentrifuge tube, and 50µl of pre-heated Elution Buffer or Milli-Q is added to the centre of the column. The column is led to stand for 1minute and centrifuged for 1 minute at 14000 RPM to elute pure plasmid DNA.

### 3.1.3.2: Plasmid DNA isolation using TELT buffer

This method is cost-effective and comparatively quick, and straightforward and regularly used in screening for positive clones from cloning experiments.

**TELT buffer preparation**: 50mM Tris-Cl (Sigma) pH 7.5, 62.5mM EDTA (Fischer Scientific) pH 8, 0.4% Triton X100 (Sigma) and 2.5M LiCl (Sigma) is added and made in autoclaved Milli-Q.

**TE Buffer preparation**: 0.5M EDTA pH 8 and 1M Tris-Cl pH 8 is added and made in autoclaved Milli-Q.

**Protocol**: A single bacterial colony is inoculated in 1.5ml of LB-antibiotic (Amp/Kana) media and incubated at 37$^{o}$C for 16 hours at 180 RPM. The bacterial culture is harvested at 14000 RPM for 1 minute. The pellet is resuspended in 150µl TELT Buffer and vortexed briefly. 5µl of 50mg/ml lysozyme is added, mixed and kept on a dry bath at 99$^{o}$C for 1 minute. The mixture is placed on ice for 10 minutes and spun at 14000 RPM for 10 minutes. The sticky pellet is removed using a toothpick. 330µl of ice-cold absolute ethanol is added to the supernatant, mixed well and incubated at -80$^{o}$C for 30 minutes. The mixture is centrifuged at 14000 RPM for 10 minutes. The supernatant is discarded. 200µl 70% ethanol is added for washing the DNA pellet and centrifuged at 14000 RPM for 5min. The pellet is dried by removing all the remaining alcohol and resuspended it in 30µl TE buffer or Milli-Q.

### 3.1.3.3: Plasmid Preparation using Cesium Chloride

**Solution I**: 50mM Glucose, 25mM Tris, 10mM EDTA in Milli-Q.

**Solution II**: 10N NaOH (SRL), 10% SDS (Sigma) in Milli-Q

**Solution III**: 5M Potassium Acetate (HI Media), Glacial Acetic Acid (MP) in Milli-Q

**Protocol**: A single bacterial colony is inoculated in 5ml of LB media added with antibiotic (Amp/Kana) and incubated at 37$^{o}$C for 16 hours at 180 RPM in a shaker incubator. The primary culture is added to 500ml of LB (Amp/Kana) and incubated at 37$^{o}$C for 16 hours at 180 RPM in a shaker incubator. The culture is spun at 5000 RPM for 10 minutes at 4$^{o}$C. The pellet is resuspended in 18ml of Solution I and vortexed briefly. 2ml of 50mg/ml lysozyme is added, mixed well and incubated at room temperature for 5 minutes. 40ml of Solution II is added and mixed by inverting few times slowly. 20ml of ice-cold Solution III was added, mixed and incubated on ice for 10 minutes. The mixture is centrifuged at 5000 RPM for 15 minutes at

4ºC. The supernatant was filtered using cotton gauze and 0.8 volumes of isopropanol (SDFCL). The mixture was spun at 8000 RPM for 15 minutes at 4ºC. The pellet is washed with 70% ethanol (Merck) by spinning at 8000 RPM at 4ºC for 10 minutes. The dried pellet is dissolved in an appropriate TE (8.5 ml) volume and an equal weight of Cesium Chloride (HI Media) (8.5g) and incubated for 5 minutes until the solution is clear. 250µl of 10mg/ml EtBr (HI Media) is added, mixed and spun at 8000 RPM for 10 minutes. The solution was loaded in ultracentrifuge tubes and spun in 90 Ti rotor for 22 hours at 60,000 RPM at room temperature. The band is pulled by placing the needle at the lower side of the band. An equal volume of water-saturated butanol is added, vortexed and spun at 3000 rpm for 2 minutes. The upper layer of butanol is discarded, and fresh butanol (SDFCL) is added, and the mixture was centrifuged. This step is repeated until both the layers become colourless. Twice the volume of Milli-Q and 6 volumes of absolute ethanol are added and incubated at 4ºC for 30 minutes. The mixture is spun at 8000 RPM at 4ºC for 15 minutes. The pellet is kept for drying and dissolved in 500µl Milli-Q.

### 3.1.4 Agarose gel electrophoresis

Agarose gel electrophoresis is a routinely used method for the analysis of DNA samples. DNA fragments can be separated based on their size using different concentrations of agarose gels.

**Ethidium bromide**: 10 mg/ml

**6X Gel loading dye:** 1.2ml glycerol (SRL), 1.2ml 0.3mM EDTA, 300µl of 20% SDS, 160µl of 0.5% Bromophenol blue stock made in nuclease free water to a final volume of 10ml.

**Sodium Borate (SB) Buffer**: 10mM NaOH adjusted to pH 8.5 with boric acid for 1X SB buffer. This buffer is used for faster separation of DNA fragments on agarose gel under high voltage.

**Tris-Acetate-EDTA (TAE) Buffer**: 40mM Tris base, 2mM EDTA, 20mM Acetic acid, adjusted pH 8.5 for 50X TAE buffer and diluted to 1X Milli-Q.

Agarose powder is weighted according to the percentage of gels (generally 0.6% - 2%), which depends on DNA fragments' size. The mixture is boiled until agarose powder dissolves entirely and subsequently cooled down to about 60$^{o}$C. Ethidium bromide (intercalates in the DNA molecule and absorbs UV light to fluoresce, making DNA visible) is added at a final concentration of 1µg/ml and mixed well. The mixture is poured into the gel tray. A comb is placed to create wells. Once the gel is solidified, the comb is removed. 1X SB / TAE buffer (running buffer) is poured into the tank containing the agarose gel. 6X gel loading dye is added to the DNA samples (Plasmid DNA, genomic DNA, PCR fragments, restriction digestion fragments) to make a final concentration of 1X. Standard 1Kb or 100bp ladders are used as molecular weight markers and run parallel to understand the size of DNA fragments being analyzed. DNA bands were visualized using a gel documentation system.

### 3.1.5 Polymerase chain reaction (PCR)

The technique is used to amplify specific DNA sequences from template DNA (yeast genomic DNA / plasmid DNA / cDNA) using two oligonucleotide sequences or primers that specifically bind to the opposite strands of DNA by complementary base pairing. A thermostable DNA polymerase is used to extend the primers from 5' to 3' direction. High fidelity DNA polymerase enzyme, Phusion is used for the PCR amplification process.

| | **Components** | **Final concentration** |
|---|---|---|
| 1 | H2O | To make up the volume |
| 2 | 5X buffer HF/GC | 1X |

| | | |
|---|---|---|
| 3 | 10mM dNTP mixture | 200 µM |
| 4 | Forward primer (100µM) | 0.5 µM |
| 5 | Reverse primer (100µM) | 0.5 µM |
| 6 | Template DNA | 50ng (Plasmid DNA)<br>100ng (Genomic DNA) |
| 7 | DNA Polymerase | 0.02 U/µl |

**Table 1: Contents of PCR reaction**

The samples are thawed on ice, and the reagents are added as per the order stated in the table. The mixture is quickly subjected to a thermocycler preheated to the denaturation temperature (98°C) to start the reaction. The PCR product is checked on agarose gel for the desired band.

| **Step** | **Temperature** | **Time** | **Cycle** |
|---|---|---|---|
| Initial denaturation | 98 ˚C | 2 minutes | 1 |
| Denaturation | 98 ˚C | 30 seconds | 30-35 |
| Annealing | Lower Tm +3 | 1 minute | |
| Extension | 72 ˚C | 1 minute/kb | |
| Final Extension | 72 ˚C | 8 minutes | 1 |
| Hold | 4 ˚C | forever | |

**Table 2: PCR cycle parameters**

### 3.1.6 **Quick change / Site-directed mutagenesis** (Liu and Naismith, 2008)

This technique introduces point mutation, insertion or deletion of a few bases using primers in a gene of interest with high fidelity Pfu Turbo polymerase. Oligo mix is prepared by mixing 5µl of each forward and reverse primers (from 100µM stock) and 40µl of Milli-Q (1:10 dilution).

The reaction set up is as follows (20µl mix):

| | **Components** | **Final concentration** |
|---|---|---|
| 1 | H2O | 15.3µl |
| 2 | 10X buffer for PfuTurbo | 2µl |
| 3 | 10mM dNTP mixture | 0.4µl |
| 4 | Primer mix | 0.4µl |
| 5 | Template DNA (50ng/ µl) | 1µl |
| 7 | DNA Polymerase | 0.4µl |

**Table 3: Contents of PCR reaction for site-directed mutagenesis**

| **Step** | **Temperature** | **Time** | **Cycle** |
|---|---|---|---|
| Initial denaturation | 95 ˚C | 2 minutes | 1 |
| Denaturation | 95 ˚C | 30 seconds | 18 |
| Annealing | 55 ˚C | 1 minute | |

| | | | |
|---|---|---|---|
| Extension | 68 ˚C | 2 minutes / kb | |
| Final Extension | 68 ˚C | 8 minutes | 1 |
| Hold | 4 ˚C | forever | |

**Table 4: Cycling conditions for PCR for site-directed mutagenesis**

0.8µl of DpnI restriction enzyme is added to the mutagenized PCR sample and incubated for 3 hours at 37$^{o}$C. DpnI selectively cleaves the parental DNA by recognizing methylated adenine sites. The mixture is then transformed into ultra-competent DH5α *E. coli* cells to remove concatemers formed during multiple cycles of PCR. Colonies obtained are screened for mutagenesis.

### 3.1.7 Gene Cloning (Higuchi *et al.*, 1976)

In the cloning procedure, the gene of interest is amplified through PCR (insert) and cleaved with one or more restriction enzymes (RE) to get blunt/cohesive ends creating compatible ends with a suitable vector plasmid digested with the same set of enzymes. For vectors, 1µl of alkaline phosphatase is added after restriction enzyme digestion and incubate for another 1 hour (Alkaline Phosphatase removes the 5'-phosphate group of DNA from both the termini of the digested vector to avoid the self-ligation of the vector). Both the insert and vector can be ligated using the T4 DNA Ligase enzyme that catalyzes phosphodiester bond formation. The ligated heterogeneous mix is then transformed into a bacterial host under selective antibiotic pressure to propagate the clones. The resulting transformed clones are then screened by RE digestion or PCR to confirm the recombinant clone.

#### 3.1.7.1: Restriction Digestion

Restriction enzymes or restriction endonucleases cut at a specific site in the template DNA. The components of preparative and analytical restriction digestion reaction are as follows:

| Components | Preparative | Analytical |
|---|---|---|
| Plasmid DNA | 2-3µg | 300ng |
| $H_2O$ | To make up the volume | To make up the volume |
| 10X buffer | 1X | 1X |
| Restriction Enzyme | 10U | 1U |

**Table 5: Content of Restriction Enzyme Digestion reaction**

All the components are added in a microcentrifuge, briefly vortexed and given a short spin. The mixture was incubated at 37˚C (or at any other temperature if explicitly mentioned for a particular enzyme) for 3-8 hours. The digested DNA fragment is visualized and analyzed on an agarose gel.

### 3.1.7.2: Purification of digested DNA or PCR product

For cloning digested DNA fragments (either vector or insert), it is vital to remove nucleotides, primers, enzymes, mineral oil, salts, agarose, ethidium bromide, and other impurities from DNA samples during all cloning procedures.

**Reagents**: Nucleotide removal kit (Qiagen); as per the manufacturer's protocol

Columns contain a silica membrane assembly for binding of DNA in high-salt buffer and eluted in deionized Milli-Q.

**Protocol**: 5 volumes of Buffer PNI is added to 1 volume of the reaction sample and mixed thoroughly. The mixture is transferred to QIA quick spin column placed on 2ml collection tube

and centrifuged for 1 min at 6000 RPM. The flow-through is discarded. 700µl of buffer PE is added to the column and centrifuged for 1 min at 6000 RPM. The collection tube was replaced with a new clean collection tube and centrifuged for 1 minute at 13000 RPM to remove any residual buffer PE. The column is placed on a clean 1.5 ml microcentrifuge tube, and 30-50µl of pre-warmed autoclaved water is added to the column's centre. It is led to stand for 1 minute and centrifuged for 1 minute at 14000 RPM to elute pure DNA. The DNA can be stored at -20˚C for further use.

### 3.1.7.3: Purification of DNA fragments from agarose gel

For cloning of digested DNA fragments (either vector or insert) or to get pure PCR product, the DNA band of the specific size must be cut and retrieved from agarose gel followed by removal of agarose from DNA samples for different cloning procedures.

**Reagent**: Gel Extraction Kit (Sigma); as per the manufacturer's protocol

**Protocol**: The agarose gel containing the DNA band of interest is placed on a UV illuminator to visualize DNA. The DNA band is cut with precision using a sharp scalpel (pre-sterilized with 70% alcohol). DNA band then is cut into small pieces and transferred to a microfuge tube. 3 volumes of the Gel Solubilization Solution are added to 1 part of the gel weight. (e.g., for every 100mg of agarose gel, 300 ml of Gel Solubilization Solution is added). The mixture is incubated at 60°C for 10-15 minutes with intermittent vortexing until the gel is completely solubilized. Meanwhile, 500 ml of the column preparation solution is added to the binding column and centrifuged for 1 minute. The flow-through is discarded. 1 gel volume of 100% isopropanol is added to the solubilized gel and mixed homogeneously. The mixture is then added to the binding column and centrifuged for 1 minute at 13000 RPM. The flow-through liquid is discarded. 700µl of wash buffer is added to the column and centrifuged for 1 min at 13000 RPM. The collection tube was replaced with a new clean collection tube and centrifuged

for 1 minute at 13000 RPM to remove any residual wash buffer. The column is then placed on a clean 1.5 ml microcentrifuge tube, and 30-50µl of pre-warmed autoclaved water is added to the column's centre. It is led to stand for 1 minute and centrifuged for 1 minute at 14000 RPM to elute pure DNA. The DNA can be stored at -20˚C for further use.

### 3.1.7.4: Ligation reaction

T4 DNA Ligase enzyme creates a phosphodiester bond between 5'-phosphate termini and a 3'-hydroxyl group of two different DNA fragments and ligates the vector and insert. The concentration of purified vector and insert DNA fragments is measured. The typical ratio of vector: insert used is 1:3. The amount of vector and insert fragment required is calculated to achieve 1:3 molar ratio as per the formula:

$$x \text{ µg of Vector} \times \frac{\textbf{size of Insert DNA (in bp)}}{\textbf{size of Vector DNA (in bp)}} \times \frac{3}{1} = \text{y µg of Insert}$$

A positive control (undigested plasmid DNA of vector with the same concentration as calculated for RE digested vector) to check the competency and negative control (another ligation mixture without the insert fragment) to check self-re-ligation of the vector is set up with each ligation reaction.

The following components are added for the ligation reaction:

| **Components** | **Control** | **Test** |
|---|---|---|
| Nuclease- free water | To make up the volume | To make up the volume |
| 10X T4 DNA Ligase buffer | 1µl | 1µl |
| Vector | As per calculated | As per calculated |
| Insert | As per calculated | - |

| | | |
|---|---|---|
| T4 DNA Ligase | 200 U | 200 U |

**Table 6: Ligation reaction mix**

The reaction is incubated at 16°C for 5-6 hours and transformed ultra-competent DH5α E. coli cells. The colonies obtained are screened for positive clones. Screening procedure is carried out only if the test plate contains more colonies than the negative control plate. Ideally, in the negative control plate, there should be no colonies.

The transformants are replica plated on LB-Amp or LB-Kan plates and inoculated simultaneously in 1.5ml antibiotic containing LB broth. The cultures are incubated at 37$^{o}$C in a shaker incubator for 12-16 hours at 200 RPM. The plasmid DNA was isolated for the clones using TELT buffer protocol. Restriction digestion reaction was set up along with vector control DNA with RE combination, which confirms the insert in the positive clones. The digested fragments are analysed in agarose gel electrophoresis for the desired band.

### 3.1.8 Bacterial freeze stocks

The bacterial colony is inoculated in 5ml LB broth containing the required antibiotic and incubated at 37$^{o}$C in a shaker incubator for 12-16 hours at 200 RPM. 0.55ml of 50% Glycerol is added to 1.25ml of the bacterial culture in a cryo-vial and mixed well. A duplicate vial is prepared for back-up as well. The vial is given a specific number in the File-Maker database in the lab and stored at -20˚C for further use.

## 3.2 Yeast Techniques

**Host**: *Pichia pastoris*

**Strain**: PPY12 (*his, arg*)

### 3.2.1 Media preparation

**YPD (Nutrient-rich media) broth**: 10g **y**east extract, 20g **p**eptone and 20g **d**extrose is dissolved in Milli-Q with the final volume adjusted to 1 litre and autoclaved. For making YPD-agar plates, 20g bacteriological grade agar powder is added. The mixture is autoclaved and poured in 90 mm sterile petri-plates, and stored at 4$^{o}$C after solidification.

**SD (Synthetic Dextrose) (Minimal-complete media) broth**: This media is transparent and is used to visualize live yeast cells under the microscope. 1.7g yeast nitrogen base (HI Media) without ammonium sulphate and amino acids, 5g ammonium sulphate (HI Media), 20g glucose and CSM (Complete Supplement Mixture) as indicated on pre-mix media bottle are dissolved in Milli-Q with the final volume adjusted to 1 litre and autoclaved.

**NSD (Non-fluorescent synthetic dextrose)**: This is a nutrient-rich non-fluorescent media ideal for growing yeast cells analysed under fluorescent microscopy. 20g dextrose, 5g ammonium sulphate, 5g potassium phosphate monobasic, 1g magnesium sulphate, 0.5 sodium chloride, 0.1 calcium chloride, 0.79g CSM, 1.7g yeast nitrogen base without ammonium sulphate and amino acids, 2ml vitamin mix, 2ml cobalt chloride and 2ml biotin are dissolved in Milli-Q. The pH is adjusted to 5.5, and the final volume is made up to 1 litre and autoclaved.

**Drop out media**: This is used for the auxotrophic selection of transformants. 1.7g yeast nitrogen base without ammonium sulphate and amino acids, 5g ammonium sulphate, 20g glucose and CSM without one or more amino acid (HIS / ARG) for selection is added in a proportion as indicated on pre-mix media bottles (CSM can also be made by individually adding each amino acid), and dissolved in Milli-Q with the final volume adjusted to 1 litre and autoclaved. They were sterilized by autoclaving.

### 3.2.2 Retrieving strains from the yeast collection

The yeast strain is retrieved from the freeze down inside UV sterilized the laminar hood. The

appropriate vial is removed from -80°C and kept on ice. A sterile toothpick/tip is used to take a small amount of the frozen cells and streak them on a YPD plate or auxotrophic dropout plate. The plate is incubated for 2 days at 30°C.

### 3.2.3 Growing yeast log phase culture

A single colony is inoculated from the plate in 5ml YPD broth or dropout broth in a round bottom 14ml tube and incubated at 30°C for 48 hours at 200 RPM. 0.1% of the saturated pre-culture (a dense pellet of cells should be settled at the bottom of the tube) is inoculated in a baffled flask (to maintain proper aeration and growth) to obtain a log phase culture.

### 3.2.4 Freezing Yeast

400µl of cell suspension from saturated pre-culture is plated on 2 YPD or auxotrophic dropout plates and incubated at 30°C until a thick lawn of cells grows on the plate. A small sterilized tip is used to scrape off the entire lawn of cells and resuspended in 15% sterile glycerol in a cryo-vial. A duplicate vial is prepared for back-up as well. The vial is given a specific number in the File-Maker database in the lab and stored at -20˚C for further use.

### 3.2.5 Manipulating Yeast Genome

Gene targeting by homologous recombination is one of the most powerful and vital techniques utilized for yeast studies. A gene at its standard chromosomal location can be removed or replaced with its variant created in vitro such that phenotypes conferred by such mutations can be analysed. Genes can be modified to fuse to the coding sequence for fluorescent proteins or other epitope tags. The tagged gene is made in the genomic context and is subjected to native regulation. A second copy or foreign gene can also be integrated into the mutated HIS / ARG genes (used for auxotrophic selection) under a constitutive or inducible promoter. A strain's

properties can be compared to an isogenic wild-type strain to study gene localization function and regulation.

### 3.2.6 **Yeast transformation** (Becker and Guarente, 1991)

*Pichia pastoris* cells are transformed by the high-efficiency electroporation method. The yeast strain was inoculated in 25ml of YPD at a 30ºC shaker incubator at 200rpm. The culture is allowed to grow overnight till $O.D_{600}$ reaches 1. 1ml of 1M DTT (Sigma) and 1M HEPES (Sigma) are added to the culture and kept at 30ºC shaker for 15 mins. The culture is centrifuged at 3000 rpm for 3 minutes at 4°C. The pellet is resuspended with 25ml of sterile ice-cold water and centrifuged at 3000 rpm for 3 minutes at 4°C. This step is repeated, and the pellet is resuspended in 10ml of sterile ice-cold 1M sorbitol (Sigma). The cells are then resuspended in 200 ul of ice-cold 1M sorbitol and kept on ice. 40µl of the competent cells are added to linearised DNA (~500ng for auxotrophic selection and 1000ng for antibiotic selection) and transferred to an ice-cold 0.2cm electroporation cuvette (the cells were tapped down to the bottom of the cuvette). The cells are subjected to electroporation using conditions;

Voltage – 1500 V

Capacitance - 25µF

Resistance – 200 ohms

1 ml of ice-cold 1M sorbitol is added to the cuvette immediately after the pulse. The mixture is transferred to a sterile 1ml microfuge tube and centrifuged at 5000 RPM for 1 min. 800µl of the supernatant is removed the remaining amount is plated on selection plates. The plate is incubated for 48-72 hours at a 30°C incubator until colonies appear. The transformants are patched on the selective plate to screen for positive colonies containing the edited gene of interest. The replica plate is incubated at the 30ºC incubator for 24 hours.

### 3.2.7 Genomic DNA isolation

**3.2.7.1: Breaking buffer**: 2% (v/v) Triton X-100, 1% (v/v) SDS, 100mM NaCl, 10mM Tris-Cl; pH 8.0, 1mM EDTA; pH 8.0 is made in sterile Milli-Q

This method is used to prepare a purified genomic DNA sample for PCR amplification of DNA fragments for cloning or sequencing.

A single colony is inoculated in a preculture tube (5-6 ml) or microfuge tube (1ml) and allowed to grow overnight at 30ºC at 200 RPM shaker incubator. The culture is spun for 5 minutes at 3000 RPM at room temperature (RT). The supernatant is discarded. The pellet is washed in 500µl Milli-Q and centrifuged at 3000 RPM for 3 minutes at RT. The pellet is disrupted by brief vortexing and resuspended in 200µl of freshly prepared breaking buffer. 0.3 g tiny glass beads, 100µl phenol and 100µl chloroform are added, and the mixture is vortexed at the highest speed for 5 minutes to achieve cell lysis. 200µl 1X TE buffer is added and mixed by brief vortexing. The cells are centrifuged at the highest speed (~14000 RPM) for 5 minutes at RT. The aqueous layer formed is transferred to a fresh tube, and 1ml of 100% ethanol (ice cold) is added, mixed by inversion and incubated at -20ºC for 1 hour for DNA precipitation. The mixture is centrifuged for 5-10 minutes at the highest speed (~14000 RPM) at RT. The pellet is resuspended in 0.4ml of 1X TE Buffer. 3µl of RNase A (Stock; l0mg/ml) is added, mixed and incubated for 5 min at 37ºC to remove RNA contamination. 10µl of 4M Ammonium acetate and 1ml of 100% ethanol are added, mixed by inversion and incubated at -20 º C for 1 hour. The mixture is centrifuged for 5-10 minutes at the highest speed (~14000 RPM) at RT, and the pellet is kept to air dry. The DNA pellet is resuspended in 20-100µl 1X TE buffer or Milli-Q and stored at -20ºC.

**3.2.7.1: Lithium chloride / SDS method** (Lõoke, Kristjuhan and Kristjuhan, 2011): This is a crude method for isolating genomic DNA from yeast sample used for screening gene

integration and knockout using PCR or sequencing in yeast transformants. Colonies are inoculated in 200µl of YPD and allowed to grow at a 30$^{o}$C shaker incubator for 4-5 hours. The cultures are spun at 3000 RPM for 3 minutes. The pellet is resuspended in 100µl 0.1M Lithium Chloride (HI media) and 100µl 1% SDS and mixed by vortexing. The mixture is kept on a 70$^{o}$C dry bath for 5 minutes. 300µl of absolute ethanol is added and mixed well. The mixture is spun at 13000 RPM for 3 minutes. The pellet is washed with 70% ethanol. The pellet is resuspended in 100µl Milli-Q and spun at 13000 for 3 minutes. The supernatant contains the genomic DNA to be used for further processing.

### 3.2.8 Checking yeast samples in an upright microscope for screening

A small amount of yeast cells is taken from the replica plate, resuspended in 200µl of SD media and allowed to grow at 30$^{o}$C shaker incubator for 4-5 hours. The slides and coverslips are adequately cleaned and air-dried. The cell suspension is put on the slide, and the coverslip placed from the top on this suspension. The coverslip is sealed with transparent nail polish. A drop of immersion oil is put on the coverslip, and the slide is observed under the microscope. Cells are focused in the bright field & then fluorescence is checked by selecting an appropriate fluorescent filter.

### 3.2.9 Preparing the yeast cells for confocal microscope

The yeast strain is inoculated from a healthy preculture and grown overnight in 10ml YPD / NSD in a 50ml baffled flask until the culture reaches an $OD_{600}$ of ~0.5-0.6. A MatTek dish with a high precision 0.170mm glass bottom is used. The dish is coated with 100µl of 2mg/ml Concanavalin A (Con-A) and incubated for 30 mins. The dish is washed thoroughly with autoclaved Milli-Q and dried. 200µl of the log phase yeast culture is added to Con-A coated glass surface and incubated for 12 minutes at room temperature. The culture is removed, and

the surface is washed gently with SD / NSD media to remove all unattached / loosely attached cells. Finally, 200µl -1.5ml of SD / NSD media is added for imaging under a confocal microscope.

**3.2.10 Electron microscopy of yeast** (Wright, 2000)

The yeast strain is inoculated from a healthy preculture and grown overnight in 50ml YPD in a 250ml baffled flask until the culture reaches an $OD_{600}$ of 0.5. The culture is filtered slowly on a bottle-top 0.22µm filter until a volume of about 5 ml concentrated media containing cells retain over the filter. 40 ml of ice-cold fixative solution (50mM KPi buffer; pH 6.8, 1mM $MgCl_2$, 2% glutaraldehyde (Ted Pella, Inc.) is added, and the cells are allowed to fix for 1 hour on ice. The fixed cells are spun for 3 min at 3000 rpm at 4°C. The pellet will be resuspended in 25 ml ice-cold 50 mM KPi; pH 6.8. The same step is repeated two more times for a total of three washes. The pellet is resuspended in 1 ml 50 mM KPi; pH 6.8 and transfer the cell mixture to a microfuge tube. The cells are spun at 5000 RPM for 1 minute at RT. The cell pellet is resuspended in 0.75 ml freshly prepared 4% $KMnO_4$ (SDFCL) and mixed end-over-end for 30 min. The cells are spun for 1 min at 5000 RPM at RT, and the cell pellet is resuspended in 0.75ml H2O. The step is repeated two more times for a total of three washes. The pellet is resuspended in freshly prepared 0.75ml 2% uranyl acetate (stored in the dark). The cells are mixed end-over-end for 1 hr and washed four times with $H_2O$. The cells are dehydrated in the graded series of EtOH solutions (50%, 70%, 80%, 85%, 90%, 95%,100%, 100%,100%, 100%). After each resuspension, the cells are mixed end-over-end for 5 min and spun for 1 min at 5000 RPM. Normal spurrs resin (Sigma) is prepared in a disposable plastic beaker according to the kit instructions' formula, and the resin components are mixed using a glass rod. The dehydrated cells are resuspended in 0.75ml of 3:1 EtOH: Spurrs mixture and mixed end-over-end for 1 hour. The cells are spun for 1 min at 5000 RPM. The pellet is resuspended in 0.75ml of 1:1

EtOH: Spurrs mixture and mixed end-over-end overnight. The cells are spun for 1 min at 5000 RPM. The pellet is resuspended in 0.75ml of 1:3 EtOH: Spurrs mixture and mixed end-over-end for 1 hour. The cells are spun for 1 min at 14000 RPM. Cells are resuspended in 0.75ml of pure Spurrs mixture and mixed end-over-end for 1 hour. The cells are spun for 1 min at 14000 RPM. This step is repeated once more. The cell pellet is finally resuspended in 300µl of pure Spurrs resin mixture and centrifuged for 1 min at 14000 RPM. The microcentrifuge tube is filled with resin and kept in a temperature-controlled oven set at 68°C. The resin is allowed to polymerize for 2 days for sectioning and staining with lead citrate. Ultrathin sections are cut on ultra-microtome (Leica UC7, Germany) and collected on copper grids. Finally, sections are subjected to contrast with uranyl acetate and lead citrate, and micrographs are taken on Jeol 1400 plus Transmission Electron Microscope, Japan at 120 KeV to capture images in bright field mode.

### 3.2.11 Functional inactivation of proteins using the anchor-away method in yeast

A PPY12 derivative is developed that is suitable for anchor-away experiments. The TOR1 gene was modified to confer rapamycin resistance (Helliwell *et al.*, 1994) to the yeast strain such that the addition of rapamycin (Sigma, R0395) only reroutes the protein of interest without any side effects on the yeast cells. A 99–base pair double-stranded DNA fragment is synthesized around the Ser-1919 codon (homologous to Ser-1972 in S. cerevisiae TOR1) containing Ser-to-Arg mutation at the position corresponding to codon 1919. The oligonucleotide fragment is transformed into PPY12 cells, and rapamycin-resistant transformants were selected on YPD plates containing 1µg/ml rapamycin. PCR amplification and sequencing confirmed mutated TOR1 alleles. The FPR1 gene, which encodes a mammalian FKBP homologue (Heitman *et al.*, 1991), is deleted by replacing the open reading frame with kanMX6 to avoid competitive binding FRB tagged protein of interest. Finally, the ribosomal protein Rpl17 was C-terminally

tagged with FKBPx4 by gene replacement. For functional inactivation, various genes of interest (Sec26, Tip20, Sec23) are tagged with one or two copies of FRB in the TOR1 mutant strain carrying the fpr1Δ and RPL7-FKBPx4 alleles. Yeast cells are grown to mid-log phase and treated with 1µg/ml rapamycin from a 1mg/ml stock in 90% ethanol/10% Tween 20. The cells are imaged after 10 minutes.

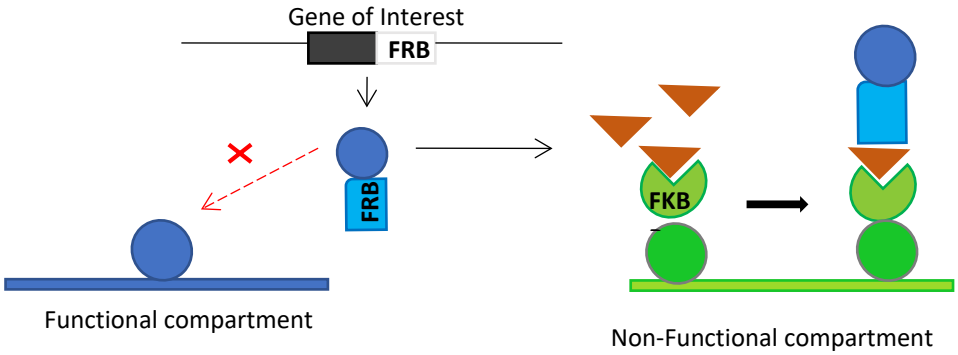


**Figure 3.1: Schematic of the Anchor-away method.**

### 3.2.12 Depletion of proteins using an AID in yeast

The yeast codon-optimized version of the plant OsTIR1 gene (provided by the National BioResource Project–Yeast Kyoto, Japan) is amplified by PCR and subcloned into the constitutive expression vector pIB2 (Sears *et al.*, 1998). The construct is then transformed for integration at the HIS4 locus in *P. pastoris* for this variable F-box protein's ectopic expression.

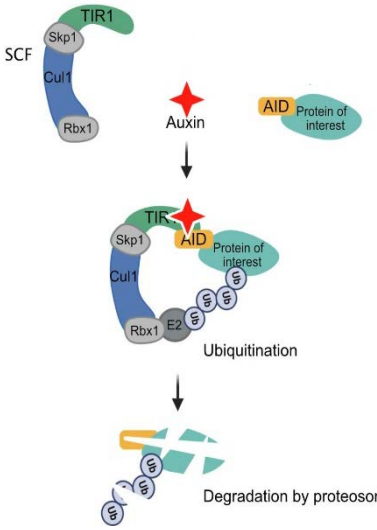


**Figure 3.2: Schematic of the auxin-inducible degron (AID) system.**

(Adapted from Ashley *et al.*, 2020, BioRxiv)

The gene of interest is tagged with a 3x-mini-AID sequence (Kubota *et al.*, 2013). Yeast cells are grown to mid-log phase and treated with 1-3mM IAA (Sigma, 45533) and are imaged after 10-30 minutes.

### 3.2.13 Overexpression of Sar1 mutant

**SY (Synthetic Yeast) Media**: 10g **y**east extract, 1.7g yeast nitrogen base without ammonium sulphate and amino acids and 5g ammonium sulphate is added to a final volume of 1 litre Milli-Q and autoclaved.

**SY-G Media**: 0.8ml 50% Glycerol is added to 40 ml of SY media

**SY-M Media**: 0.8ml methanol (Merck) is added to 40 ml of SY media

Dominant-negative GDP-locked form of Sar1 containing Threonine to Asparagine mutation at the position corresponding to codon 34 is cloned into an inducible expression vector containing methanol-inducible *AOX1* promoter. This construct is then transformed for integration at the HIS4 locus in *P. pastoris*. The cells are transferred from SYG to methanol-containing SYM medium in the early log phase to induce *AOX1*-driven over-expression and imaged after 4 hours.

### 3.2.14 HaloTag labelling of yeast cells

The yeast cells are grown in NSD media to the mid-log phase. 0.4ml of the yeast culture is added to an equal volume of 1µM of JF646 HaloTag (Promega) ligand (200µM Stock solution is diluted to 1:200 with NSD) that binds to HaloTag fusion protein. The mixture is incubated in a shaker incubator at 23$^{o}$C for 30 minutes. The cells are spun at 3000 RPM for 3 minutes and washed with NSD. Finally, resuspend the cells in 200µl of NSD and adhered on Con-A coated plates and imaged.

## 3.3 Mammalian Cell Culture Techniques

Origin of the cells –All are established mammalian adherent epithelial cell lines are used:

| Name | Tissue Origin | Medium |
|---|---|---|
| Int407 | Human Intestine epithelial immortalized | DMEM |
| HCT116 | Human Colon epithelial transformed | DMEM |
| U2OS | Human Bone epithelial transformed | DMEM |

**Table 7: Origin of mammalian cell lines**

**Dulbecco's Modified Eagle Medium (DMEM)**:13.5gpowdered medium (GibCo) is dissolved in 900 ml autoclaved distilled water. 3.7 g sodium bicarbonate ($NaHCO_3$) is added, and the pH is adjusted to 7.2 with concentrated HCL or 5M NaOH to a final volume of 1litre. The medium is filtered through a 0.22μm sterile filter and stored at 4°C.

**Complete medium (CM)**: DMEM is supplemented with 10% FBS (GibCo) and 1% antibiotics [Anti-bacterial Anti-mycotic (Gibco)]

### 3.3.1 Reviving mammalian cell frozen stocks

The media is pre-warmed at 37ºC. The laminal hood is UV sterilized, and all the surfaces and materials to be used are thoroughly cleaned 70% alcohol before starting cell culture. The frozen cryovial is removed from liquid nitrogen and immediately placed in a 37°C water bath. Thawing and recovery of cells from liquid nitrogen must be made quickly. The outside of the

vial is wiped with 70% ethanol. The thawed cells are gently added to pre-warmed 10ml complete DMEM kept in a 90mm petri dish and incubate at 37°C in a $CO_2$ incubator. The media is changed after 4-5 hours once the cells are attached to remove DMSO and non-adherent dead cells and replenish nutrients. Alternatively, the thawed cells can be resuspended in pre-warmed 10ml complete DMEM and spun at 500 RPM for 5 minutes. The pellet is gently resuspended in 1ml complete DMEM and added to pre-warmed 10ml complete DMEM kept in a 90mm petri dish and incubate at 37°C in a $CO_2$ incubator.

### 3.3.2 Cell passaging

**Phosphate buffered saline (PBS)**: 8g NaCl, 0.2g KCl, 0.24g $KH_2PO_4$ (HI Media) and 1.44g $Na_2HPO_4$.2H2O (HI Media) are dissolved final volume of 1 litre distilled water, and the pH is adjusted to 7.4 and sterilized by autoclaving.

**Trypsin–EDTA**: 0.01g EDTA disodium salt, 0.1g D-glucose, 0.04g KCl, 0.8g NaCl, 0.058g $NaHCO_3$ (Merck) and 0.025g Trypsin (Merck) is dissolved to a final volume of 1 litre distilled water, and the pH is adjusted to 7.2 and sterilized by passing through 0.22µm sterile filter and stored at 4°C.

Once the cells are 80-90% confluent, the liquid media covering the cells is removed without disrupting the attached cells. 5 ml of 1X PBS is added, and the cells are washed gently by swirling the petri-plate or flask. The PBS is removed. 1-2ml of trypsin-EDTA is added to cells such that it covers the entire cell surface and incubate at 37°C in a $CO_2$ incubator for 2-5 minutes. Trypsin cleaves proteins on the cell surface and extracellular matrix and removes adhesion molecules to detach the cells from the surface of the petri-dish or flask. EDTA is added to enhance the activity of trypsin, Ca 2+ chelator, removes calcium and causes cell rounding, cell adhesion through cadherins and selectins is calcium-dependent, low calcium causes cells to internalize adhesion molecules, rounding or detachment. The cells are checked

intermittently under a microscope until the cell becomes rounded from their normal spread morphology to confirm detachment (Longer incubation harm the cells). 10 ml of serum-containing complete media is added to deactivate trypsin. The cells are resuspended carefully, and the cell suspension is transferred to a 15 ml centrifuge tube and centrifuged cells for 4 min at 500 RPM. The supernatant is discarded, and the cell pellet is resuspended 1 ml media. An appropriate volume of cell suspension is aliquoted into 10ml complete DMEM kept in a 90mm petri dish or T25 culture flask. The media and cells are adequately mixed by swirling and kept at 37℃ in a CO2 incubator.

### 3.3.3 Preparing frozen stocks of mammalian cells

Cells are harvested from an 80% confluent plate. The liquid media covering the cells is removed without disrupting the attached cells. 5 ml of 1X PBS is added, and the cells are washed gently by swirling the petri-plate or flask. The PBS is removed. 1-2ml of trypsin-EDTA is added to cells such that it covers the entire cell surface and incubate at 37ºC in a $CO_2$ incubator for 2-5 minutes. 10 ml of serum-containing complete media is added to deactivate trypsin. The cells are resuspended carefully, and the cell suspension is transferred to a 15 ml centrifuge tube and centrifuged cells for 4 min at 500 RPM. The supernatant is discarded, and the cell pellet is resuspended in cold 2.7ml serum. 300µl of DMSO is added to the single-cell suspension and mixed well. 1ml aliquot of the cell suspension is added immediately into the cryovial, placed in an isopropanol chamber chiller and stored at –80°C overnight. The next day, the frozen cells are transferred to a liquid nitrogen cylinder.

### 3.3.4 Primary hippocampal neuronal culture

**Neurobasal Complete Media:** 48.85ml of neurobasal incomplete media, 1ml of 50X B27, 100µl of 200mM Glutamax and 50µl of antibiotic are mixed.

**HBS solution**: 4.2g NaCl, 0.112g KCl and 1.19g HEPES is added to a final volume of 500ml with Milli-Q and sterilized through a 0.2 µm filter.

Rat is sacrificed on the 18$^{th}$ day of pregnancy, and rat embryos are collected in a petri-plate kept on ice. The embryos are decapitated, and the heads are placed in freshly prepared HBS solution. The brains are dissected in HBS solution, and the hippocampus is collected in HBS solution. The excess HBS solution is removed. 100µl of 0.3% trypsin (made in HBS solution) is added and incubated at 37$^{o}$C for 5 minutes. 200µl (double the volume of trypsin) of serum is added to inhibit the action of trypsin. The hippocampal tissue is washed 4-5 times with fresh media. The hippocampal tissue is transferred to a fresh T15 tube containing 1ml media and vigorously mixed using a pipette to make an apparent single-cell suspension. 20000-40000 cells are seeded on 0.05mg/ml poly-D-Lysine coated coverslips/ glass bottom 35mm petri plates and incubated at 37$^{o}$C for 24 hours. The media is changed on the next day with 2-3ml fresh media without serum, and the culture is maintained for 19-20 days. The cultures are transfected from the 9$^{th}$ to 14$^{th}$ day for studying biological processes in neurons.

### 3.3.5 Transfection of DNA in cell lines

**X-treme GENE HP DNA Transfection Reagent (Roche)**: **Established mammalian cell lines**

**Lipofectamine 2000 reagent (Invitrogen)**: **Primary neuronal cells**

The cells are seeded in 50-60% confluency to achieve healthy and well-spread cells for imaging experiments in the glass bottom chamber (35mm dish) / coverslips the day before. The required DNA and transfection reagents are diluted in 2 different tubes containing 100µl of DMEM medium or incomplete neurobasal media. X-tremeGENE HP DNA Transfection Reagent/ Lipofectamine 2000 reagent is used in 1:1 DNA to transfection reagent ratio and incubated separately for 5 minutes at room temperature. The diluted transfection reagent is added to the

diluted DNA and incubated for another 30 minutes. 200µl of the mixture to the culture drop-wise and mixed by rocking the culture plate gently. The dish is incubated at 37ºC in a $CO_2$ incubator for 48-72 hours and imaged after that.

**Transfection of mammalian cells with $CaCl_2$**

**2X BES Buffer**: 50mM BES, 280nM NaCl and 1.5mM $Na_2HPO_4$ is dissolved to a final volume of 100ml of $H_2O$, and the pH is adjusted to 6.96. The buffer is sterilized using a 0.22µM filter. 100µl of 2.5M $CaCl_2$ is added to 900µl of Milli-Q and mixed. 10-20µg of DNA is added to the mixture. 1ml of 2X BES buffer is added dropwise and incubated for 1 hour at room temperature. (White coloured precipitation is observed.) The mixture is added to the cells (90mm petri-dish) dropwise with constant rocking and incubated at 37ºC in a $CO_2$ incubator for 16 hours. The media is changed with fresh media and imaged or processed after 24-48 hours.

### 3.3.6 Exosome isolation (Théry *et al.*, 2006)

**Exosome free-FBS**: Fetal Bovine Serum is thawed and loaded onto 70Ti ultracentrifuge tubes and spun at 120000 x g for 18 hours at 4ºC. The supernatant was collected and stored at 4ºC.

**Exosome production media**: 10% exosome free serum and 1% antibiotic is added to incomplete DMEM.

The cells are grown in exosome production media, and the conditioned media is collected when cells are about 90% confluent. The conditioned media (minimum 200ml) is spun at 300 x g for 10 minutes at 4ºC. The supernatant is collected and again spun at 2000 x g for 20 minutes at 4ºC. The supernatant is collected and passed through a 0.22µm filter. The filtrate is collected and subjected to ultra-centrifugation at 120000 x g for 2 hours at 4ºC. The supernatant is

discarded, and the pellet is washed with 1X PBS by spinning at 120000 x g for 18 hours at 4$^{o}$C. The pellet is resuspended in 100µl 1X PBS.

Note: Cells transfected with CD63-GFP produces fluorescently labelled exosomes as the tetraspanin protein CD-63 is enriched in exosomes.

**Exosomes labelling by PKH26**: This is a general lipid membrane labelling dye that labels the bilayer lipid membranes of a pure pool of small vesicles, exosomes. The pellet obtained after PBS wash in the above protocol is resuspended in 1ml if Diluent C (Solution A). 4µl of PKH26 dye is added to 1ml of Diluent C (Solution B). Solution A and B are mixed for 5 minutes with intermittent mixing. The reaction is stopped by adding an equal volume of 1% BSA or exosome-free serum and incubated for 1 minute. This mixture is made to a final volume of 26ml (volume capacity of 70 Ti) and subjected to ultracentrifugation at 120000 x g for 2 hours at 4$^{o}$C. The supernatant is discarded, and the pellet is washed with 1X PBS by spinning at 120000 x g for 18 hours at 4$^{o}$C. The pellet is resuspended in 100µl 1X PBS.

**EM Characterization**: Purified exosomes are diluted in 2% PFA, adsorbed to a 400-mesh Formvar-coated copper grid (Nisshin EMCo. Ltd, Tokyo, Japan) and placed in 1% uranyl acetate solution for 10s. After drying, the samples are observed under a transmission electron microscope (JEM-1400Plus; Jeol Ltd, Tokyo, Japan) at an acceleration voltage of 120 kV.

### 3.3.7 Immunofluorescence of mammalian cells

Cell line: U2OS

Anti-Sec16A antibody: Bethyl Laboratories (product no. A300-648A)

Anti-RINT1 antibody: Santa Cruz Biotechnology (product no. sc-19404)

Anti-Syntaxin18 antibody: Santa Cruz Biotechnology (product no. sc-293067)

Double labelling of Sec16A and RINT1; secondary antibodies from Thermo Fisher Scientific; Alexa Fluor 488–conjugated chicken anti-rabbit IgG (product no. A-21441) Alexa and Fluor 568–conjugated rabbit anti-goat IgG (product no. A-11079), respectively.

Double labelling of Sec16A and Syntaxin18: secondary antibodies from Thermo Fisher Scientific; Alexa Fluor 594–conjugated chicken anti-rabbit IgG (product no. A-21442) and Alexa Fluor 488–conjugated donkey anti-mouse IgG (product no. A-21202), respectively.

**4% Paraformaldehyde (PFA)**: 4g of EM grade paraformaldehyde (SDFCL) is added to 50ml of Milli-Q. 1ml NaOH id added to the solution and dissolved at 60$^{o}$C. 10ml of 10X PBS is added, and the solution is allowed to cool to room temperature. The pH is adjusted to 7.4 with 1M HCl, and the final volume is adjusted to 100ml with $H_20$. The solution is sterilized through a 0.45 µl filter.

The cells are seeded in 35mm glass-bottom plates to a 60-70% confluency. The media is discarded, and the cells are washed in 1X PBS for 5 mins, twice. 4% of pre-warmed PFA is added and incubated for 15 mins at 37$^{o}$C. The cells are washed with 1X PBS for 5 mins thrice. 0.3% Triton X100 (made in 1X PBS) and incubated for 10-15 minutes at RT. The cells are washed with 1X PBS for 5 mins thrice. 5% BSA (Sigma) (made in 1X PBS) is added to the cells and incubated for 1 hour at RT. The cells are washed with 1X PBS for 5 mins. The cells are incubated with primary antibody (diluted 1:100 with 1X PBS) at 4$^{o}$C overnight. The cells are washed with 1X PBS for 5 mins thrice. The cells are incubated with the secondary antibody (diluted 1:200 with 1X PBS) at 4$^{o}$C overnight. The cells are washed with 1X PBS for 5 mins thrice. 1X PBS is added to the cells and imaged.

## 3.4 Microscopy and Image Processing (Day, Papanikou and Glick, 2016)

### 3.4.1 Image Acquisition Parameters

Following parameters were used for the live-cell imaging using Leica SP8 imaging platform.

• 100x (yeast cells), 63x (mammalian cells) objective, NA=1.4

• Frame size (width x height): 256 x 128 (yeast cells), 512 x 512 (mammalian cells)

• Zoom: 7 (yeast cells), 2 (mammalian cells)

• Pixel size: 60-70 nm

• XY scan direction: bidirectional, phase = 3.15,

• Pinhole: 1.2 AU

• Line averaging: 8 (yeast cells), 1 (mammalian cells)

• Slice thickness: approximately 0.3µm (yeast cells), 0.8µm (mammalian cells)

• Bit depth: 8-bit is almost always adequate

• Laser settings for green and red fluorescence channels:

- 488: 3-10%, HyD, collection window = 495-550 nm, gain = 400-500

- 561: 3-10%, HyD, collection window = 575-750 nm, gain = 400-500

• PMT for bright field, gain = 300-600; store in blue channel of RGB images

### 3.4.2: Deconvolution

Images are deconvoluted using Huygens professionals. First, the raw Lif file is opened by Huygens professionals. The parameter wizard is opened to set the embedding media refraction to 1.35, rest of the default parameters are kept as it is and accepted. Next, the deconvolution wizard is opened for the selected image/movie, and once all the parameters are set, the deconvolution plug-in is run. The same is repeated for other fluorescence channels as well. The deconvolved image is saved as Tiff 8-bit.

### 3.4.3: Image Processing

This software is used for image processing. The deconvolved image sequence is imported as Hyperstack using the appropriate number of channels, slices per Z-stack and frames. The channels are assigned their corresponding colour. For simple projection, Image > Stacks > Z Project with “Average Intensity” plug-in is used. Further, the brightness and contrast of the individual channels are adjusted. For advanced processing, each channel is converted from 8 bits to 16 bits. After that, the plug-in Process > Math > Multiply to 256 is used, followed by auto-adjusting the brightness for each channel using Image >Adjust > Brightness/Contrast plug-in, and finally, the image is averagely projected using Image > Stacks > Z Project with “Average Intensity” plug-in. The individual channel in the PNG format and merged image in TIFF file format. The averagely projected fluorescence micrographs were assembled using Adobe Photoshop.

**3.4.4 Colocalization Overlap Quantification:**

The overlap between two differently fluorescent-tagged punctate compartments is quantified as done by Levi et al., 2010. Using ImageJ, the red and green channels from a merged RGB image are separated and maximally projected. Using the Photoshop software, red and green channels are converted to grayscale, inverted to give dark spots on a light background, processed with the Despeckle filter and saved as separate TIFF files. The TIFF file corresponding to the red and green channels are then opened in ImageJ, and a binary thresholded image of black spots on a white background was created using the Dynamic Threshold 1d plug-in (http://www.gcsca.net/IJ/Dynamic.html) with the parameters: mask size= 15, threshold = [*(*max + min*)/*2] −C, where C = 7. The TIFF file was then inverted to give light spots on a dark background, and the binary thresholded image was subtracted that displayed only the punctate spots from the red channel. The total signals from each cell's red and green spots were then obtained using the Measure command in ImageJ. The binary thresholded image from the green channel was subtracted from the TIFF file for the red channel to determine the

fraction of the punctate red signal that overlapped with the punctate green signal. The resulting signal was measured and was divided by the total signal previously measured for the red spots. Alternatively, 4D movie series were deconvoluted using Huygens Professional. The deconvoluted image sequence stacks were bleach corrected for each channel and converted into 4D montage series. The latter is further converted into an 8bit hyper-stack. 4D movie analysis provides masked values for each channel with the other. The red masked was divided by the total red signal to determine the fraction of the punctate red signal overlapped with the punctate green signal.

**3.4.5 Quantification of fluorescence at puncta**:

The DIC and coloured channels are split and averagely projected. The image is background-corrected from the region outside the cell. The image was then duplicated. One image was made into binary, and another was further background corrected by adjusting the rolling ball radius pixel such that only signal coming from the ERIS or ERES site is visible. Further, the image was made into binary by adjusting the threshold between 0(min) and 255(max). Both the images were then measured for mean intensity. The mean intensity values for the later image were divided by the former to find the fraction of the total intensity at the respective sites.

**3.4.7 Quantification of *de novo* formation of fluorescent spots**

4D movie series are deconvoluted using Huygens Professional. The deconvoluted image sequence stacks are bleach corrected for each channel and converted into 4D montage series. Using the edit montage series plug-in, the all the fluorescent spots except the one of interest is erased. The edited file is converted into an 8bit hyper-stack that contains the one fluorescent

spot to be studied. 4D movie analysis provides the fluorescent intensity of the spot over each progressing frame.

### 3.5: Statistical tests

For every experiment, the quantification data is plotted using GraphPad Prism software. Datasets are first checked for normal distribution by column statistics. In the case of normally distributed datasets, paired two-tailed student t-test is used. Graphs are plotted in column type mean with standard error mean.

# 4. Results and Discussion

# 4.1 ER Arrival sites in the budding yeast *P. pastoris*, together with ER exit sites, form a bidirectional transport portal.

### 4.1.1 Introduction

The biogenesis of proteins begins in the Endoplasmic Reticulum (ER). The proteins are correctly folded and subjected to various post-translational modifications in the ER. While misfolded proteins undergo ER-associated degradation, the rest of the secretory proteins enter the secretory pathway (Vitale and Denecke, 1999). The proteins are transported to Golgi via COPII-coated vesicles. These anterograde vesicles are formed at designated sites on the ER known as ER Exit sites (ERES) (Kurokawa and Nakano, 2019). The coat proteins (Sec23, Sec24, Sec13, Sec31) are recruited at these sites by Sar1 GTPase that anchors the ER membrane and initiates COPII-coated vesicle formation. The ER-resident proteins (facilitating cargo-loading, export and fusion of COPII vesicles to Golgi membrane) that escape the ER membrane and misfolded Golgi proteins are transported back to the ER by COPI vesicles using their ER retrieval signals (Spang, 2013). These retrograde vesicles are recognized by the multi-subunit tethering complex known as Dsl1 complex (comprising three soluble proteins, namely, Dsl1, Dsl3 and Tip20) on the ER membrane. The Dsl1 complex docks the COPI vesicle and is associated with the ER t-SNARE proteins (Ufe1, Use1 and Sec20) that recognize the cognate v-SNARE (Sec22) on the COPI leading to fusion of the lipid bilayer. The COPI vesicles must fuse at the ER Arrival sites (ERAS) on the ER membrane by analogy.

We aim to test if multiple Dsl1 complex self-assemble to organize the ERAS. We have used the budding yeast *Pichia pastoris* for our studies. This model organism provides a simple platform where fluorescent studies have shown few countable stacked Golgi units positioned next to the ERES (Bevis *et al.*, 2002). ERES are persistent dynamic structures that appear de novo, undergo expansion and shrinkage, and fuse to probably maintaining their numbers between 3 – 6. Electron microscopy tomographic images have shown that multiple COPII vesicles emerge from ERES, which aggregate in between the ER membrane and the adjacent cis-Golgi membrane. Another set of smaller COPI vesicles, were identified to be distributed

around the COPII vesicle clusters (Levi *et al.*, 2010). So, it seems reasonable that ERES and the presumptive ERAS might be associated sites.

### 4.1.2 COPI vesicles fuse at the ER Arrival sites formed by the Dsl1 complex on the ER membrane

We first aimed to investigate whether the Dsl1 complex formed an organized structure. To answer that, we fluorescently labelled the subunits of the Dsl1 complex, Tip20 and Dsl3, such that the proteins would display a punctate pattern only if multiple tethering complexes assemble, creating a particular microdomain. We C-terminally tagged Tip20 with iGFP and Dsl3 with mCherry and found that both the proteins individually formed punctate structures that resembled partial rings. Sometimes a central zone of clearance was observed in few puncta (Fig 4.1A). The signal from the two subunits more or less wholly overlapped with each other, as shown by the percentage overlap graph (Fig 4.1B), confirming that the two subunits form part of the same complex and must behave indistinguishably. To determine whether these puncta were a part of ER, we fused the ER signal sequence, 'HDEL' with DsRed fluorescent tag under a constitutive promotor to label the ER network in yeast and co-expressed Tip20-iGFP. The Tip20 punctate structures were visible on the nuclear and peripheral ER network (Fig 4.1C). These results show that the Dsl1 complex is localized at specific ER sub-domains. To answer whether the ER-localized SNARE proteins that collaborate with the Dsl1 complex in COPI vesicle fusion to the ER membrane organize into the same microdomain, we N-terminally tagged Sec20 with GFP in the yeast strain expressing Tip20-mCherry. The SNARE's fluorescent signal was, in general, weak and displayed a punctate pattern with a background fluorescence that presumably reflected diffused localization to the ER network (Fig 4.1D). The punctate signal showed visible association with Tip20 signifying their connectivity.

The SNARE proteins are integrated into the ER membrane during translocation, and on the

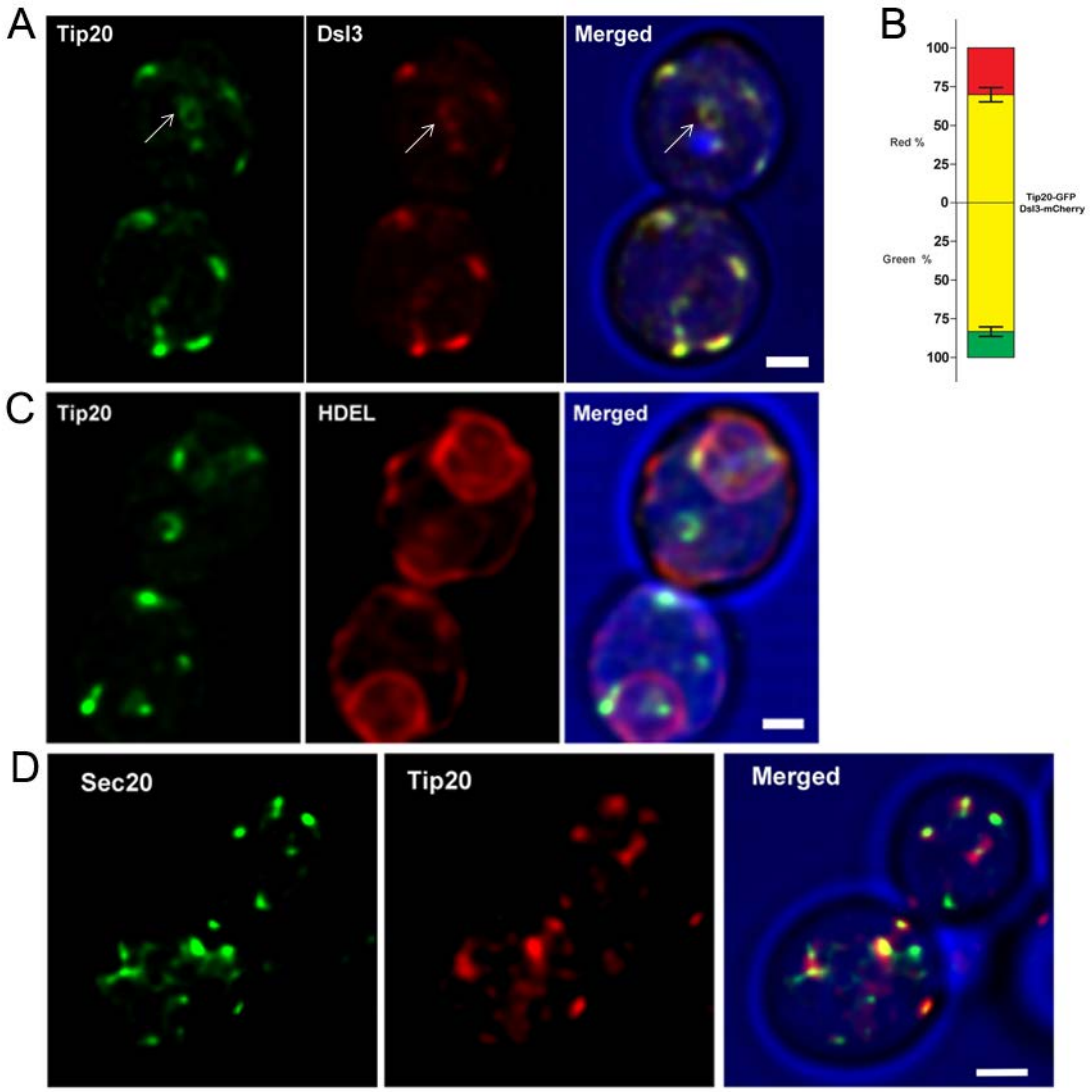


**Figure 4.1: Dsl1 complex forms specific sub-domains of the ER**

**(**A) Colocalization of the Dsl1 complex subunits Tip20 and Dsl3 in *P. pastoris*. Arrowhead showing ring-like pattern with central clearance zone. Scale bar, 1μm. (B) Signal overlap of Tip20-GFP and Dsl3-mCherry was measured for ~20 individual cells. Above the horizontal axis, yellow indicates the percentage of the red signal that coincided with green pixels, while below the horizontal axis, yellow indicates the percentage of the green signal that coincided with red pixels. Bars represent SEM. (C) Tip20-GFP localization with the ER, marked by the ER signal sequence, DsRed-HDEL. Scale bar, 1μm. (D). A strain co-expressing Dsl1 complex subunit, Tip20-GFP and ER-localized SNARE protein, GFP-Sec20. Scale bar, 1μm.

contrary, the tethering complex is recruited to the ER membrane (Cai, Reinisch and Ferro-Novick, 2007). ER-localized SNAREs are mostly present throughout the ER membrane but become concentrated at the site of fusion machinery. However, the Dsl1 complexes are

specifically localized into particular sites and facilitate the assembly of the SNAREs. Therefore, we presume that the Dsl1 complex can be the potential representative of the ER Arrival sites (ERAS).

The Dsl1 complex tethers COPI vesicles. Therefore, it is essential to see whether COPI docking and fusion occurs at sites formed by the Dsl1 complex. We tagged Sec26, the essential β-COP subunit of the COPI coat in a strain co-expressing a Dsl1 complex subunit, either Tip20-mCherry (Fig 4.2A) or Dsl3-mCherry (Fig 4.2B). Sec26 displayed a similar ring-like structure and strongly overlapped with the pattern formed by the Dsl1 complex, quantified by the % colocalization graph (Fig 4.2C and 4.2D). These partial ring-like patterns formed by COPI vesicles must be because of COPI vesicle budding sites present at Golgi cisternal rims. To test this, we co-labelled Sec26 with the GDP-mannose transporter, Vig4, an integral membrane protein localized at cis-Golgi (Abe, Hashimoto and Yoda, 1999) and Guanine nucleotide exchange factor, Sec7, a peripheral membrane protein localized at trans Golgi (Richardson, McDonold and Fromme, 2012), separately. Both the proteins uniformly distribute throughout the respective Golgi cisterna. Sec26 lie adjacent to Golgi and could be seen to form partial or complete ring-like structures around the early and late Golgi markers, fitting the previously held concept that emerging COPI vesicles decorate the Golgi outer periphery (Tie *et al.*, 2018) (Fig 4.2E and 4.2F). All these results suggest that the incoming COPI vesicles tether to the ER with the help of the Dsl1 complex, which in turn links the ER-localized SNAREs to that of the v-SNARE and bring about COPI fusion in specific vesicle capturing hotspots in the ER membrane; ER Arrival sites (ERAS).

### 4.1.3 ERAS are located around ER exit sites (ERES) and adjacent to Golgi

Tomographic reconstructions of electron micrographs showed COPI vesicles originating from Golgi clustered around centrally placed COPII vesicles budding at the ER exit sites (ERES) on

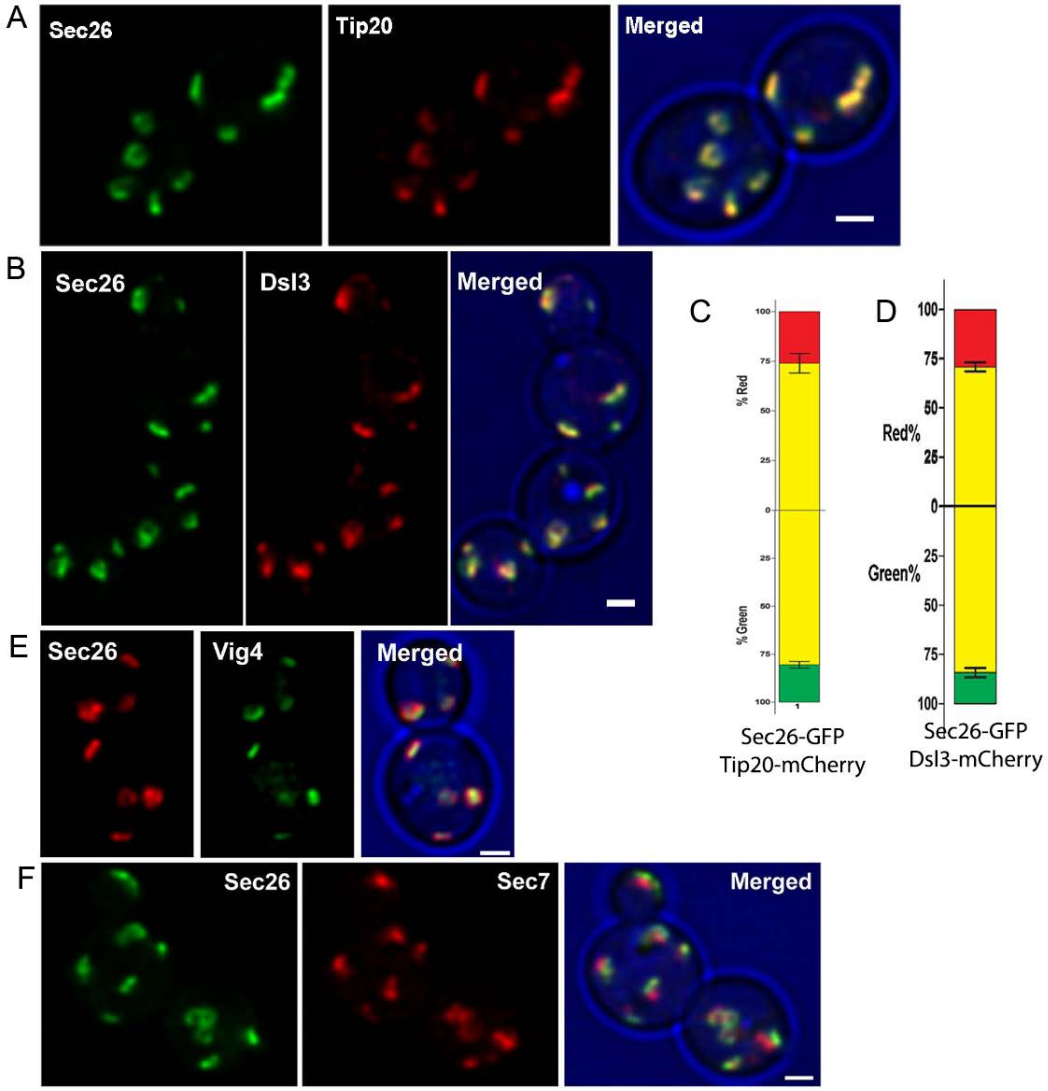


**Figure 4.2: Golgi-derived COPI arrives at the ERAS**

(A) Colocalization of the Dsl1 complex subunit, Tip20 with COPI coat protein, Sec26. Scale bar, 1µm. (B) Colocalization of the Dsl1 complex subunit, Dsl3 with COPI coat protein, Sec26. Scale bar, 1µm. (C) Colocalization quantification from A for ~20 cells. Bars represent SEM. (D) Colocalization quantification from B for ~20 cells. Bars represent SEM. (E) Localization of Sec26 with early Golgi marker, Vig4. Scale bar, 1µm. (F) Localization of Sec26 with late Golgi marker, Sec7. Scale bar, 1µm.

the ER membrane (Levi *et al.*, 2010). We utilized fluorescence microscopy to look at the COPI and COPII distribution in *P. pastoris*. To label COPII vesicles originating at the ER, we tagged the COPII subunit, Sec13, with DsRed in a strain expressing Sec26-GFP. Sec13 formed tight solid puncta, and Sec26 signal was found adjoining it, often partially or entirely encircling it (Fig 4.3A), consistent with the EM data. COPI vesicles almost entirely colocalize with the

Dsl1 complex that holds the COPI vesicles and form the ERAS, so the next obvious question was to look at the localization of ERAS to that of ERES. Polymerization of the COPII coat for vesicle formation occurs at the ERES, and further uncoating leads to pinching off the COPII vesicles causing recycling of the COPII subunits for the next round of vesicle formation. Hence COPII coat proteins mark the ERES. We constructed a *P. pastoris* strain co-expressing Sec13-DsRed and either of the two Dsl1 subunits, Tip20 or Dsl3, with GFP (Fig 4.3B), marking the ERAS. As predicted, the ERAS was found to form larger structures partially surrounding the ERES. We further checked the localization of two ERAS-associated SNAREs, GFP-Ufe1 or GFP-Sec20, with ERES marker Sec13-DsRed. The SNAREs were associated with ERES,

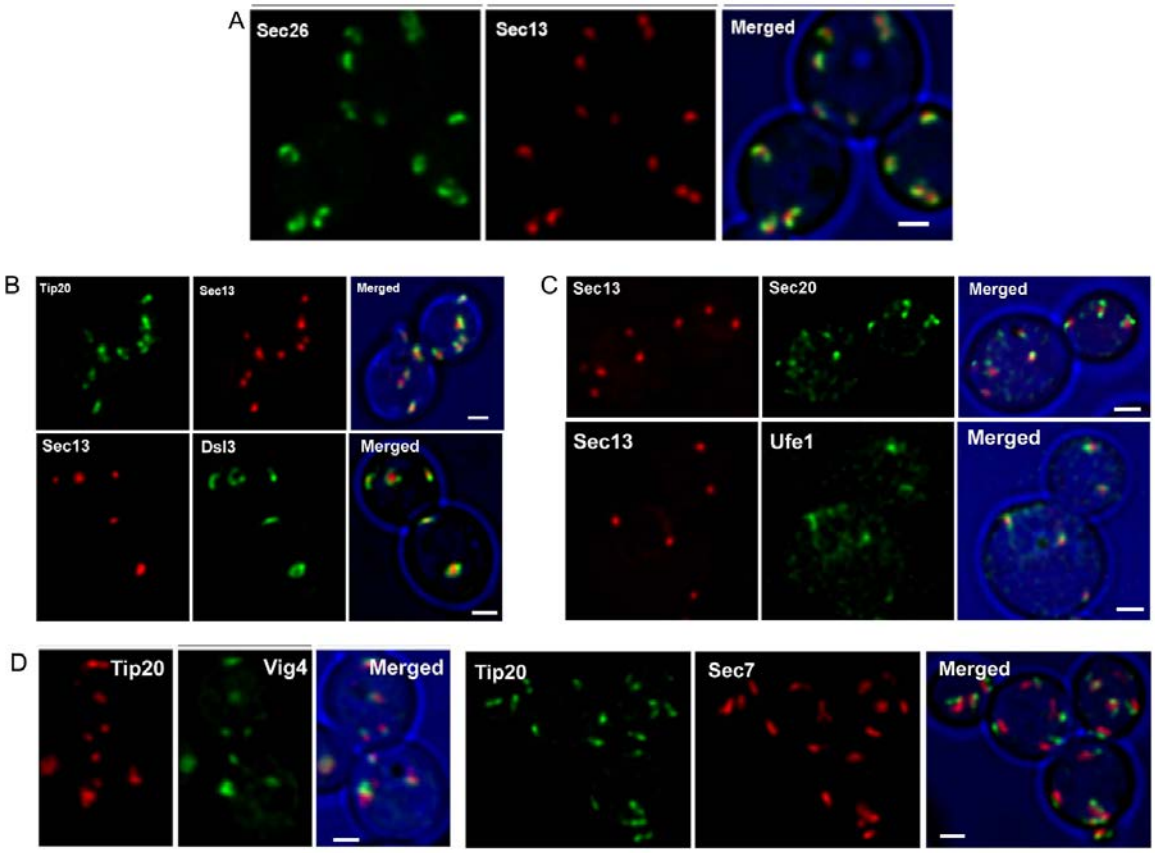


**Figure 4.3: ERAS encircles ERES adjacent to Golgi**

(A) Colocalization of the COPI coat subunit, Sec26 with COPII coat subunit, Sec13. Scale bar, 1μm. (B) Colocalization of the ERES marker, Sec13 with ERAS markers or Dsl1 complex subunits; Tip20 (upper panel) and Dsl3 (lower panel). Scale bar, 1μm. (C) Colocalization of the ERES marker, Sec13 with ER-localized SNAREs, Sec20 (upper panel) and Ufe1 (lower panel), associated with the Dsl1 complex. Scale bar, 1μm. (D) Localization of Tip20 with cis Golgi marker, Vig4 (left panel) and trans Golgi marker, Sec7 (right panel) Scale bar, 1μm.

sometimes partially surrounding them (Fig 4.3C). Since the Golgi apparatus lies next to the ERES, the logical implication would be that ERAS must also lie in the same plane as ERES adjacent to the Golgi. To document this, we expressed Tip20-mCherry with early Golgi marker, Vig4 and Tip20-GFP with late Golgi marker, Sec7. We found that the ERAS or Dsl1 complex was localised adjacent to Golgi in general, closer to cis-cisterna than trans-cisternae (Fig 4.3D).

### 4.1.4 The universality of association between ER arrival site and ER exit site

We next swapped the fluorescent tags corresponding to the ERES marker, Sec13, and ERAS marker, Tip20, in a dual labelled strain co-expressing Tip20-mCherry and Sec13-GFP. We found ERAS to form a larger punctate pattern around a smaller solid punctum formed by ERES (Fig 4.4A). Due to the higher PSF of the red fluorescent tag, we could not observe the central clearance zone seen in the ERAS signal when viewed from a correct orientation. We, therefore, quantified the data to find that the Sec13-GFP signal completely colocalized with the Tip20-mCherry signal; however, only a fraction of the Tip20 signal overlapped with Sec13 due to its additional surrounding area (Fig 4.4B). We further used different ERAS and ERES markers, the Dsl1 complex subunit, Dsl3 and COPII coat protein, Sec31 and found the same co-localization pattern (Fig 4.4C).

From all the previous experimental evidence in *P pastoris*, it has been clear that for each ERAS, there is always an associated ERES. We checked whether this association occurred in higher eukaryotes using immunofluorescent studies. ERAS marker, Tip20 homolog, Rint1, was associated with the ERES marker, Sec16 (Fig 4.4D). Moreover, similar co-localization was observed between ERES marker, Sec13 and ERAS marker, Rint1 in the dendritic region of primary hippocampal neurons (Fig 4.4F). We further investigated the localization pattern of Rint1 and ER associated t-snare, Ufe1p homolog, Syntaxin18. In our fluorescent studies, Rint1and Syntaxin18 showed incomplete co-localization similar to that in *P. pastoris* results

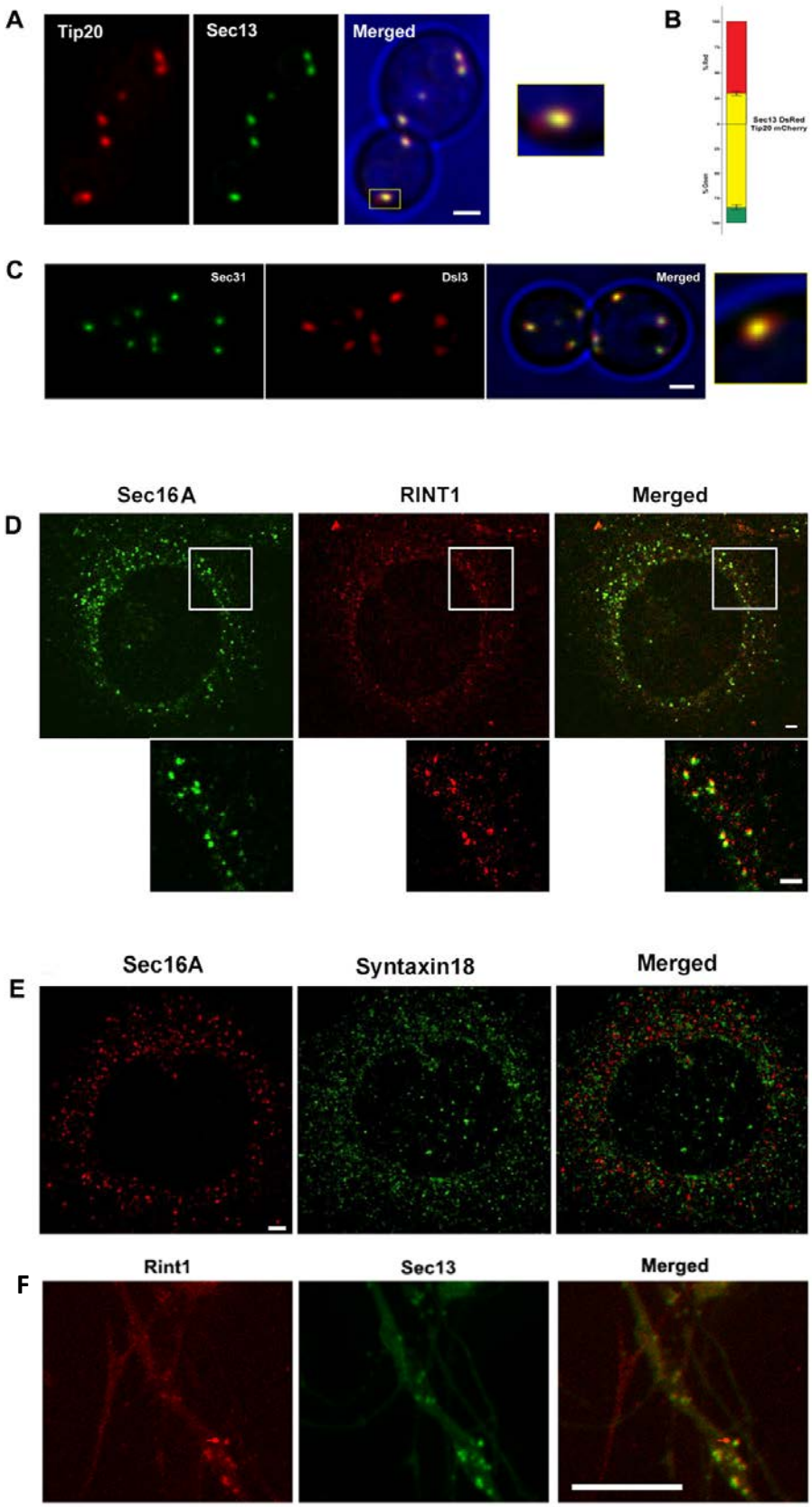


**Figure 4.4: The universality of association between ER arrival site and ER exit site**

(A) Colocalization of the Dsl1 complex subunit, Tip20-mCherry with COPII coat protein, Sec13-GFP. Scale bar, 1μm. (B) Colocalization quantification from A for ∼20 cells. Bars represent SEM. (C) Colocalization of the Dsl1 complex subunit, Dsl3-mCherry with COPII coat protein, Sec31-GFP. Scale bar, 1μm. (D) Immunofluorescence microscopy to visualize localization of ERES marker, Sec16A with NRZ complex subunit, RINT1, marking ERAS. Scale bars, 5μm. (E) Immunofluorescence microscopy to visualize localization of ER-localized SNARE, Syntaxin18 with Sec16A. Scale bar, 5μm. (F) Co-localization of ERES marker, Sec13 and ERAS marker, RINT1 in the dendritic region of primary neurons. Scale bar, 10μm.

(Fig 4.4E). These results are in concordance with the previous yeast results and provided evidence for the universality of distinct ER domains, namely ERES and ERAS, that might form a bipartite structure.

### 4.1.5 ERAS exhibit similar dynamics as ERES

The proximity of ER arrival sites to the COPI vesicles and the ER exit sites raises the question of ER arrival sites' dynamics. Previous studies have shed detailed evidence on the *denovo* formation, homotypic fusion, expansion and shrinkage of ERES in P. pastoris (Rossanese *et al.*, 1999; Bevis *et al.*, 2002). Since ERAS and ERES are closely associated, we tried to explore the possibility that weather the appearance of either compartment precede the other and provide the template for its biogenesis. We did 4D imaging of the two-colour strain labelling both ER Arrival sites and ER Exit sites to address this issue. We first used Sec13-DsRed and Tip20-GFP marked spots that were found to form *de novo* almost simultaneously (Fig 4.5A). We could not discriminate their time of appearance during the *de novo* formation, and even if there was any slight difference, it was beyond the detectable limits of our instrumental measurements. The spots were visualized as a new small coupled fluorescent spot that gradually increased in size, quantified by an increase in the fluorescence signal with progressing time frame and represented in % fluorescence over time graph (Fig 4.5B). The Tip20 structures were more variable and dynamic in shape, making the quantification for Tip20 signal noisier as compared to Sec13. The explanation can be that the Dsl1 complex is dynamic

structures that extend to capture the COPI vesicles and retract back to bring them closer to the ER membrane (Travis *et al.*, 2020). This process depends on the availability of COPI vesicles emerging from rims of cis Golgi cisterna that may be non-uniform at a particular point in time. Therefore, the ring-like pattern formed by the Sec26 signal the adjacent Tip20 signal does not display an even fluorescence but fluctuates within the ring area over time. Further, using live-cell imaging, we have documented that ER arrival sites fuse with similar kinetics as that of ER exit sites (Fig 4.5C), i.e., when ERES fused, the associated ERAS fused as well. Hence, the biogenesis and dynamics of ERAS and ERES ultra-structures are tightly coupled. We repeated the experiment with a yeast strain co-expressing Sec13-GFP and Tip20-mCherry, to see whether a swap of the fluorescent tags to ERES and ERAS markers affects the similarity in their behaviour. However, we found similar results (Fig 4.6 A, B, C). Together these results suggest that ER exit and ER arrival sites are inseparable entities and perhaps are a part of the same structure most of the time.

### 4.1.6 Loss of ERES lead to loss of ERAS structures.

All the previous results suggest that possibly both ER exit and ER arrival sites are bipartite structures. If that is so, a natural question arises about the fate of one in the absence of the other. The co-localization events direct us to cross-examine ER arrival sites' fate (ERAS) when ER exit sites (ERES) are disrupted or vice versa. We have decided to approach this question by studying the effect of individual perturbation of different ERES constituent protein's functions on ER arrival sites in general. Moreover, to get accurate answers, we have simultaneously explored various methods for perturbation of protein functions. The efficacy of perturbation of protein function by these independent methods varies and greatly dependent on the individual proteins.

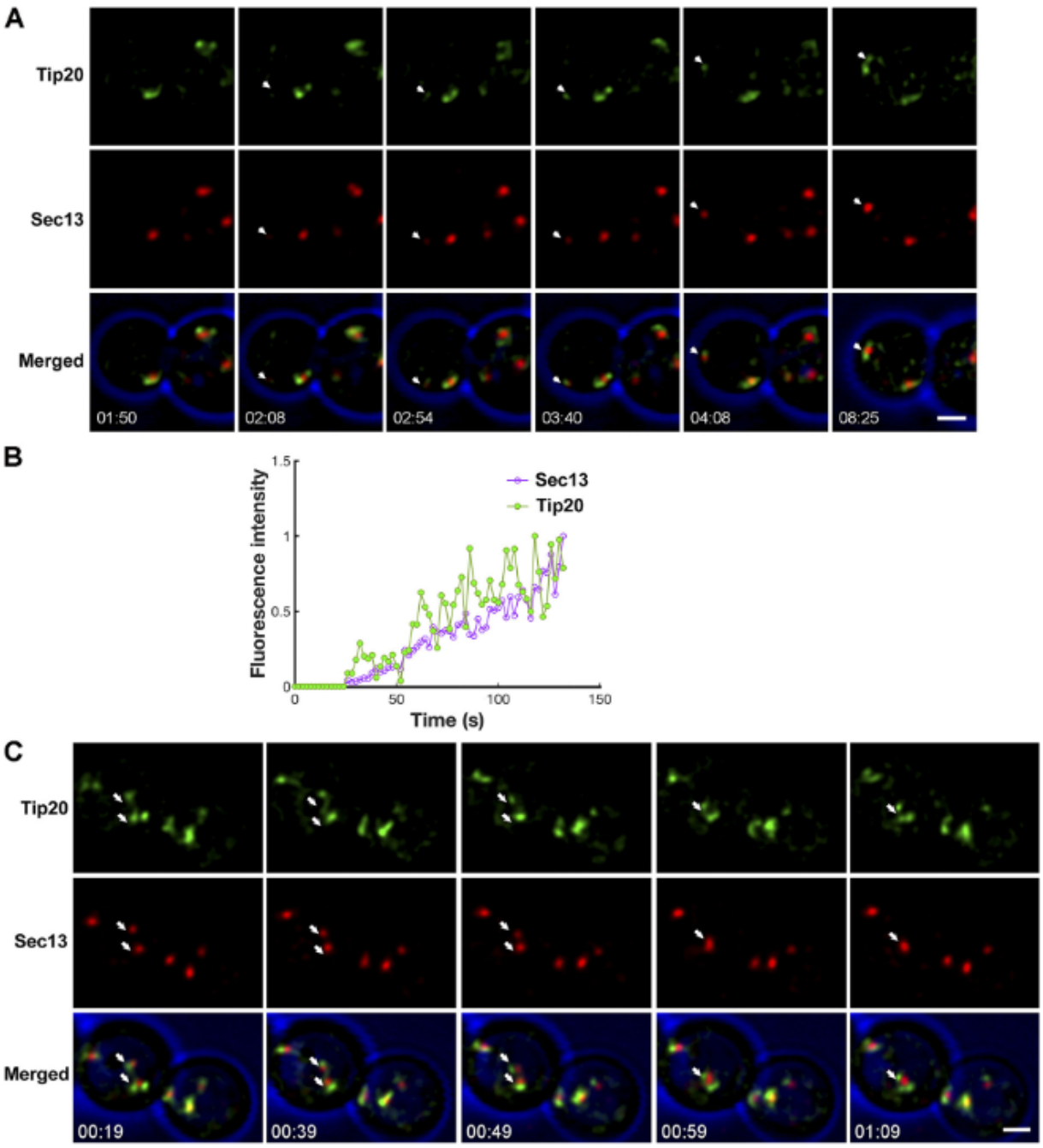


**Figure 4.5: Coupled behaviour of ERAS and ERES**.

(A) Simultaneous *de novo* formation of ERAS structures marked with Tip20-GFP and ERES structures marked with Sec13-DsRed. Arrowhead mark parallel appearance of new ERAS and ERES spots tracked by 4D confocal microscopy and represented in the movie time-frames. Scale bar, 1μm. (B) Quantification of the fluorescence signals from the newly formed spots marked by arrows in A. Plot normalized by setting the highest value to 1. (C) Coupled fusion of Tip20-GFP and Sec13-DsRed spots. Arrowheads mark ERAS-ERES pairs undergoing fusion event, tracked by 4D confocal microscopy and represented in the movie time-frames. Scale bar, 1μm.

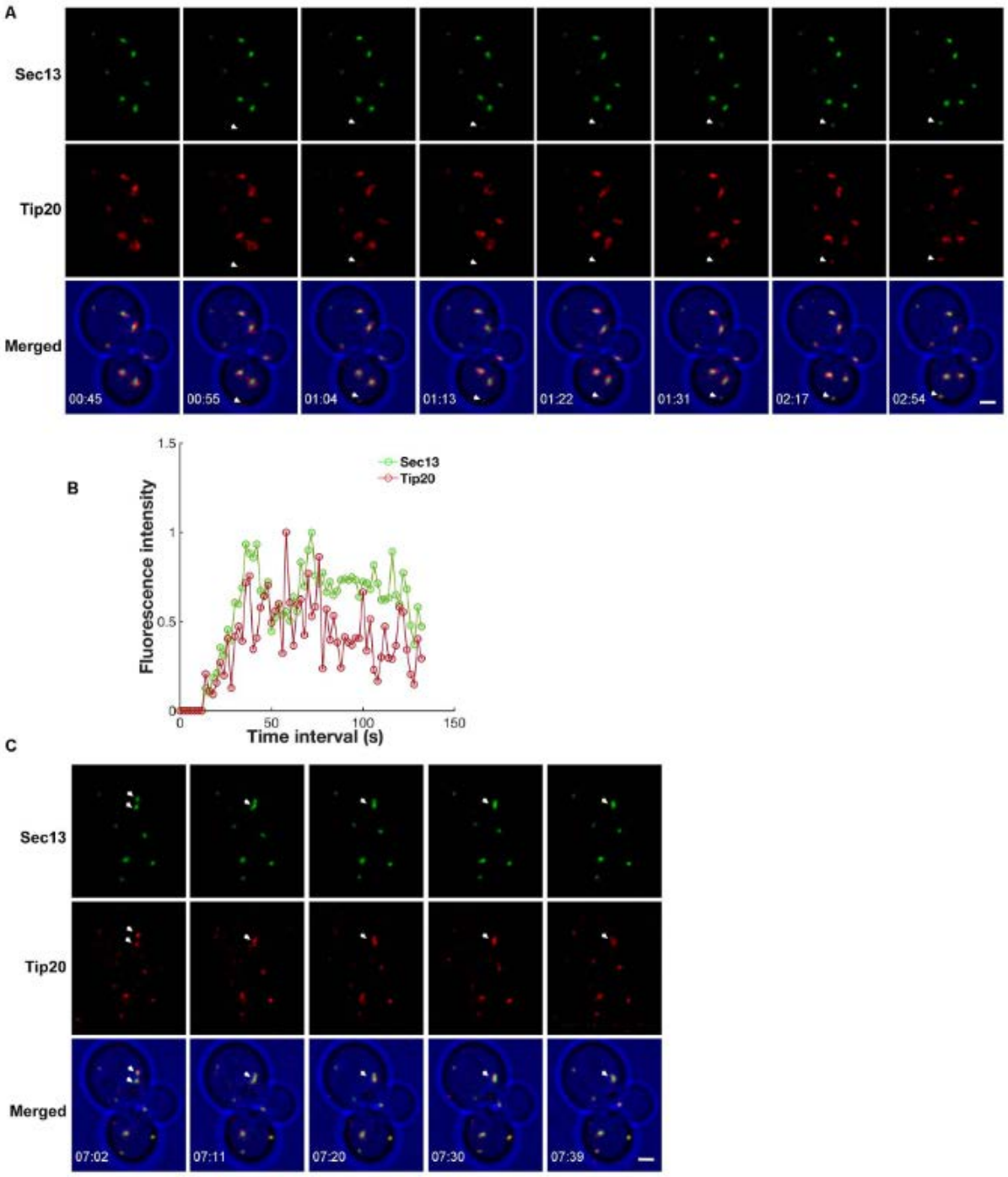


**Figure 4.6: Coupled behaviour of ERAS and ERES with swapped fluorescent tags.**

(A) Simultaneous *de novo* formation in a strain expressing ERAS structures marked with Tip20-mCherry and ERES structures marked with Sec13-GFP. Arrowhead mark parallel appearance of new ERAS and ERES spots tracked by 4D confocal microscopy and represented in the movie time-frames. Scale bar, 1μm. (B) Quantification of the fluorescence signals from the newly formed spots marked by arrows in A. Plot normalized by setting the highest value to 1. (C) Coupled fusion of Tip20-mCherry and Sec13-GFP spots. Arrowheads mark ERAS-ERES pairs undergoing fusion event, tracked by 4D confocal microscopy and represented in the movie time-frames. Scale bar, 1μm.

The anchor away system (Haruki, Nishikawa and Laemmli, 2008) is an elegant method that employs a rapamycin inducible system to reroute any FRB (FKBP12-rapamycin-binding domain of human mTOR) tagged endogenous protein of interest to a different cellular location such as ribosomes using a specific FKBP (human FK506 binding protein) tagged anchor protein. Rapamycin binds to the FKBP12 domain, and this establishes an interaction surface for the FRB domain to form a tight ternary complex. Rapamycin is toxic to wild-type yeast. Therefore, a rapamycin-resistant strain is developed containing a mutated *TOR1* (*tor1-1*). *FPR1*, the yeast homolog of the human FKBP12 gene, encoding the most abundant FK506 and rapamycin binding protein, is deleted (Δ*fpr1*). This deletion is necessary not only for rapamycin resistance but also to reduce competition between Fpr1p and the anchor-FKBP12 recombinant protein for binding to the FRB domain.

We tried to look at the effect of COPII coat proteins on ERAS biogenesis and stability. Rerouting of the inner layer COPII coat protein, Sec23 (representative protein of ERES), along with its homologue Shl23 (Esaki, Liu and Glick, 2006), has been shown previously to cause complete abolition of ER exit sites (Bharucha *et al.*, 2013). We have used a strain carrying the ribosomal protein Rpl17 tagged with FKBP and expressing Sec23-FRB and Shl23-FRB. The addition of rapamycin caused the FRB tagged Sec23 and Shl23 protein to tether at the ribosomal anchored FKBP site within 5-10 minutes, thereby preventing Sec23/Shl23 from carrying out their cellular activities. We documented this by expressing the outer layer COPII coat protein, Sec31-GFP (another representative protein of ERES) in the above background (Fig 4.7A). As predicted, we found loss of distinct Sec31 punctate structures. Further when we co-expressed the ERAS marker, the Dsl1 subunit, Tip20-GFP in above strain, we found that the ERAS no longer maintained its organized punctate nature after 10 minutes of adding rapamycin, rather diluted into a network pattern resembling that of the ER (Fig 4.7B). The %

fluorescence at the ERAS was measured and found to be significantly lower than control cells not treated with rapamycin (Fig 4.7C).

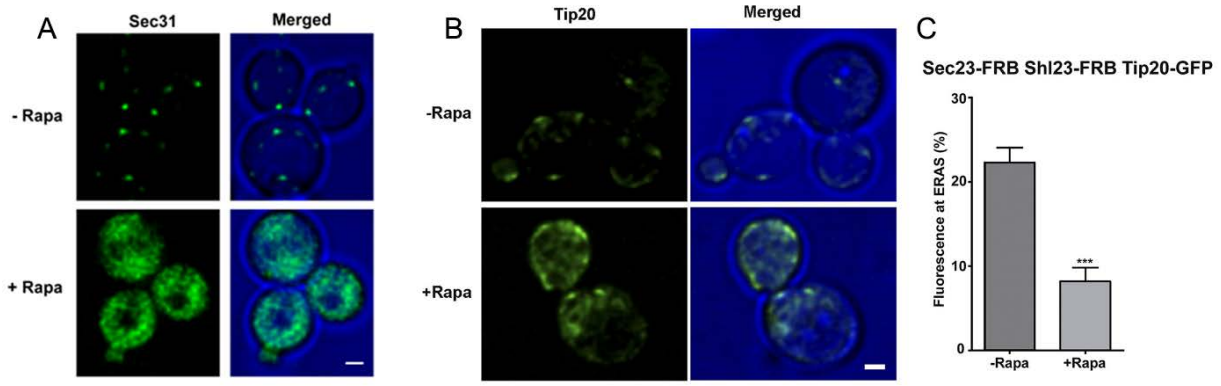


**Figure 4.7: Effect of anchoring away ERES on ERAS.**

(A) Distribution of the ERES marker, Sec31, in a strain expressing the ribosomal anchor, Rpl17-FKBPx4, Sec23-FRB and Shl23-FRB. Images were captured before and after 10 mins treatment with 1µg/µl rapamycin (Rapa). Scale bar, 1µm. (B) Distribution of the ERAS marker, Tip20, in a strain expressing the ribosomal anchor, Rpl17-FKBPx4, Sec23-FRB and Shl23-FRB. Images were captured before and after 10 mins treatment with 1µg/µl Rapa. Scale bar, 1µm. (C) Quantification of the data from B. The percentage of the total GFP signal present at punctate ERAS was measured for ~30 cells in treated and untreated samples. Bars indicate SEM. ***, the punctate fluorescence in the treated sample was significantly lower at $P < 0.0001$.

To further authenticate ERAS and ERES's dependence on each other's existence, we utilized the 'Auxin Induced Degron' system (Nishimura *et al.*, 2009). The AID system allows rapid degradation of target proteins in response to auxin. It makes it possible to generate efficient conditional mutants of essential proteins in yeast to offer a powerful tool to control protein expression and study protein function. The auxin-inducible degron (AID) system employs auxin-dependent poly-ubiquitination of proteins containing AID/IAA sequence by auxin-responsive F-box protein in plants. The SCF complex comprises a cullin subunit, a catalytic RING finger protein (RBX1), the adaptor SKP1 and a variable F-box responsible for substrate recruitment to the SCF complex. In the presence of Indole-3-Acetic Acid (IAA) or auxin hormones, F-box transport inhibitor response 1 (TIR1) associates with the AID degron sequence of the target protein. Ectopic expression of TIR1 and fusing the proteins of interest

with an AID sequence allows reconstitution of the AID system. *Oryza sativa* TIR1 (OsTIR1) was expressed under the control of constitutive *GAP* promoter in *P. pastoris*, which forms a functional SCF ubiquitin ligase and recognize the protein of interest carrying AID tag derived from *Arabidopsis thaliana*, IAA17. SCF-TIR1 acts as an E3 ubiquitin ligase to recruit an E2 ligase, resulting in the AID tagged target protein's polyubiquitylation and proteasomal degradation. The endogenous copy of Sec23 of *P. Pastoris* was C-terminally tagged with 3xmini-IAA. Control experiments using another ERES component, Sec31-GFP, showed pronounced and statistically significant loss of fluorescent signal at ERES (Fig 4.8A, B). Remnant Sec31 spots / ERES are seen, which might be because the Sec23 homologue, Shl23, was not degraded. Shl23 not as efficiently as Sec23 but compensates the activities done by Sec23. However, live-cell imaging of strain expressing OsTIR1 and ER arrival site marker Tip20-3xiGFP and Sec23-3xmini-IAA showed complete dispersal of Tip20 signal within 10-20 minutes upon addition of IAA. The % fluorescence at the ERAS significantly reduced than control cells not treated with IAA (Fig 4.8C, D). Moreover, it was evident that most of the Tip20 were relocated to the general ER. To confirm this, we expressed the translocon protein, Sec63, fused with 3xmCherry, that locates on the rough ER and is evenly distributed over the ER membrane. In a similar experiment, we showed that Tip20 colocalizes with Sec63 under IAA-induced depletion of Sec23, supporting the fact that Tip20 indeed diffuses and redistributes into general ER (Fig 4.8E). These results suggest that the destruction of ER Exit sites lead to disruption of ER Arrival sites.

Further, we overexpressed a dominant-negative GDP-locked mutant of Sar1 GTPase, Sar1(T34N) (Connerly *et al.*, 2005) in a dual colour strain co-expressing Tip20-GFP and Sec13-DsRed. The Sar1(T34N) mutant is expressed under the control of methanol-inducible AOX1 promotor such that transferring the yeast cells to methanol containing media produces a high level of mutant proteins in the cell. Although the Sar1(T34N) mutant overexpression

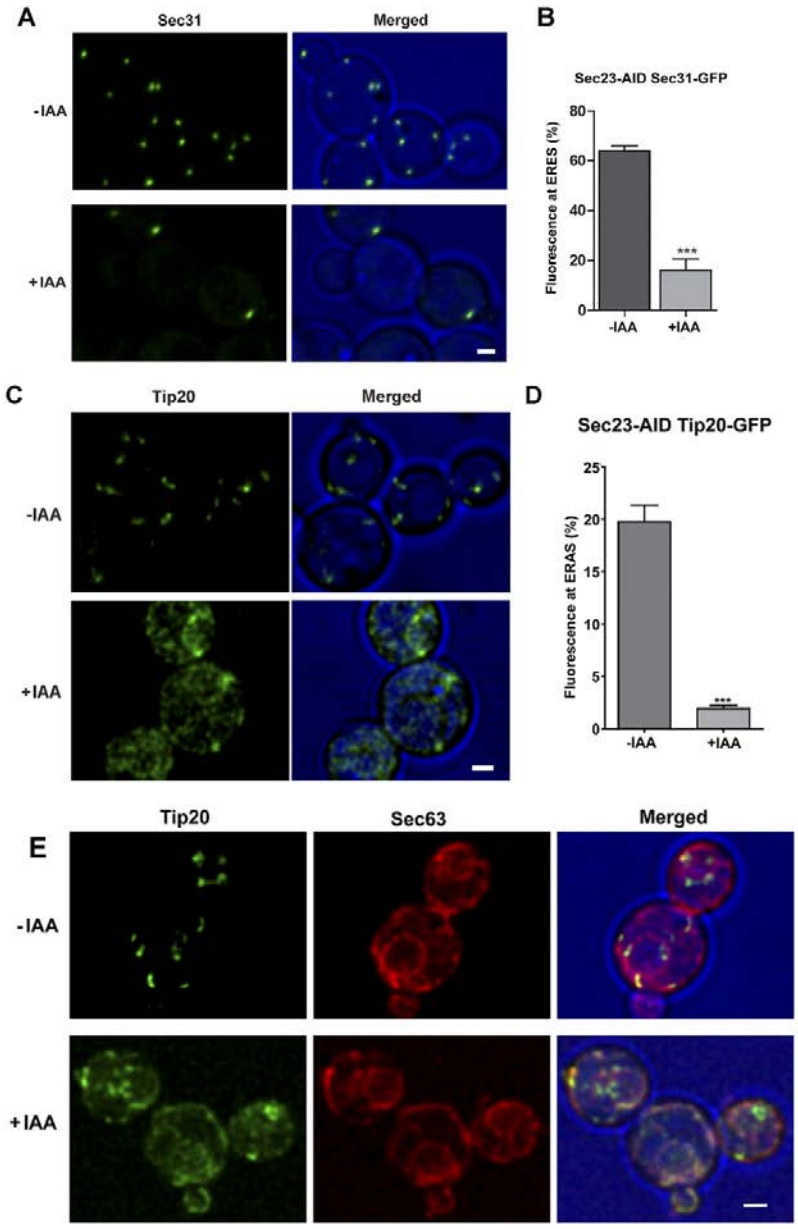


**Figure 4.8: Effect of degradation of ERES on ERAS**

(A) Distribution of the ERES marker, Sec31, in a strain expressing OsTIR1 and Sec23-AID. Images were captured before and after 30 mins treatment with 1mM Indole-3 Acetic acid (IAA). Scale bar, 1μm. (B) Quantification of the data from A. The percentage of total GFP signal present at punctate ERES was measured for ~30 cells in treated and untreated samples. Bars indicate SEM. ***, the punctate fluorescence in the treated sample was significantly lower at $P < 0.0001$. (C) Distribution of the ERAS marker, Tip20, in a strain expressing OsTIR1 and Sec23-AID. Images were captured before and after 15 mins treatment with 1mM IAA. Scale bar, 1μm. (D) Quantification of the data from C. The percentage of the total GFP signal present at punctate ERAS was measured for ~30 cells in treated and untreated samples. Bars indicate SEM. ***, the punctate fluorescence in the treated sample was significantly lower at $P < 0.0001$. (E) Distribution of the Tip20-GFP in a strain expressing the general ER marker, Sec63-

mCherry, OsTIR1 and Sec23-AID. Images were captured before and after 15 mins treatment with 1mM IAA. Scale bar, 1μm.

inhibits cell growth, it does not dislocate the ER exit sites. However, it does drastically decrease the *de novo* formation events of ERES. On shifting the yeast cells from glycerol to methanol-containing media, the number of Sec13 puncta drastically reduces as compared to control cells growing in non-inducing glycerol containing media. On the other hand, the effect on ERAS was drastic such that there was a complete delocalization of the Tip20 signal from its specific punctate nature (Fig 4.9). This result indicates that the biogenesis of ERES is necessary for the organization of ERAS.

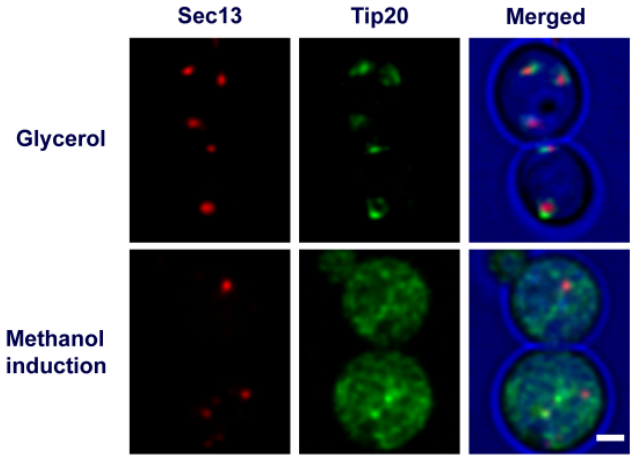


**Figure 4.9: Effect of perturbed de novo formation of ERES on ERAS.**

Distribution of Sec13-DsRed and Tip20-GFP in a strain overexpressing dominant-negative GDP-locked Sar1(T34N) mutant under methanol induction. Images were captured for control cells grown in non-inducing glycerol containing media (upper panel) and cells grown in methanol-containing media for 4 hours (lower panel). Scale bar, 1μm.

Next, we looked at the effect of an essential ER exit site associated factor, Sec16, on ER Arrival sites' stability. Sec16 has been proposed to influence COPII assembly and regulate COPII turnover by retarding Sar1-GTP hydrolysis (Connerly *et al.*, 2005; Bharucha *et al.*, 2013). As

previously reported, a temperature-sensitive Pro-1092-to-Leu mutation within the central conserved domain (CCD; residues 1030–1459) of Sec16 strain (P1092L) displayed changed ERES patterns at 37°C. ERES became numerous, smaller and dynamic as compared to wild-type cells. We wanted to see ER arrival sites' fate when the ER exit sites are forcefully modulated through this temperature-sensitive Sec16 mutation that was reported to cause fragmentation of ER exit sites at non-permissive temperatures (Bharucha *et al.*, 2013). We labelled both ER exit site by Sec13-DsRed and ER arrival sites by Tip20-GFP in this Sec16 temperature-sensitive mutant strain. We found that ER arrival sites showed weak fluorescence spread over the cells. However, punctate signal was visible that co-localized with fragmented ER exit sites (Fig 4.10A). For further clarification, we functionally depleted Sec16 by the anchor away system. Such depletion of Sec16 has shown a minor effect on the overall stability of ER exit sites. However, due to accelerated COPII turnover, the steady-state size of ERES drastically reduces and leads to multiple ERES formation (Bharucha *et al.*, 2013). We tested the behaviour of ERAS under such condition in a strain carrying the RPL17-FKBP ribosomal anchor and expressing Sec16-FRB, and Tip20-GFP. Upon addition of rapamycin, Sec16 was removed from ER exit sites, and Tip20 labelled punctate structures seemed a little dispersed, but distinct ER arrival sites remained visible. When we compared the fraction of fluorescence at ERAS, we found very little insignificant difference between the wild-type and the ‘Sec16 anchor away' conditions (Fig 4.10B). These results indicate that perturbation of Sec16 function has mild or almost no effect on ER arrival sites’ stability. Alternatively, in other words, Sec16 possibly does not regulate ER arrival site assembly the way it does for ERES. Hence, we can extrapolate that the presence and biogenesis of ERES are essential for the maintenance of ERAS; however, its organization and dynamics may not interfere with the immediate behaviour of ERAS.

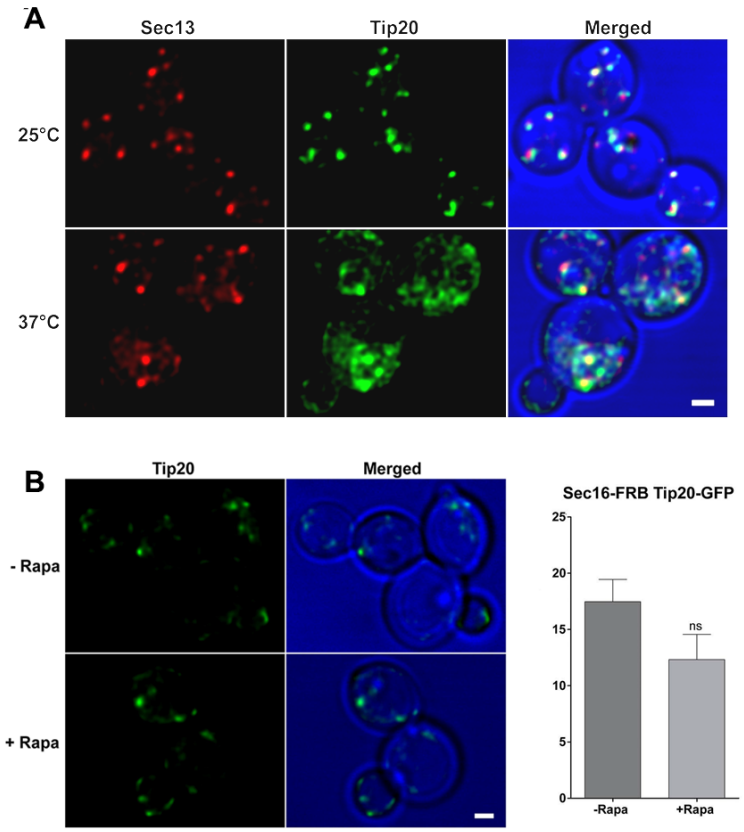


**Figure 4.10: Effect of depleting Sec16 on ERAS.**

(A) Distribution of Sec13-DsRed and Tip20-GFP in a strain carrying P1092L mutation in Sec16. Images are captured from cells grown at a permissive temperature at 25°C (upper panel) and non-permissive temperature at 37°C for 1h (lower panel). Scale bar, 1µm. (B) Distribution of Tip20 in a strain expressing Rpl17-FKBP ribosomal anchor and Sec16-FRB. Images were captured before and after 30 mins treatment with 1µg/µl Rapa. Scale bar, 1µm. (C) Quantification of the data from B. The percentage of the total GFP signal at punctate ERAS was measured for ~30 cells in treated and untreated samples. Bars indicate SEM. ***, the punctate fluorescence in the treated sample was significantly lower at $P < 0.0001$.

### 4.1.7 Destruction of ER arrival sites (ERAS) does not affect ER exit sites (ERES).

As a complementary experiment, we wanted to examine the destruction of ER arrival sites on the ER exit site. For this purpose, we first tried to functionally inactivate the ERAS component Tip20 by anchor away in a control experiment. We expressed Tip20 with dual FRB-GFP tag in a strain along with ribosomal protein Rpl17 tagged with FKBP. We saw Tip20 lose its punctate nature within 5-10 mins of rapamycin treatment (Fig 4.11A). In the test experiment, the ERES marker, Sec31-GFP, was expressed in a strain along with RPL17-FKBP ribosomal

anchor and Tip20-FRB. Tip20 anchor away did not affect the Sec31 localization pattern (Fig 4.11B). Even after 60 minutes of rapamycin treatment, the Sec31 localization pattern remained the same as untreated cells. We found a slight increase in the % fluorescence intensity at ERES in ‘Tip20 anchor away' conditions compared to the wild type. To further authenticate our results, we depleted Tip20 by AID in a strain expressing OsTIR1 and another ERAS component, Dsl3-3xiGFP. Within 10 mins after IAA addition, most of the Dsl3-GFP punctate structures diffused into ER pattern (Fig 4.11C), suggesting, AID of Tip20 is sufficient to destroy ER arrival sites. When we expressed AID tagged Tip20 in a strain expressing OsTIR1 and Sec31-GFP, we found no effect on Sec31 localization upon auxin-mediated degradation of Tip20. Sec31 maintained its punctate pattern even after 60 minutes of IAA treatment (Fig 4.11D). When we compared the percentage fluorescence at ERES before and after degradation of Tip20, we again found a minor increase in the fluorescence at the ER exit sites. All these results suggest that disruption of ER arrival sites might have a little or almost no visible effect on the stability or organization of ER exit sites. However, the quantification result is somehow concomitant with earlier reports that show the mutant form of Tip20 causes back-fusion of the COPII vesicles (Kamena and Spang, 2004), which might be due to a lack of ER retrieval of ER-resident adaptor and transport proteins required for the anterograde movement of vesicles.

### 4.1.8 Depletion of COPI have a dramatic effect on ERAS but does not affect ERES.

Next, we wanted to ask whether depletion of incoming COPI proteins affects ER arrival sites' stability. We have approached this question both by AID and anchor away methods as earlier. To verify whether we can successfully deplete Sec26, an essential beta-COPI coat subunit of COPI vesicles by anchor away, we created a strain where Sec26 was simultaneously labelled with FRB along with a GFP tag to visualize its localization post rapamycin treatment. After

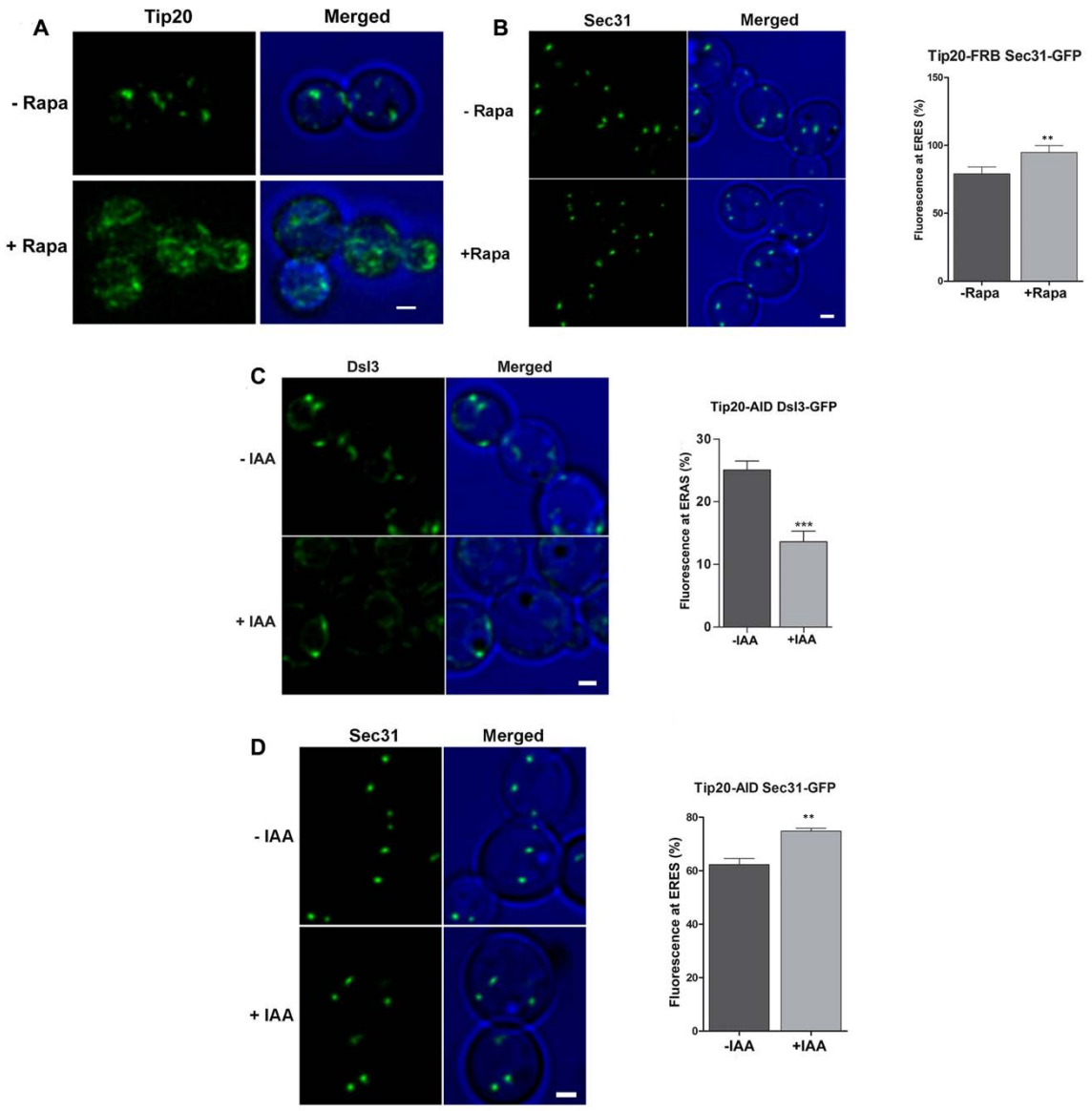


**Figure 4.11: Effect of disruption of ERAS on ERES.**

(A) Redistribution of Tip20-FRB-GFP in a strain expressing Rpl17-FKBPx4 ribosomal anchor. Images were captured before and after 10 mins treatment with 1µg/µl Rapa. Scale bar, 1µm. (B) Distribution of the ERES marker Sec31-GFP before and after anchor-away of the ERAS component, Tip20. Images were captured before and after treatment 40 mins with 1µg/µl Rapa. Scale bar, 1µm. The percentage of the total GFP signal at punctate ERES was measured for ~30 cells in the treated and untreated samples. Bars indicate SEM. **, $P < 0.005$. (C) Diffused pattern of the Dsl1 complex subunit, Dsl3-GFP after auxin-induced degradation of Tip20. Images were captured before and after 15 mins treatment with 1mM IAA. Scale bar, 1µm. The percentage of the total GFP signal at punctate ERAS was measured for ~30 cells in the treated and untreated samples. Bars indicate SEM. ***, the punctate fluorescence in the treated sample was significantly lower at $P < 0.0001$. (D) Distribution of Sec31-GFP before and after auxin-induced degradation of Tip20. Images were captured before and after 50 mins treatment with

1mM IAA. Scale bar, 1μm. (D) The percentage of the total GFP signal at punctate ERES was measured for ~30 cells in the treated and untreated samples. Bars indicate SEM. **, P < 0.005.

rapamycin addition, the strain shows complete disintegration of the COPI localization pattern and depletion from its native congregated ring-like pattern within 10 minutes (Fig 4.12A). We then depleted Sec26 by anchor away method in a strain expressing Tip20-GFP. We observed dispersal of Tip20 signal as it becomes readily displaced to a general ER pattern on the addition of rapamycin, and all the ER arrival sites were destroyed within 10 minutes (Fig 4.12B). We saw the same result on degrading Sec26 by AID. Upon addition of IAA, within 10 minutes, Tip20 labelled sites tend to disappear and relocate to ER network. (Fig 4.12D). We quantified the remaining fluorescence at the ERAS when COPI was degraded upon AID and found it to be significantly lower than the control cells not treated with IAA. These results suggest that possibly COPI proteins stabilize the Dsl1 complex organization. In other words, a constant flow of COPI is required for the maintenance of ER Arrival sites. The next immediate complementary question was whether COPI has any effect on ER exit sites. Surprisingly, rerouting or degrading Sec26 by anchor away or AID did not affect Sec31 localization to punctate ERES (Fig 4.12C, F).

Therefore, COPI is essential for ER arrival site's stability but not essential for ER exit site's stability. However, we found a slight increase in the % fluorescence at the ERES upon COPI depletion by AID compared to the control cells not treated with IAA (Fig 4.12G). This result was similar to the earlier result, where the loss of ERAS had the same effect on ERES. It is clear from the above results that the effect of COPI depletion on the biogenesis of ERAS is direct. The role of ERES is upstream of COPI as COPI depletion does not affect the biogenesis of ERES structure. All these results intrigued us to investigate further the mechanism of ERAS organization.

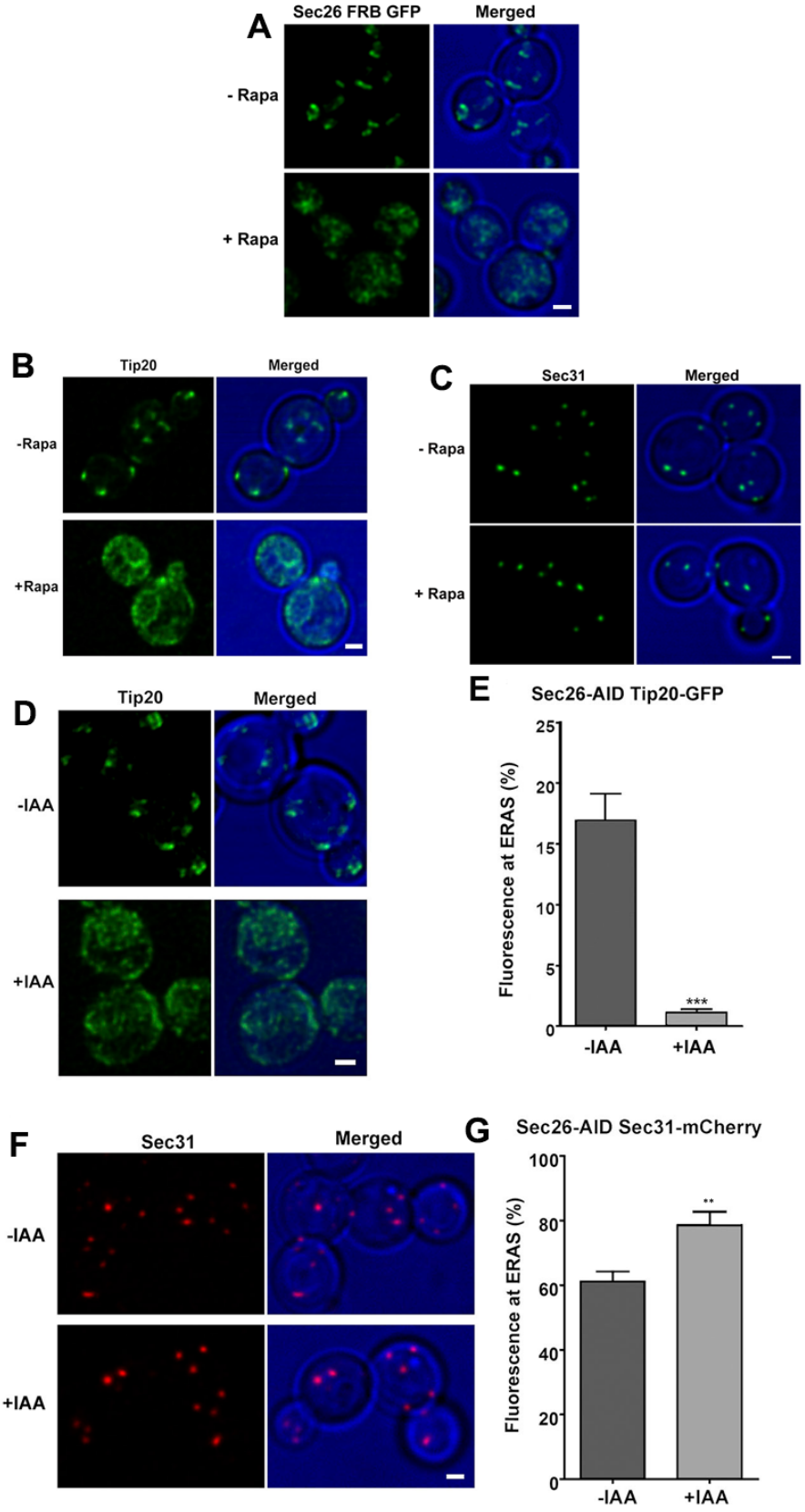


**Figure 4.12: Effect of COPI depletion on ERAS and ERES**

(A) Redistribution of COPI coat subunit, Sec26 simultaneously tagged with FRB and GFP, to ribosomes by the anchor-away. Images were captured before and after 10 mins treatment with

1μg/μl Rapa. Scale bar, 1μm. (B) Distribution of Tip20-GFP before and after rerouting COPI in yeast cells, expressing Rpl17-FKBPx4 and Sec26-FRB. Images were captured before and after 10 mins treatment with 1μg/μl Rapa. Scale bar, 1μm. (C) Distribution of Sec31-GFP before and after COPI anchor-away. Images were captured before and after 40 mins treatment with 1μg/μl Rapa. Scale bar, 1μm. (D) Distribution of Tip20-GFP before and after degradation of COPI in yeast cells, expressing OsTIR1 and Sec26-AID. Images were captured before and after 10 mins treatment with 1mM IAA. Scale bar, 1μm. (E) Quantification of percentage of the total GFP signal at punctate ERAS from D, measured for ~30 cells in treated and untreated sample. Bars indicate SEM. ***, the punctate fluorescence in the treated sample was significantly lower at $P < 0.0001$. (F) Distribution of Sec31-mCherry before and after auxin-induced degradation of COPI. Images were captured before and after 40 mins treatment with 1mM IAA. Scale bar, 1μm. (G) Quantification of percentage of the total GFP signal at punctate ERES from F, measured for ~30 cells in treated and untreated sample. Bars indicate SEM. **, $P < 0.005$.

### 4.1.9 Loss of ERES depletes COPI vesicles.

Perturbation of ERES biogenesis and depletion of COPI leads to displacement of ERAS. Moreover, COPI depletion does not affect the punctate organization of ERES. The following missing link that remains to be explored is the effect of ERES loss on COPI vesicles. To investigate this issue, we utilized the anchor away method to reroute the essential ERES component, Sec23 and its homologue Shl23, to ribosomes to sequester its functional activity upon rapamycin induction. As shown in earlier experiments, functional inactivation of Sec23 and Shl23 inhibits punctate ERES sites. We expressed GFP tagged Sec26 or beta subunit of the COPI in a strain expressing Sec23-AID and Shl23-AID together with Rpl17-FKBP ribosomal anchor. Upon addition of rapamycin, we found that Sec26 lost its ring-like punctate pattern and became cytosolic within 10 minutes (Fig 4.13A). We further perturbed the *de novo* formation of ERES by expressing the GDP-locked Sar1(T34N) mutant under methanol induction in a strain expressing Sec26-GFP and found a similar dispersal of the COPI signal (Fig 4.13B). This result suggests that ERES may influence COPI formation and localization. Since ERES also influence ERAS organization, it might result in two possibilities. One, that absence of ERES disrupts the ERAS that in turn causes delocalization of COPI. Reports in *S.*

*cerevisiae* have shown mis-localization of COPI in a strain carrying a mutation in the lasso domain of Dsl1, rendering it unable to interact with the COPI vesicles such that no BiFc spots are formed between the Dsl1 complex and COPI vesicles (Schröter, Beckmann and Schmitt, 2016). Second, since COPII vesicles fuse to form the cis Golgi cisterna (Glick and Malhotra, 1998), the above result can be explained by the hypothesis that ERES functions in Golgi biogenesis, which in turn bud COPI vesicles that further organize ERAS. We investigated the problems one by one.

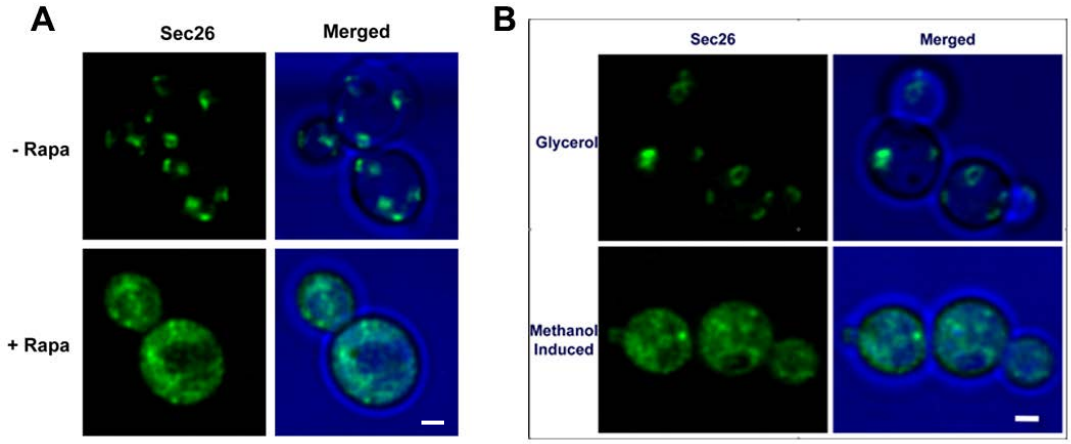


**Figure 4.13: Perturbation of ERES biogenesis depletes COPI vesicles.**

(A) Redistribution of COPI coat subunit, Sec26-GFP on disruption of ERES by anchor away. Images were captured before and after 10 mins treatment with 1µg/µl Rapa. Scale bar, 1µm. (B) Distribution of Sec26-GFP in a strain overexpressing dominant-negative GDP-locked Sar1(T34N) mutant under methanol induction. Images were captured for control cells grown in non-inducing glycerol containing media (upper panel) and cells growing in methanol-containing media for 4 hours (lower panel). Scale bar, 1µm.

### 4.1.10 Loss of ERAS leads to accumulation of COPI vesicles.

We expressed the COPI marker, Sec26-GFP, in yeast cells along ERAS component, Tip20-FRB and ribosomal protein, Rpl17-FKBP. Upon addition of rapamycin, Tip20 was delocalized to ribosomes (shown earlier), but there was no difference in COPI's localisation that formed a typical ring-like punctate pattern. However, we could see a visible increase in the fluorescence intensity of the puncta under 'Tip20 anchor away conditions' compared to the control cells not

treated with rapamycin. We could see a decrease in the rings' central area of clearance (Fig 4.14A). To confirm our observation, we quantified the fraction of fluorescence at the puncta before and after 30 mins rapamycin treatment. We found a significant increase in % fluorescence comparable to the former observation (Fig 4.14B). These results suggest that COPI vesicles might not fuse to the ER and accumulate at the periphery of the Golgi. The result can be supported by earlier observations that show a similar accumulation of vesicles in *tip20* mutant cells (Zink *et al.*, 2009).

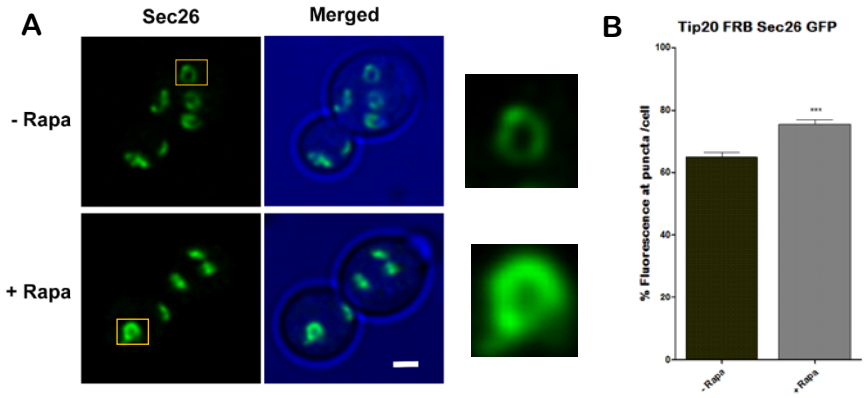


**Figure 4.14: Perturbation of ERAS leads to accumulation COPI vesicles.**

(A) Distribution Sec26-GFP in a strain expressing Rpl17-4xFKBP ribosomal anchor and Tip20-FRB. Images were captured before and after 30 mins treatment with 1µg/µl Rapa. Scale bar, 1µm. (B) Quantification of percentage of the total GFP signal at punctate COPI from A, measured for ~30 in each sample. Bars indicate SEM. ***, the punctate fluorescence in the treated sample was significantly higher at $P < 0.0001$.

### 4.1.11 Disruption of ERES affects Golgi organization

We destroyed the ERES by anchoring-away the COPII subunit, Sec23 and its homologue Shl23 in a yeast cells expressing Vig4, early/cis-Golgi marker. Upon addition of rapamycin, Vig4 punctate structures lost its regular pattern (Fig 4.15A). The same result was obtained with late/trans Golgi, labelled with Sec7-GFP under ‘Sec23/Shl23 anchor away’ conditions. Sec7 puncta also lost its punctate pattern after rapamycin treatment (Fig 4.15B).

We further perturbed the *de novo* formation of ERES by overexpressing Sar1(T34N) GDP-locked mutant under AOX1 promotor in a Golgi two-colour strain expressing GFP-Vig4 and

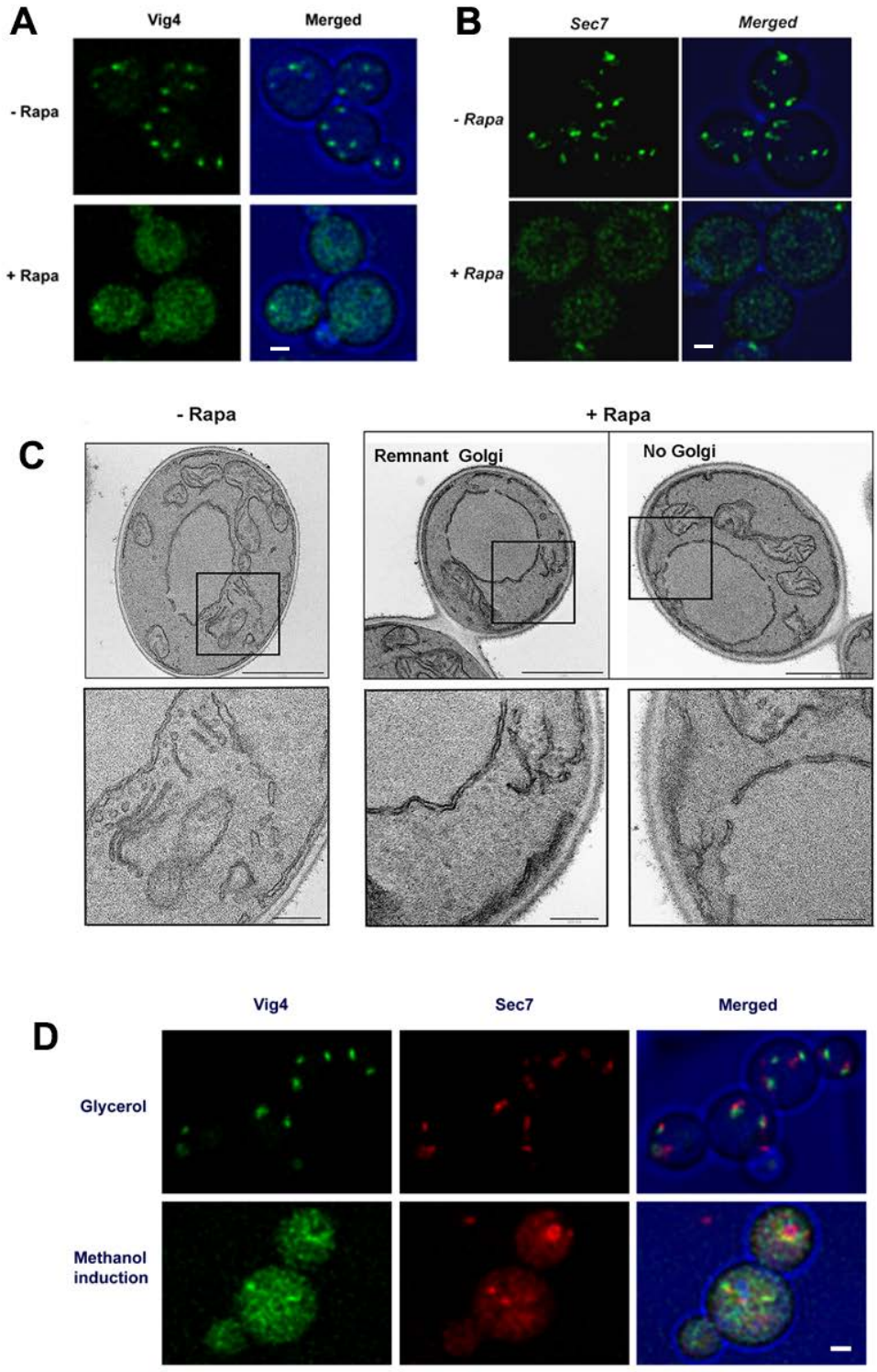


**Figure 4.15: Disruption of ERES affects Golgi organization**

(A) Redistribution of early Golgi marker, GFP-Vig4 in yeast cells carrying Rpl17-4xFKBP ribosomal anchor along with Sec23-FRB and Shl23-FRB. Images were captured before and after 10 mins treatment with 1µg/µl Rapa. Scale bar, 1µm. (B) Redistribution of late Golgi marker, Sec7-GFP on sequestering Sec23 and Shl23 by anchor away. Images were captured before and after 10 mins treatment with 1µg/µl Rapa. Scale bar, 1µm. (C) Representative thin-section electron micrographs of *P. pastoris* cells on depletion of ERES by anchor away,

showing either complete absence of tightly stacked Golgi structures or remnant loose Golgi structures, after treatment with 1μg/μl Rapa for 15 min. Scale bars, 1μm (top) or 200 nm (bottom). (D) Distribution of cis and trans cisterna in dual labelled Golgi strain with GFP-Vig4 and Sec7-GFP, overexpressing dominant negative GDP-locked Sar1(T34N) mutant under methanol induction. Images were captured for control cells grown in non-inducing glycerol containing media (upper panel) and after growing in methanol-containing media for 4 hours (lower panel). Scale bars, 1μm

Sec7-DsRed. On shifting the cells from SY- Glycerol to methanol containing media, the typical stacked green and red traffic-light pattern displayed by cis and trans cisterna, respectively, was lost entirely (Fig 4.15D).

Moreover, we performed thin-section Transmission Electron Microscopy (TEM) with *P. pastoris* cells expressing Sec23-FRB and Shl23-FRB along with RPL17-FKBP ribosomal anchor. We processed the cells for EM after 15 mins of rapamycin treatment. We observed tight stacks of Golgi cisternae in the untreated control cells. By contrast, the Golgi was almost absent in the cells where ERES was disrupted. However, few cells showed remnant membranous structures assumed to be less-organized Golgi stacks (Fig 4.15C). All these results conclude that the absence of ERES lead to the complete abolition of the Golgi organization. The result supports the earlier possibility that ERES give rise to Golgi cisterna that produces COPI vesicles, which organize ERAS.

### 4.1.12 Loss of COPI affects Golgi organization.

We labelled early Golgi marker Vig4 and late Golgi marker Sec7 separately in a strain expressing Sec26-FRB to deplete COPI vesicles and Rpl17-FKBP ribosomal anchor. Interesting, we found that Vig4 no longer showed punctate structure (Fig 4.16A); however, distorted and larger aggregated residual Sec7 puncta was still visible after 20 minutes of rapamycin treatment (Fig 4.16B). COPI vesicles are responsible for Golgi to ER as well as intra-Golgi anterograde transport. Golgi-resident enzymes that escape during cisternal maturation are retrieved from the previous cisternae via COPI vesicles (Glick, Elston and Oster,

1997). As expected, the cis cisternae marked by Vig4 is primarily depleted due to lack of incoming intra-Golgi COPI vesicles from late Golgi cisterna and, as a consequence, trans cisternae marked by Sec7 become aggregated due to accumulation of cargo. Therefore, in the absence of COPI, the Golgi organization is affected, but no effect is seen on the ERES organization (shown earlier). Hence, we can extrapolate that loss of Golgi organization does not affect ERES structure, strengthening the fact that ERES generate Golgi.

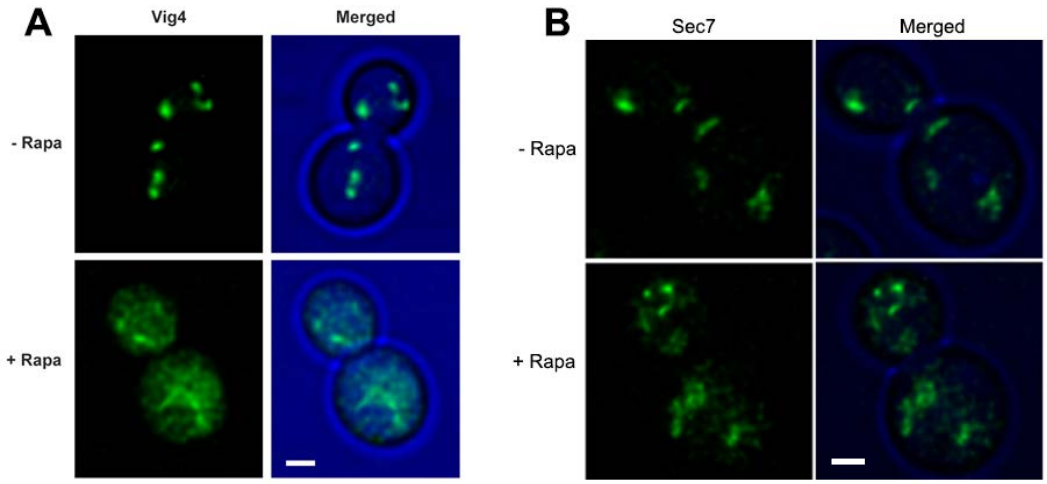


**Figure 4.16: Loss of COPI affects Golgi organization**

(A) Distribution of early Golgi marker, GFP-Vig4 in yeast cells expressing Sec26-FRB and Rpl17-FKB ribosomal anchor. Images were captured before and after treatment with 1µg/µl Rapa for 20 min. Scale bar, 1µm. (B) Distribution of late Golgi marker, Sec7-GFP under COPI anchor away conditions. Images were captured before and after treatment with 1µg/µl Rapa for 10 min. Scale bar, 1µm.

### 4.1.13 Perturbation of ERAS do not affect Golgi structure.

We performed additional experiments to test the effect of ERAS in supporting the Golgi morphology. When ERAS were perturbed by sequestering Tip20 to ribosomes by anchor away, fluorescence studies showed no detectable change in the Golgi pattern depicted by GFP-Vig4 (Fig 4.17A) and Sec7-GFP (Fig 4.17B) expressed separately with Tip20-FRB and Rpl17-FKBP. Upon quantifying the above data after 40 minutes of rapamycin treatment, we found a significant increase in the % fluorescence of the Vig4 signal compared to the untreated control

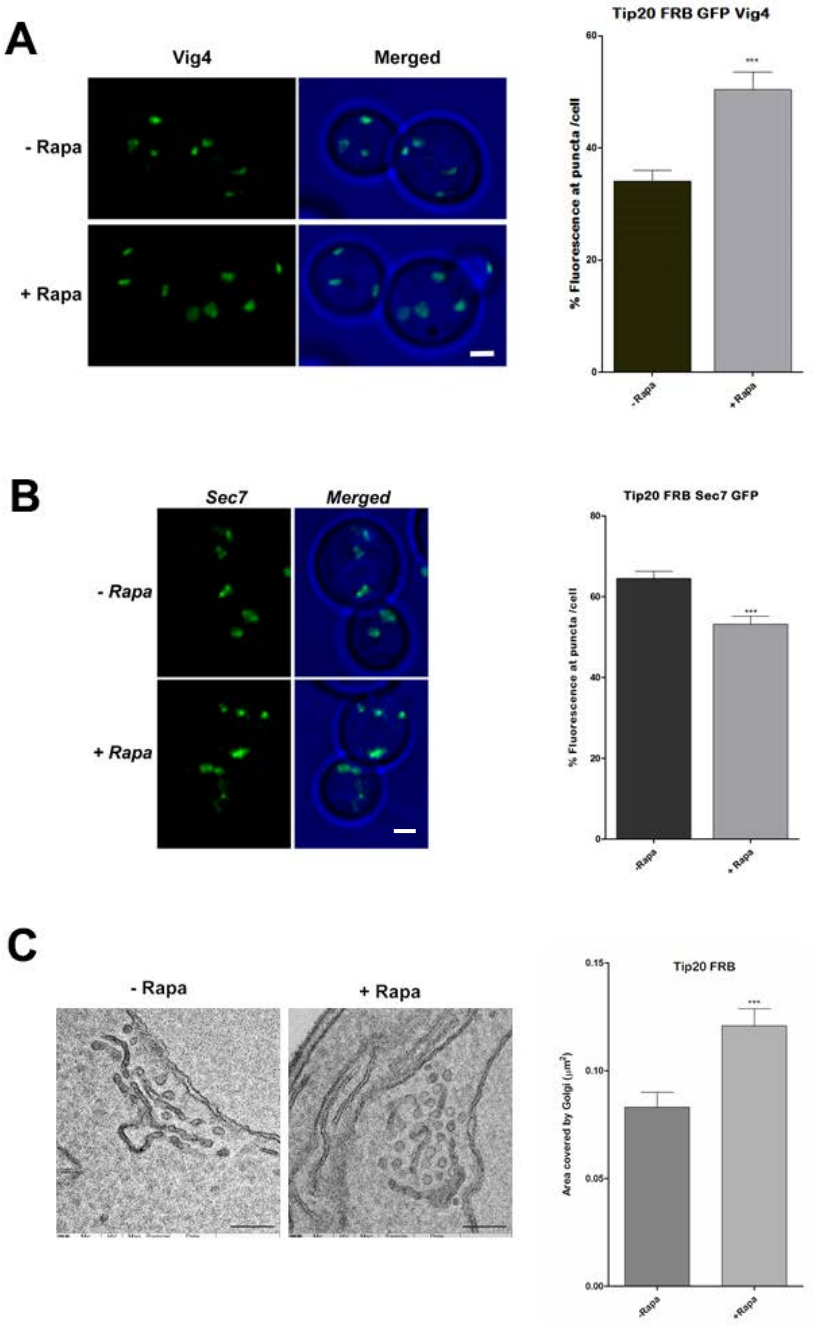


**Figure 4.17: Effect of ERAS perturbation on Golgi structure.**

(A) Distribution of early Golgi marker, GFP-Vig4 in yeast cells carrying Tip20-FRB and Rpl17-FKB ribosomal anchor. Images were captured before and after 40 mins treatment with 1µg/µl Rapa. Scale bar, 1µm. The percentage of the total GFP signal at punctate cis Golgi was measured for ~30 cells in treated and untreated samples. Bars indicate SEM. *** indicate statistical significance at $P < 0.0001$ (B) Distribution of late Golgi marker, Sec7-GFP under Tip20 anchor away conditions. Images were captured before and after 40 mins treatment with 1µg/µl Rapa. Scale bar, 1µm. The percentage of the total GFP signal at punctate trans Golgi was measured for ~30 cells in treated and untreated samples. Bars indicate SEM. *** indicate statistical significance at $P < 0.0001$ (C) Representative thin-section electron micrographs yeast cells on depletion of ERAS by anchor away, showing enlarged vesiculated stacked Golgi units

after treatment with Rapa for 30 mins. Scale bar, 200nm. Quantitative data from thin section electrograph were measured using iTEM software. The total area covered by Golgi apparatus was measured by drawing outline along the boundary of the entire stacked Golgi unit. Bars indicate SEM for ~20 individual cells. *** indicate statistical significance at $P < 0.0001$.

cells, whereas, on the contrary, Sec7 puncta showed a mild decrease in % fluorescence. These results indicate a block in the retrograde transport and support the earlier result that COPI vesicles accumulate at the cis-Golgi periphery. Retrograde block leads to enlargement of the early Golgi due to accumulated cargo, and shrinkage of the late Golgi might be due to depletion of cargo. The plausible fact can explain the latter that back-fusion of COPII vesicles in the absence of the Dsl1 tethering complex restricts COPII movement to Golgi, limiting the cargo reaching trans-Golgi. We further resorted to electron microscopy to look at the structural details of Golgi apparatus under 'Tip20 anchor away' conditions. We found an enlarged and visibly vesiculated Golgi structure in the rapamycin-added cells compared to typical tight Golgi stacks in the untreated control cells. We quantified the EM micrographs using iTEM software and found the Golgi apparatus area significantly more than the wild type cells in the absence of ERAS.

#### 4.1.14 Discussion

We found that the Dsl1 complex assembles into an ER sub-domain for receiving incoming COPI vesicles defining the ER arrival site in *P. pastoris*. The idea of a site was postulated for vesicle budding and tethering at ER and Golgi (Spang, 2009). Studies in *S. Cerevisiae* have shown Dsl1 complex form numerous hotspots for COPI vesicle capturing (Schröter, Beckmann and Schmitt, 2016), the organization and dynamics of which were not clearly defined. Many groups have shown the proximity between COPI and COPII function at the ER-Golgi interface (Stephens *et al.*, 2000; Levi *et al.*, 2010; Lerich *et al.*, 2012). We found that ERES and ERAS form a typical bipartite sub-domain on the ER membrane; ERES forming a central core with

multiple budding COPII vesicles and ERAS encircling it with concentrated COPI vesicles (Fig 4.18C) together creating a bidirectional transport site. The ER exit sites play a central role in maintaining the secretory unit in *P. pastoris* comprising the COPII, COPI, and Golgi in a closely associated ultrastructure depicted in a three-colour strain; Sec13-HaloTag, Sec26-mCherry and GFP-Vig4, respectively showing their relative arrangement (Fig 14.8A). According to our findings, we generated a working model (Fig 14.8B); ERES generate the Golgi apparatus that produces COPI vesicles that mostly emerge and cluster at the periphery of early Golgi cisterna around 400 nm in size (Tie *et al.*, 2018). Hence, by diffraction-limited microscopy, we see a ring-like pattern formed by the fluorescent fusion of beta-COP protein Sec26 when observed from an ideal orientation. Based on our results, we suggest that in the Dsl1 complexes assemble directly adjacent to the Golgi-derived COPI vesicles. Dsl1 complex tethers the COPI vesicles (Ren *et al.*, 2009) and anchors and assembles ER-localized SNAREs at the base on the ER membrane (Meiringer *et al.*, 2011). Therefore, the Dsl1 complex decorates in a similar ring-like fashion corresponding to COPI vesicles as ER Arrival sites. For this reason, we can see Tip20 or Dsl3 also forming a similar ring as illustrated by the Sec26 signal. It is to be noted that Tip20/Dsl3 and Sec26 signals are not entirely resolved, although the ER and Golgi membranes' flat surfaces are 150 nm apart. It can be explained by the fact that the estimated length of the Dsl1 complex anchored at ER plane by ER-localized COPI SNARE proteins is approximately 70 nm (Travis *et al.*, 2020) that can extend and form a dynamic bridge between ER to early Golgi plane by reaching out back and forth to connect and capture budding COPI vesicles. Thus, all the components of the secretory unit in *P. pastoris* are inter-related to each other. To summarize, in the absence of ERES, there is no formation of Golgi apparatus that further is unable to bud COPI vesicles which creates the ERAS. In the absence of ERAS, COPI vesicles accumulates at the cis Golgi blocking the retrograde transport which further might lead to block in the anterograde ER-Golgi transport.

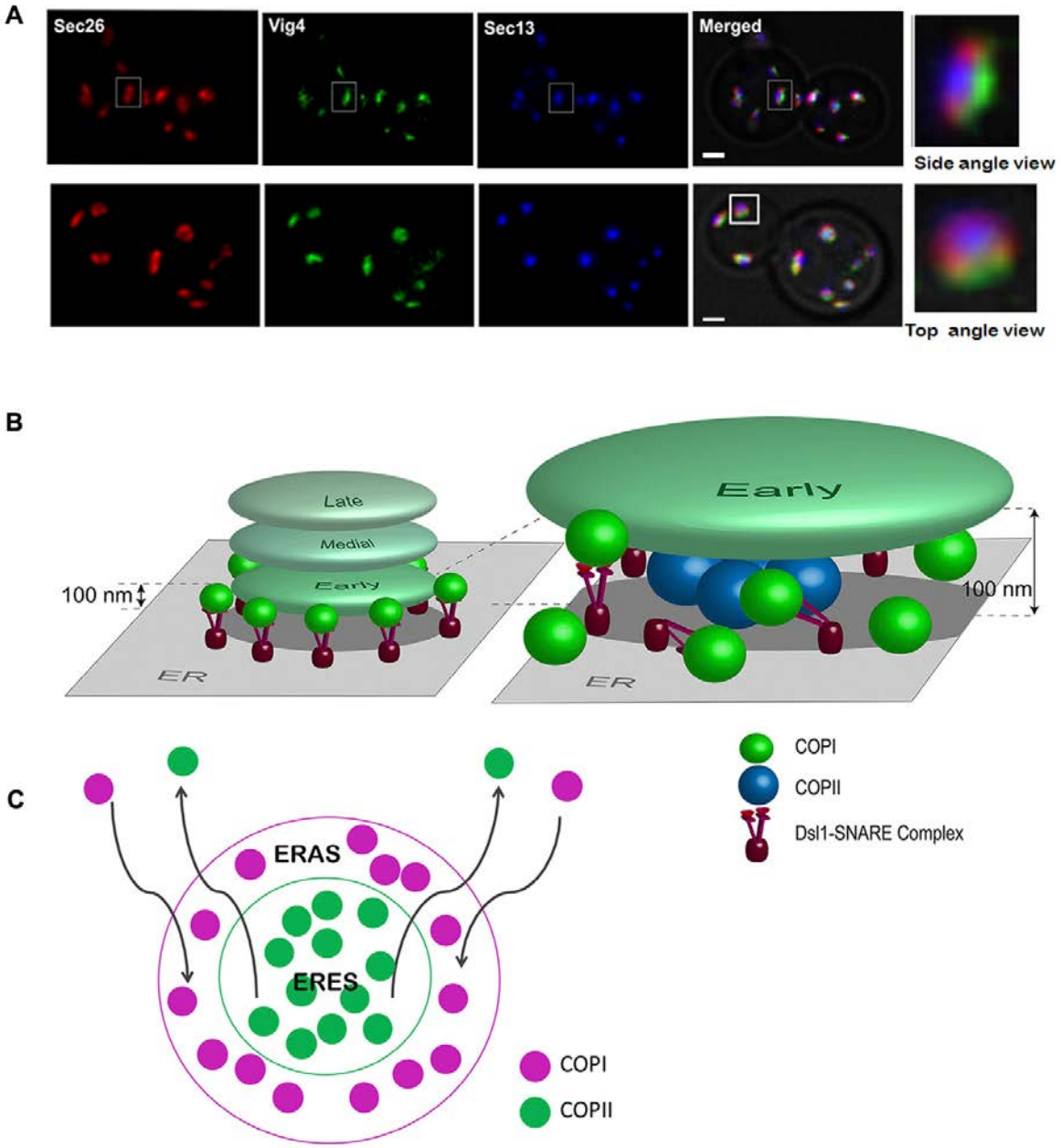


**Figure 4.18: Working model of the Secretory unit in P. pastoris**

(A) Relative localizations of the early Golgi, COPI and COPII labelled in a strain expressing GFP-Vig4, Sec26-mCherry and Sec13-HaloTag, respectively. Cells were stained with $JF_{646}$ before three-color 4D imaging. Scale bars, 1μm. (B) Schematic diagram showing the arrangement of the secretory unit in *P. pastoris*. The right panel shows the enlarged and more elaborated representation of the distribution of COPI and COPII vesicles at the ER–Golgi interface. COPII arise from ERES and fuse to adjoining early Golgi cisterna. COPI emerge from the periphery of cis Golgi and tether to the Dsl1 complex anchored to ER-localized SNAREs. (C) Model showing ERAS capturing COPI vesicles and surrounding COPII producing ERES.

## 4.2 Exosome Entry Sites in mammalian cells.

### 4.2.1 Introduction

Exosomes are small extracellular vesicles, ranging from 30-100 nm in size. These membrane-bound vesicles transport proteins, lipids, nucleic acid and other metabolites between cells. The functions of exosomes have been implicated in immune response, neurodegenerative diseases and cancer progression. Exosomes originate from the endomembrane system. Inward budding of the endosomal membrane sorts cytosolic components and endosomal membrane components into the intraluminal vesicles (ILVs) inside the lumen of the endosomes called multi-vesicular bodies (MVBs). MVBs fuse with the plasma membrane to release exosomes in the extracellular milieu (Kowal, Tkach and Théry, 2014). Various mechanisms have been reported for the uptake of exosomes in the recipient cells; however, it is much debated depending on the source of exosomes and the type of recipient cells and downstream function that the exosomes are meant to execute (McKelvey *et al.*, 2015). We hypothesize that exosomes, like most other vesicles, must possess an entry site on the recipient cell's plasma membrane.

### 4.2.2 Exosomes enter the recipient cell via a specific entry point

We isolated exosomes from cultured mammalian cells by differential centrifugation of the conditioned media. We characterized the purified vesicle population using electron microscopy. The negatively stained sections showed vesicles in a size range of 50-100 nm (Fig 4.19A) that resembled the morphology of previously described electron micrographs of exosomes (Théry *et al.*, 2006). We labelled the dense pool of exosomes (HCT116-derived) with a general lipophilic dye, PKH26. Labelled exosomes were incubated with the Int407 cell line. Punctate structures became visible within 6 hours of incubation, and a more significant number of punctate structures became visible within 12 of exosome addition (Fig 4.19B).

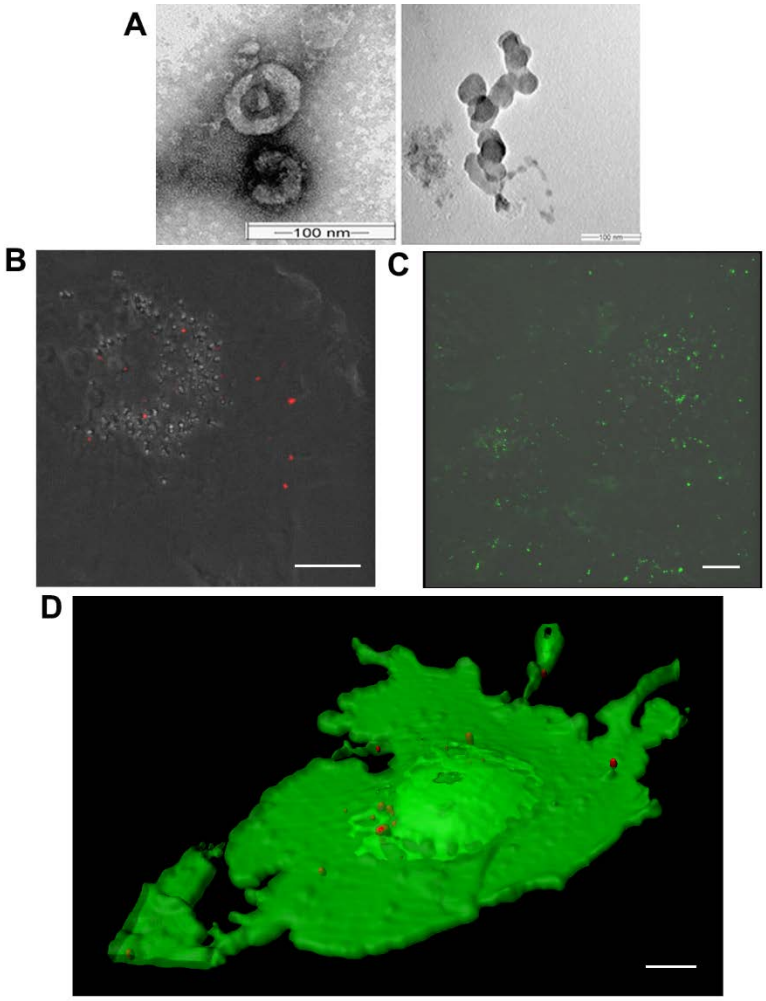


**Figure 4.19: Exosome entry site**

(A) EM micrograph showing negative staining of exosomes. Scale bar, 100nm. (B) Distribution of PKH26-labelled HCT116-derived exosomes incubated with Int407 mammalian cell line for 12 hours. Scale bar, 10μm. (C) Distribution of GFP-CD63 labelled U2OS-derived exosomes incubated with U2OS mammalian cell line for 12 hours. Scale bar** (D) 3D reconstruction of U2OS transiently transfected with farnesylated-GFP and incubated with PKH26-labelled U2OS-derived exosomes for 12 hours. Scale bar, 10μm.

A punctate pattern indicated that multiple exosomes might accumulate on the plasma membrane at a putative Exosome Entry Site (EES). We confirmed this phenomenon by labelling the exosomes using GFP fusion of the tetraspanin CD63 that is specifically enriched in exosomes. We found a similar punctate pattern within 8-12 hours of incubation of fluorescent exosomes (U2OS-derived) with the U2OS cell line (Fig 4.19C). We further labelled the plasma membrane of U2OS cells using farnesylated-GFP and incubated them with PKH26

labelled exosomes (U2OS-derived). Localization of the labelled exosomal membrane remnants on the surface would have suggested membrane fusion at entry sites. Using the surface filling tool in Imaris software, we found out that the exosome congregation existed even inside the cell (Fig 4.19D).

### 4.2.3 Exosomes' entry into recipient cell

Since earlier results indicated EES's existence, our next aim is to investigate the mode of entry of exosomes into the recipient cells. For any membrane-bound vesicles like exosomes, the plasma membrane's uptake can be through direct membrane fusion or endocytosis. We transiently transfected the cells with mCherry Clathrin LC-15 that marked the clathrin-coated vesicles and added GFP-CD63 labelled exosomes (U2OS-derived) and incubated them for 12 hours. However, we observed no co-localization between the exosome clusters and clathrin vesicles, suggesting no clathrin-dependent endocytosis of exosomes in our case (Fig 4.20).

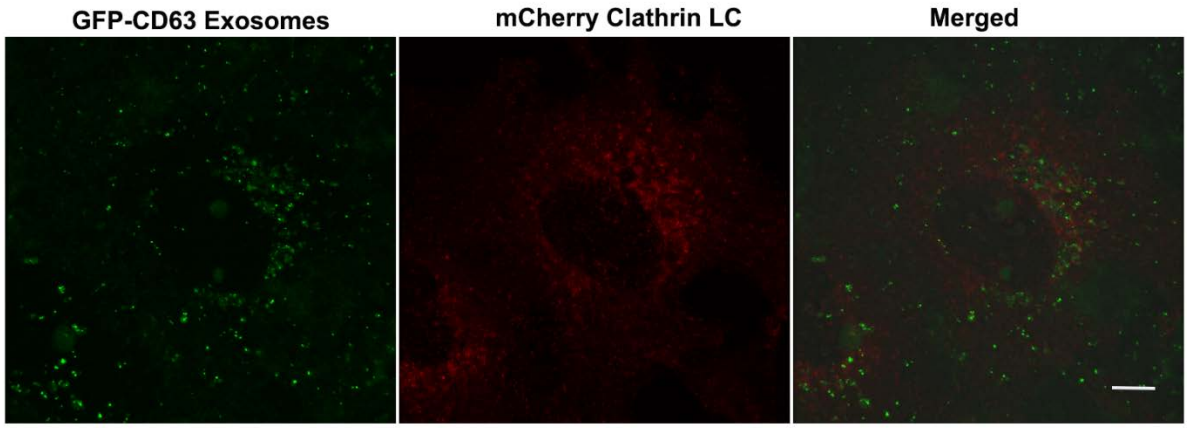


**Figure 4.20: Localization of exosomes with respect to clathrin-coated vesicles.**

Distribution of CD63-GFP labelled U2OS-derived exosomes incubated with U2OS mammalian cell line transiently transfected with mcherry-Clathrin LC for 12 hours. Scale bar, 10µm.

### 4.2.4 Discussion

We could conclude the existence of an exosome entry site, where exosomes concentrate for internalizing into the cells. However, we could not find any direct evidence of direct or clathrin-

mediated endocytosis with our results. Earlier reports have shown a decrease in exosomes' uptake where clathrin-mediated endocytosis is perturbed (Tian *et al.*, 2014). Clathrin-coated vesicles are involved in the transport and regulation of several endocytic pathways, which might hamper additional cellular activities and indirectly affecting the uptake of exosomes.

## 1.1 Summary:

Our study provides evidence that Dsl1 multi-subunit tether complex assembles and organizes ER arrival sites (ERAS) on the ER membrane by anchoring the ER-localized SNAREs. The interaction of COPI vesicles with the Dsl1 complex is documented by their complete localization. The ERAS organisation is directly dependent on the budding COPI vesicles emerging from cis Golgi as depletion of COPI vesicles disrupts the punctate nature of ERAS. The COPI vesicles emerge from the cis Golgi cisterna rim, fluorescently visualized in a ring-like pattern around the cis-Golgi that tether to the Dsl1 complex decorating them in a similar ring-like pattern. The ring pattern of the Dsl1 complex displays a central zone of clearance occupied by the ER exit sites. The organization of ERAS is lost in the absence of ERES. Loss of ERES leads to depletion of COPI and disruption of Golgi organization. However, loss of ERAS or COPI do not affect the ERES organization. This suggested that ERES plays a central role in maintaining the secretory unit in *P. pastoris*. ERES generates Golgi that in turn buds COPI vesicles which further organizes the ERAS. Loss of ERAS blocks the fusion of COPI vesicles that accumulate at the cis-Golgi cisterna visualized by increase in fluorescence intensity of COPI and early Golgi.

We also found that labelled exosomes concentrate at the plasma membrane that might form an entry site for them. However, the characterization of Exosome Entry Sites (EES) needs further investigation.

## 1.2 Conclusion:

Therefore, we conclude that both COPI vesicles (intracellular) and exosomes (extracellular) congregate at particular sites on their target membrane. These sites create hotspots for high vesicle capturing activity. In COPI vesicles, these sites are formed by Dsl1 complexes that arrange around the ER exit sites and create the ER's bidirectional transport portal.

# CONTENTS

## 1.1 Summary:

Our study provides evidence that Dsl1 multi-subunit tether complex assembles and organizes ER arrival sites (ERAS) on the ER membrane by anchoring the ER-localized SNAREs. The interaction of COPI vesicles with the Dsl1 complex is documented by their complete localization. The ERAS organisation is directly dependent on the budding COPI vesicles emerging from cis Golgi as depletion of COPI vesicles disrupts the punctate nature of ERAS. The COPI vesicles emerge from the cis Golgi cisterna rim, fluorescently visualized in a ring-like pattern around the cis-Golgi that tether to the Dsl1 complex decorating them in a similar ring-like pattern. The ring pattern of the Dsl1 complex displays a central zone of clearance occupied by the ER exit sites. The organization of ERAS is lost in the absence of ERES. Loss of ERES leads to depletion of COPI and disruption of Golgi organization. However, loss of ERAS or COPI do not affect the ERES organization. This suggested that ERES plays a central role in maintaining the secretory unit in *P. pastoris*. ERES generates Golgi that in turn buds COPI vesicles which further organizes the ERAS. Loss of ERAS blocks the fusion of COPI vesicles that accumulate at the cis-Golgi cisterna visualized by increase in fluorescence intensity of COPI and early Golgi.

We also found that labelled exosomes concentrate at the plasma membrane that might form an entry site for them. However, the characterization of Exosome Entry Sites (EES) needs further investigation.

## 1.2 Conclusion:

Therefore, we conclude that both COPI vesicles (intracellular) and exosomes (extracellular) congregate at particular sites on their target membrane. These sites create hotspots for high vesicle capturing activity. In COPI vesicles, these sites are formed by Dsl1 complexes that arrange around the ER exit sites and create the ER's bidirectional transport portal.

## 1.1 Summary:

Our study provides evidence that Dsl1 multi-subunit tether complex assembles and organizes ER arrival sites (ERAS) on the ER membrane by anchoring the ER-localized SNAREs. The interaction of COPI vesicles with the Dsl1 complex is documented by their complete localization. The ERAS organisation is directly dependent on the budding COPI vesicles emerging from cis Golgi as depletion of COPI vesicles disrupts the punctate nature of ERAS. The COPI vesicles emerge from the cis Golgi cisterna rim, fluorescently visualized in a ring-like pattern around the cis-Golgi that tether to the Dsl1 complex decorating them in a similar ring-like pattern. The ring pattern of the Dsl1 complex displays a central zone of clearance occupied by the ER exit sites. The organization of ERAS is lost in the absence of ERES. Loss of ERES leads to depletion of COPI and disruption of Golgi organization. However, loss of ERAS or COPI do not affect the ERES organization. This suggested that ERES plays a central role in maintaining the secretory unit in *P. pastoris*. ERES generates Golgi that in turn buds COPI vesicles which further organizes the ERAS. Loss of ERAS blocks the fusion of COPI vesicles that accumulate at the cis-Golgi cisterna visualized by increase in fluorescence intensity of COPI and early Golgi.

We also found that labelled exosomes concentrate at the plasma membrane that might form an entry site for them. However, the characterization of Exosome Entry Sites (EES) needs further investigation.

## 1.2 Conclusion:

Therefore, we conclude that both COPI vesicles (intracellular) and exosomes (extracellular) congregate at particular sites on their target membrane. These sites create hotspots for high vesicle capturing activity. In COPI vesicles, these sites are formed by Dsl1 complexes that arrange around the ER exit sites and create the ER's bidirectional transport portal.

# List of Figures

# List of Tables

# Thesis Highlight

**Name of the Student:** Sudeshna Roy Chowdhury **Enrolment No.:** LIFE09201504010
**Name of the CI/OCC:** Advanced Center for Treatment Research and Education in Cancer
**Thesis Title:** Biogenesis Dynamics and Functions of Cargo vesicles in early secretory pathway and extracellular milieu.
**Discipline:** Life Sciences **Sub-Area of Discipline:** Membrane Trafficking
**Date of viva voce:** 23.07.21

Distinct vesicles mediate an efficient cargo trafficking system to execute intracellular and extracellular communications in a tightly regulated manner. The primary focus of our study is to investigate whether vesicles have designated domains to fuse/enter their target membrane. In the early secretory pathway, cargo proteins are transported to Golgi via anterograde COPII vesicles originating from specialized sub-domains at the Endoplasmic Reticulum called ER Exit Sites (ERES). However, the site of the arrival of Golgi-derived retrograde COPI vesicles at the ER membrane is poorly understood. Our study characterized the ER Arrival Sites (ERAS) in the budding yeast *P. pastoris*, a simple system consisting of 4-5 stacked Golgi units positioned next to ERES. We showed that the Dsl1 multi-subunit tether complex acts as the potential candidate for organizing the putative ERAS. We also showed that fluorescently labeled exosomes congregated at particular sites (putative Exosome Entry Sites (EES) on the Plasma Membrane while entering the recipient cells.

Fluorescently labeled Dsl1 complex proteins decorated distinct domains on the ER membrane that colocalized with the COPI vesicles (marked by coat subunit, Sec26) and ER-localized SNARE proteins, confirming their role in linking the COPI vesicles to the ER-localized SNAREs for fusion. Further, the ERAS shared similar dynamics with the ERES, such that they behaved as bipartite ultrastructure, with ERES in the center and ERAS forming a ring-like pattern around it (Fig 1). Loss of ERES leads to loss of ERAS. Further, depletion of COPI vesicles also caused the disintegration of ERAS. We later observed the absence of typical Golgi stacks that failed to produce COPI vesicles when we destroyed ERES. All these results suggested that the biogenesis ERAS depends on the ERES. ERES generates Golgi, which produces COPI vesicles from rims of cis-cisterna that further organize the Dsl1 complex around the ERES. Additionally, loss of ERAS resulted in the accumulation of COPI vesicles at the Golgi, leading to an enlarged Golgi.

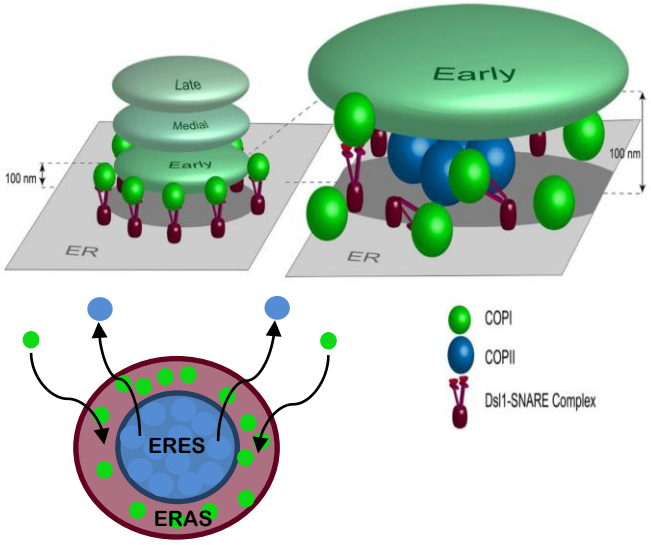


*Figure1: The schematic showing the working model of ER transport site.*